Bulletin 36
Part 2
(of 7 Parts)



# THE SHOCK AND VIBRATION BULLETIN

JANUARY 1967

A Publication of
THE SHOCK AND VIBRATION
INFORMATION CENTER
Naval Research Laboratory, Washington, D.C.


Office of
The Director of Defense
Research and Engineering

Bulletin 36
Part 2
(of 7 Parts)

# THE SHOCK AND VIBRATION BULLETIN

JANUARY 1967

A Publication of
THE SHOCK AND VIBRATION
INFORMATION CENTER
Naval Research Laboratory, Washington, D.C.

The 36th Symposium on Shock and Vibration was held in Los Angeles, California, on 18-20 October 1966. The U.S. Air Force was host.

Office of
The Director of Defense
Research and Engineering

## SYMPOSIUM MANAGEMENT

The Shock and Vibration Information Center

William W. Mutch, Director

Henry C. Pusey, Coordinator

Rudolph H. Volin, Coordinator

Jean B. Goldbecker, Editor

Katherine G. Jahnel, Administrative Secretary

### 36th Program Committee

William R. Forlifer, NASA Goddard Space Flight Center

Edward H. Scheil, Air Force Flight Dynamics Laboratory

George Stathopoulos, Naval Ordnance Laboratory

James M. Taylor, U.S. Army Missile Command

### Air Force Liaison

Los Angeles Scientific and Technical Liaison Office, Research and Technology Division, Air Force Systems Command

Lt. Col. Kenneth W. Cook

Arthur E. Kimberly

### Bulletin Production

Graphic Arts Branch, Technical Information Division, Naval Research Laboratory

# CONTENTS

PART 2



PAPERS APPEARING IN PART 1
Part I - Confidential
(Titles Unclassified)

PAPERS APPEARING IN PART 3

Vibration Testing

PAPERS APPEARING IN PART 4

Damping



PAPERS APPEARING IN PART 5

Analysis and Prediction

PAPERS APPEARING IN PART 6

Data Analysis and Instrumentation

Carl Irwin Vigness, 1905-1966

About twenty years ago, the present Shock and Vibration Information Center was born at the Naval Research Laboratory. Dr. Vigness helped to bring this organization into being, and since its inception, worked untiringly to interest engineers and scientists in this field of technology. Many of his contributions to the research studies of shock, vibration and applied mechanics were presented at the Shock and Vibration Symposia and appear in the Bulletins which the Center has published since 1946. Dr. Vigness served ably as Associate Editor, and wrote a large part of Chapter 5 on Instrumentation, of the handbook, "Fundamentals of Guided Missile Packaging," prepared at the request of the Assistant Secretary of Defense. R&D, in 1954. His persistent efforts have stimulated the development of new knowledge and techniques to further practical applications. Thus, it is a fitting tribute to dedicate the 36th Shock and Vibration Bulletin to IRWIN VIGNESS.

Irwin Vigness was born in Bismarck, North Dakota, on August 21, 1905. He attended the University of Minnesota where he earned the BEE degree in 1929, the MS in mathematics in 1931, and the Ph.D. in physics in 1934. From 1930 to 1934 he was a teaching fellow in physics, and between 1934 and 1939 he taught biophysics at that university. During this time, Dr. Vigness pursued studies on such varied subjects as the piezoelectric properties of Rochelle salt crystals, ultraviolet photometry, the effect of radiation on oil drops, and the medical applications of radium, x-rays, and diathermy. This diversity of technical experience formed an excellent background for his first research task at NRL in 1939. In the Mechanics and Electricity Division, he immediately plunged into the study of "Eddy Current Type Flow Detectors for Non-Magnetic Metals." This was followed by an investigation of the elastic properties of curved tubes. Then came the studies of fatigue tests and shock loading. At the time of his death on September 13, 1966, Dr. Vigness was Head of the Shock and Vibration Branch in the Mechanics Division. It was his guiding spirit that assembled the groups now in the Branch who are capable of testing and evaluating the effects of shock, vibration and other environments on almost any type of equipment.

Dr. Vigness contributed some forty articles to scientific journals and wrote as many NRL Reports. Under the sponsorship of the ASME and other professional societies, he lectured at various

universities over a number of years. He achieved national recognition as a consultant on mechanical vibration and shock, particularly for the Department of Defense, and served on a scientific advisory committee of the National Academy of Sciences. His committee responsibilities included being Chairman of the American Standards Association S-2 Committee, Chairman of the Acoustical Society of America Technical Committee on Shock and Vibration and President of the International Standards Organization Committee on Mechanical Vibration and Shock. He was an Associate Editor and Member of the Editorial Board of the Journal of the Acoustical Society of America, Past President of the Society for Experimental Stress Analysis, and a Fellow of the Institute of Environmental Sciences, the Acoustical Society of America and the Washington Academy of Sciences. He also held memberships in the American Physical Society, Sigma Xi, the Research Society of America, the Philosophical Society of Washington, Tau Beta Pi and Eta Kappa Nu.

Despite the demands of his work and his numerous professional activities, Irwin Vigness found time to enjoy the company of congenial friends and to participate actively in church work and in civic and community projects. He turned the skills of experimental physics and precision instrument making into a hobby from which he derived much pleasure and satisfaction — the building of electronic instruments and fine cabinetwork. He enjoyed hearing good music, and often relaxed by playing the organ. In the pursuit of these activities he found a congenial companion in Mrs. Vigness, herself a skilled weaver and an excellent homemaker. No doubt her sympathetic interest and culinary skill had much to do with his uniformly pleasant disposition.

In the untimely death of Dr. Irwin Vigness we, his friends and colleagues, sorely miss his calm approach to complex problems and his mature understanding of them. Some of the Nation's scientific societies will feel the loss of the man-of-action whom Dr. Vigness usually portrayed, and the Naval Research Laboratory has lost a dedicated and inspiring public servant.

Elias Klein
NASA Goddard Space Flight Center

# OPENING SESSION

## THE CHALLENGE OF THE SECOND HALF OF THE DECADE

R. G. Loewy*
University of Rochester
Rochester, New York

R. G. Loewy

"Challenge" is a word frequently used in the titles of papers and speeches, and for good reason. It is supposed to stir the senses and make the blood run quicker. It implies a threat or a dare, and the notion of "challenge" has a long and respected lineage.

In the fantastically technological world of the 20th century, one challenge likely to stir most of those assembled here is a purely intellectual one. The St. George's in this room have slain, imprisoned, or held at bay a family of dragons including transient dynamic overstress, resonance, instability, limit cycle behavior and other often invisible, somewhat sneaky fire-breathers whose effects are nonetheless very real, always troublesome, usually expensive, and too often tragic.

The tools we have forged to wage the good fight have constantly improved. But our dragons are continually changing, too — sort of like mosquitoes with their pesky way of developing immunity in succeeding generations to DDT and other insecticides. As technology goes through its rapid changes, the vibrational, aeroelastic, shock and acoustic dragons find different forms to take and new developments and projects in which to hide. In spite of this, our field is championed by a fearless group that rarely avoids an encounter. We are subject at turning points in the course of scientific and engineering affairs, however, to a kind of dread that there may be no more of our kind of dragons to slay, and, of course, we all prefer to be St. George rather than Don Quixote.

I remember one of these turning points shortly before the start of this decade. On December 6, 1957, a small group of specialists met at the Martin Company in Baltimore, Maryland. This was the so-called E-4 Panel of the Aircraft Research Testing Committee of the Aircraft Industries Association, and it was comprised of aircraft vibration and flutter experts. The meeting was one of many called at regular intervals to discuss technological problems in these specialities. This meeting, however, was different from any which preceded it. Almost two months before, the USSR launched the first man-made earth satellite, Sputnik I, and the reaction in the United States was already shaping national policy. The tone of our meeting was gloomy. These men were largely devoted to the theory and practice of structural dynamics, unsteady aerodynamics, aeroelasticity, and control theory — focused, as it was at that time, on aircraft. From the discussion it was clear that they viewed the launching of Sputnik I as proclaiming an era of flight in which concern with the atmosphere and dependence on lifting surfaces would be deemphasized, if not reduced to a technologically typical level. No one seemed convinced as to what his role would be when ballistic flight became the rule, or at least an inherent part of the most important developments of the age. To some, the only possible recourse was an exodus to greener pastures. Only a few insisted that there were important dynamics problems before the era of aircraft, and that they would continue to arise if and when wings became unimportant; these

*Formerly Chief Scientist of the Air Force.

few were regarded, I fear, as "whistling in the dark."

It is interesting and, I think, instructive to look back over the almost nine years since that meeting, to see how this one rather specialized branch of dynamics has fared. It is true that some specialists in vibration, structural dynamics, aeroelastic, and unsteady aerodynamics left the field. Perhaps a few thought they were leaving a sinking ship. But I suspect the majority of those who decided they would rather switch than fight recognized a need to adapt their skills to the revitalized activities centering on ballistic and orbital dynamics — the disciplines classically reserved for particle physicists, astronomers, and artillerymen. Those who remained active in our field found that instead of decreasing, the problems to be solved in the space age were, in fact, increasing both in number, variety, and importance.

Let us confine our review for the moment to some of the shock and vibration problems which have been associated with ballistic and space vehicle technology. The need to minimize structural weight, of course, was clear, because of the huge amount of propellant needed. This, together with design load conditions which in many ways were less severe than those associated with aircraft, led to structural-weight to take-off-weight fractions ten to twenty times less than those for aircraft. It is not surprising then that new phenomena became important. Wind-induced bending vibrations of big boosters, unlaunched but erected for the count-down, became a critical structural criterion. These oscillations were in response to the vortices formed on the leeward side of the rockets when winds blew across the launch complexes. The theory showing that periodic patterns of these eddies would form was developed as early as 1911 by Von Karman, and they were long ago identified as the source of "galloping transmission lines" and similar vibratory phenomena. The so-called "smoke stack" vibrations of the large rockets, however, were complicated by the close proximity of structures needed to erect and launch our spacecraft. Other serious dynamic response problems arose from the vehicle rising rapidly through horizontal winds which characteristically have the highest velocities in the vicinity of 20 to 40,000 feet, with lesser winds at higher and lower altitudes.

Such problems perpetuated the need to predict natural frequencies and mode shapes. Clustered configurations, such as Saturn I with eight bodies around a center body in the first stage and Titan III-C with two solid rockets strapped onto a single liquid-rocket center body, have renewed interest in branched beam systems. Similarly, the characteristics of large solid rockets required new attacks on the problems of short, deep composite beams with viscoelastic properties.

Space stations rotating with some nonzero absolute angular velocity in the gravity field of the planet about which they orbit are subject to purely mechanical instabilities which constitute, in a real sense, a new problem. From another viewpoint, however, there is a close relationship to the mechanical instabilities encountered with helicopter rotors. These were for years mistaken for "resonance" until explained in a fundamental NACA report by Robert Coleman in 1943. In the light of his work, it was clear why short, stiff airplane propellor blades never had the problem, and why the lower natural frequencies of long, thin rotor blades put them in the susceptible range. In an analogous way, MIT's Holt Ashley points out in a recent paper that orbiting structures are likely to be safe from such mechanical instabilities until periods as long as 1000 seconds result from their very large, limp structural characteristics. It is becoming increasingly evident that, once the loads associated with being boosted into orbit have been endured, space is — for structures — a very benign environment. The orbiting stations likely to be erected, inflated, or unwound in space are such that periods of this sort may not be out of the question.

But a really new kind of instability has been encountered. This one gave new meaning to an old word, for the phenomenon became popularly described as POGO oscillations. Here, for the mathematically minded, the two or more degrees of freedom coupled so as to have lags in the feedback from one to another, which are always required for classical dynamic instabilities, have several mechanisms to exploit. One system is provided by the fuel line and tank and the fuel they contain. A second is established by the oxidizer and its tankage and delivery system. A third can be considered to be associated with the pumps and combustion dynamic characteristics; the latter, of course, provides the point of energy input for the instability. And, finally, a fourth system capable of coupling all the foregoing, is inherent in the longitudinal natural modes of the complete launch vehicle structure. Now, such instabilities usually are encountered only if two or more frequencies are close to one another. One of the puzzling aspects of the POGO oscillations was how these conditions could exist, since the natural frequencies of the liquids in the tanks and feeder lines was quite high compared to those of the other systems. The riddle has been solved only

fairly recently. It was discovered that the cavitation bubbles associated with high-speed pump operation lowered the fundamental natural frequencies of the fuel and/or oxidizer liquids to where the coupling necessary for instability could indeed take place.

I have so far mentioned only problems associated with ballistic missiles and space vehicles. There are, however, related problems which are very much down to earth. If this sounds paradoxical, it can be explained by noting that the emergence of nuclear weapons as our principal deterrent force has been paced by the successful development of reliable, accurate launch vehicles, ballistic missiles such as the Atlas, Titan, Minuteman, and Polaris. In this situation, attempts to prevent nuclear war include (among other things) both insuring that our "hardened" missile launch complexes and civil defense shelters can survive a sneak attack, and also extending the nuclear test ban treaty, hopefully, to the point where permanent arms control and perhaps even disarmament are feasible. These efforts have reemphasized the importance of shock wave propagation in the earth's crust, its mantle, and its core. A review of the 1963 Shock and Vibration Symposium papers will show how fully the importance of this field was appreciated by the meeting planners. The Atomic Test Ban Treaty of that year is considered by many to be the first opening in the dark and threatening clouds of nuclear holocaust hanging over us all. This treaty, as you know, applies only to tests in the atmosphere, and it is enforceable only because such tests are detectable.

A recent development which combines seismological techniques well known in radar, sonar, and radio astronomy promises to put underground nuclear testing in the same monitorable category as atmospheric tests. This development is called LASA, Large Aperture Seismic Array. Under ARPA sponsorship, research at the Air Force Technical Applications Center and MIT's Lincoln Laboratory has led to an installation in Montana which is now operative. The installation consists of 525 seismometers placed in 21 clusters, buried 200 feet deep and spread over an area more than 100 miles in diameter. The signals from the seismic transducers are amplified, filtered, digitized and telemetered to a central computer where they are combined, analyzed, correlated, displayed, and recorded.

The success of the system as a test monitor, of course, depends on its ability to discriminate between minor and distant natural earth tremors and underground nuclear blasts of low yield. Aside from the geological knowledge to be gained, this development holds great promise of extending the detection of nuclear tests throughout the world, and thereby of perhaps sidestepping at least one aspect of the crucial diplomatic issue of inspection.

Seismic techniques have become an integral part of our civilian space program as well. The Ranger 5 spacecraft contained a passive seismic instrument as part of its payload, and one of the first Apollo lunar surface experiments will probably include active seismic measurements. It is likely that wave propagation and impact measurements will continue to be important to lunar investigations and even planetary research for many years to come.

Admittedly, it would take a much longer time than that allotted to me to even list the important dynamics problems of the space age to date. But we can hardly ignore what is often described as "a resurgence of aircraft" on the national scene. Helicopters, for example, have in Viet Nam approached a density and almost universal usage which only visionaries would have predicted when the currently operational generation of aircraft was first designed. The technology resulting in variable sweep wings and turbofan engines with multistage afterburners has made possible aircraft capable of performing an unusually great variety of missions. Furthermore, it is clear that a supersonic transport is practically at the end of the runway. Lifting reentry bodies and other hypersonic aircraft, perhaps with a supersonic combustion ramjet mode of propulsion, seem to be waiting just offstage. And even recoverable launch vehicles threaten to bring about aircraft applications with challenge enough for us all.

In the light of all this, no keynote speaker would have difficulty in enumerating problems to which the attenders of this Symposium can profitably address themselves. The difficulty lies in choosing a few to mention from among the many.

Helicopter vibratory loads and comfort levels remain vexing problems, particularly in high-speed forward flight, in spite of the fact that they are now quite well understood. We now require design techniques which will, for example, keep fuselage natural frequencies at the proper values or multidegree-of-freedom rotor isolation systems from bottoming over a very wide range of payloads. The development of engine, nacelle, and very large propeller packages for VTOL aircraft required advances in whirl-flutter prevention, fatigue life prediction and tolerance to small-particle impact.

Very large conventional aircraft such as the C-5A are likely to need special attention to problems of man-machine interactions, since the frequencies of the fundamental aircraft modes can approach those that a pilot might inadvertently use in cycling the flight controls. Aircraft noise of all kinds will be a matter of continuing importance from both military and commercial viewpoints, and design advances to minimize it will be much in demand. For spacecraft, the need to quantify impulsive excitation such as results from ascent or descent engine firing and docking impacts will become increasingly evident. Structural panel response to acoustic excitation will continue to be an important problem, and if "external burning" fulfills its promise as a propulsive, lifting, or control mechanism, we may have an interesting example of complete aerodynamic-combustion-elastic stability.

To insure performance gains in all these areas, it will be most important that we become well versed in the mechanics of composite structural materials such as filamentary composites. Their great potential virtually assures widespread applications, and we sorely lack experience with inhomogeneous, anisotropic materials as structures. Finally, I could hardly conclude even such a sketchy listing as this without mentioning the important contributions to be made in the field of high-speed mass transport. The development of 200 plus mph railroads, monorails, or tube trains can hardly hope to succeed without a great deal of attention to the structural dynamics problems with which you are all most familiar.

It has been an honor and a pleasure to be allowed to keynote this meeting. I am sure that it will be as successful and profitable as the Shock and Vibration Symposia of previous years, and I am looking forward with you all to the talks and papers which we are about to hear.

* * *

# SHOCK AND VIBRATION—A PERSPECTIVE

Alan Powell
David Taylor Model Basin
Washington, D.C.

A. Powell

From time to time it is well to stand back from the problems of the moment and to ponder a little over our field of endeavor in a more general way. In taking stock of where we stand now — and what led us here — we may be able to look ahead to see in what ways the subject which brings us together today may be best advanced.

I do not have to tell you that our field is a very complex one, even though I am including only shock and vibration and those aspects of acoustics which are inseparable from these. To analyze it, a choice of approaches must be made, and it is convenient to consider, firstly, albeit very cursorily, the nature of the fields of engineering application, which has produced the engineering needs; secondly, the different cross-cut of the way in which these needs have been met; and thirdly, some aspects of the educational processes by which people have been able to accept and carry off the challenges. These different points of view, taken together, should bring out the special features of our field, whether these features solve problems or create problems, and what developments we can either expect or for which we can reasonably have hope.

It is proper to consider first the fields of engineering application, on the basis that the field as we know it today has engineering development as its base in contrast to its beginnings as part of physical science, as in Lord Rayleigh's day. Rather than scientific curiosity producing the new basic problems, it is the developing techniques (such as Dr. Loewy has just described so well) which nowadays ruthlessly expose almost all of them, or provides new twists on classical problems which can be tackled properly only through engaging in basic research.

From the point of view of motivations, this base of engineering development falls rather clearly into two parts.

Firstly, vibration, and to a much lesser extent shock, can be put to work for us. Here the vibration is desired, and the problem is to acquire control of it so as to exploit it for useful purposes, whether for moving materials, drilling teeth or oil wells, or for artificial aging of beer.

Secondly, because shock and vibration are damaging, the motive is to exert control over it. Here it is usually best to banish it or, if that is not possible, then its adverse effects must be minimized.

In the first case it is a tool, the effort being justified for its own productive merits, but in the second case it is justified because it would otherwise be an unavoidable brake on the development, or even the very usefulness, of engineering systems. Often major systems are involved, as is the case of acoustic fatigue of airliners, launch vehicles and reentry vehicles, reliability of control systems, and the vulnerability of missile sites and naval vessels.

The total effort in this second category is by far the larger of two. Every paper in this Symposium and the vast majority of those in the professional journals fall into it, and it is on this aspect that I will concentrate. But even so, there will be many common elements within the first category of the exploitation of vibration.

What are the major characteristics of this "defense against shock and vibration" category?

Firstly, it cuts across the boundaries between diverse engineering systems, between static machines and structures and all vehicles — land, sea, air and space.

Secondly, there is obviously an indispensable mechanical element in its nature, in most cases more precisely described as structural dynamics.

Thirdly, "pure" problems are very rare, in the sense that they can be isolated from the systems in which they occur; and this is more so than for most other disciplines of very wide application, such as electric power. Thus machine unbalance, so nice and pure in a textbook, in practice is usually intimately tied up with such things as bearing technology, mount and perhaps noise considerations, material fatigue and more often than not entangled in production and economics. Another source of excitation lies in the field of fluid mechanics, a tremendously broad field in itself. This has a key role in the vibration of missiles, ship propellers, fans piping systems, in flutter, shock hardening against air blast, and so on.

This very broadness of the areas of application, compounded with the intimate and inseparable connection with many scientific and engineering specialties, has continually posed a special and serious problem.

Each of the fields of engineering has had necessary interests in the subject, but it is only to be expected that no one has had both the breadth and strength to become a focal point for them all. The need for a focus has existed, nonetheless, and as a consequence a few organizations such as this Center have sprung up with shock and vibration as their central theme (acoustics likewise). The outstanding characteristic of these, naturally, is their interdisciplinary scope.

Another problem posed to the profession is no less serious. This is the enormous complexity of most vibration problems when taken in their proper context. They are in very many cases incapable of a "paper solution" from beginning to end, and this has resulted in a mismatch between the scientific and engineering workers in the field.

Although the public does not seem to distinguish between our ideas of science and engineering, there is, of course, a vital difference if one thinks in terms of motivation of the individual rather than in terms of the scientific approach -- which all good engineers use all the time! The engineer has to achieve a certain result; the problems are very complex and the engineer is often driven to ad hoc test work because he dare not risk changing a parameter because of the danger of being nonrepresentative. The scientist's job is to explain something; to be successful, he has to get the problem into a form that is amenable to his special methods. For the same reason that the engineer is so often driven to test work, the scientist must all too often consciously or unconsciously sidestep solving the real problem, so that if his work is to be put to use, it still needs backup by test work (all too often full-scale) so that the engineer can bridge the gap between the scientist's idealized system and the real world. Of course, a mismatch between the basic researchers and the designers is a widespread problem that receives less attention than it should. It is just that the extremely complex nature of the real problems in shock and vibration has amplified the mismatch.

This in turn is compounded by the fact that, because the problem lies mainly in that second motivational category -- of shock and vibration in need of suppression -- it has not been of central importance to the designer as is, say, acoustics to the sonar designer. Historically it has been quite satisfactory to neglect it in most designs, giving it attention only if troubles developed during development or service. In this way, the subject has traditionally come to receive heavy emphasis in test, evaluation and remedial measures. There have been a few notable exceptions. Flutter was so catastrophic that the basic research had to be done very early and the results have been systematically used in subsequent aircraft design as a matter of course. Acoustic fatigue was not considered until difficulties arose -- difficulties which obviously would worsen at such a rate that patching things up was no approach. The airframe designer soon became aware that he had another criterion to meet. Nevertheless, the acquiring of the support information in a form that the designer can use still involves a tremendous amount of test and evaluation.

This complexity of our subject has been a major factor in the educational picture -- an adverse one. As in the case of professional engineering societies, so it is with engineering departments in the universities and colleges; the very breadth and complexity of the subject makes it ill-fitted to neat and elegant deductive analysis without a real danger of emasculation. But unfortunately, focusing has been a long time coming here. Instruction beyond the most elementary notion of vibration has traditionally depended upon the interest and enterprise of individuals, usually residing in physics or engineering departments, in pushing an area that Rayleigh did not polish off, but lacking in glamor and, therefore, interest to the uninitiated student, to the public at large, and to the benefactors, who have a vested and lively interest in

the use of the educational tax or gift million support. But it is a happy characteristic of human affairs that long-standing needs often seem to be met sooner or later if they are real enough. Indeed, a couple of most promising developments have been the recent recognition of engineering-acoustics as a bona fide field of study for higher degrees carrying that name, and the National Science Foundation's provision of some very basic institutional support.

The area of shock, however, is unfortunately even less well placed than are vibration and acoustics — shock is an item yet to be found in any college curriculum (except perhaps in psychology!), even where engineering design is prospering.

The situation has all the earmarks of a vicious circle — the nature of the profession and the academic outlook react on each other, and the woeful lack of graduates with a strong background is a key element in the circle. These educational steps forward and a few more like them have the potential for introducing a new element in this feedback circuit, and this could well change markedly the technological outlook over not too many years.

In the meantime, what are the virtues of the situation?

The fact that most workers in the field had been active in some other discipline or field of application adds a breadth that would be hard to cultivate. The result is quality essential to the health of an interdisciplinary field, i.e., more than just a superficial notion of the other closely involved specialties. I sometimes wonder if it is this diversity of related disciplines, or rather the stimulation of these interdisciplinary aspects as well as the various areas of application which is one of the big attractions. It is noticeable that many people move into the field, and perhaps move around in it, but very few leave it.

You will observe the irony of the situation; specialization built on an interdisciplinary base is a real strength so far as the professional is concerned, but the educational system has developed in such a way that it has been ill-conditioned to provide such a foundation.

To summarize at this point, we see a profession with strong interdisciplinary connections, heavy at the test and evaluation end of the scale, with a continuing inadequate input of appropriately highly trained graduates, scholars generally distant from the real engineering problems which are most certainly not going to go away, but we also see signs of some leadership beginning to emerge in the educational field.

With this base, one may reasonably speculate about the future.

These new educational developments should begin to add a new strength in the professional field but the acute shortage of talent will last at least five or ten years. For a long time the bulk of the burden of education in shock, vibration, and acoustics will still fall largely on the profession itself through on-the-job training, with a continuing, and probably growing, dependence on either part-time or further (post-graduate) education.

As our overall understanding of the usually very complex problems of shock and vibration improves, it should be possible to reduce the enormous cost of test and evaluation work. By overall understanding here, I mean having a basic knowledge adequate not only to analyze new situations, but also with the know-how for translating the results into a form the designer can use. With reduced uncertainties, it will be possible to reduce it by being able to design better and farther reaching tests — in other words, the test would take on more and more the nature of a controlled experiment. But the largest gains to be realized will come from feeding the shock and vibration aspects more fully into the design spiral, really getting down to a comprehensive systems approach. This leads to the next point.

The full impact of the mushrooming computer technology has yet to be felt. The computer has a great value simply as a super-calculating machine, to get existing calculations accomplished in a useful time, in reformulating problems so that telling sensitivity and parametric design studies become feasible. But the advancing computer technology will make quite new approaches possible, particularly in analysis and design, both system and detail, and in the bridging between the two, where many of the most stubborn vibration problems have their roots. It is going to call for the highest talent, which will become employed very effectively, and it will be expensive. For example, there is the tremendous amount of support data required, both for the establishment of specifications and for design, much of which does not exist now. This is thin enough in the vibration area, but it is even more sparse for shock, where realistic tests are even more expensive because "non-destructive" often means academic. But the long-term possibilities can obviously revolutionize our approach — and much of computer-aided and automated engineering design will be

limping until shock and vibration have their proper roles in it.

These will be exciting developments — and they contain many elements which are very likely to be taken up by the academic community, adding more impetus to the changing scene. The far-reaching developments are apart from the emergence of new techniques of analysis, which they will embrace. These techniques are those such as energy and statistical or averaging methods in random vibration, which are already under way. A freer movement of top talent to and fro between the universities, government and industry would be especially valuable here, apart from the general benefits from working exchanges, but it really needs more than an occasional sabbatical leave — the individual must get more deeply involved than is possible in a short temporary status (the common pension scheme of the British universities and the Scientific Civil Service is a potent factor, the likes of which does not exist in this country).

The interdisciplinary nature, which can be such a handicap, should then encourage fuller realization of the real needs and the relatively early introduction of such things as new materials and sensors. The latter, in conjunction with computer developments, may well bring about considerable changes in the way experiments are done

I have offered you a perspective, one of many possible, but the conclusions of them all are likely to be much the same. We are in all probability at a turning point in our field — the question is not so much whether these changes will take place, but rather how fast we can push them forward.

Central to this is the contribution from the educators who have such a key role in determining the vitality of rate of progress, and hopefully will capitalize on the interdisciplinary aspects of the real problems to impart a richer education. It is up to us to help this along by all means at our disposal, not to be too preoccupied in tackling the complex and urgent problems of the moment, at which — considering the handicaps — we have had singular success. There is reason to feel that progress, which already has been, in retrospect, quite remarkable, will quicken in the years just ahead.

* * *

# SHOCK

## YIELDING EFFECTS ON SHOCK SPECTRA

William R. Mentzer, Jr.
Bowles Engineering Corporation
Silver Spring, Maryland

and

Patrick F. Cunniff
Department of Mechanical Engineering
University of Maryland, College Park, Maryland

An undamped two-degree-of-freedom spring-mass system, representing an equipment attached to a nonrigid foundation subjected to shock, is analyzed to determine the shape of the shock spectrum curve when the equipment spring is allowed to yield. Analytical solutions for the equations of motion are presented for the system response as a perfectly elastic system and as a system yielding under a constant force. The system base mass response is used to obtain the shock spectrum data by a high-speed digital computer. The shock spectrum curves for the yielding systems and for the perfectly elastic systems, with equivalent design parameters and shock loading, are compared. The results indicate that certain difficulties exist for proper interpretation of field data when the equipment has yielded, particularly if the analyst, unaware that yielding has taken place, wishes to compile data for a design shock spectrum curve.

P. F. Cunniff

### INTRODUCTION

The concept of shock spectra is used to evaluate the damaging potential of a shock motion to equipment structures. A shock spectrum curve is defined as a plot of the maximum absolute values of the relative displacement of a set of damped or undamped single-degree-of-freedom oscillators subjected to a shock motion versus the natural frequencies of the various oscillators employed. This information can also be presented in velocity or acceleration units by choice of the proper scaling factors.

Past studies at the Naval Research Laboratory toward developing meaningful shock spectra have produced two significant results: (a) the discovery of the shock spectrum dip effect [1], and (b) the initiation of the concept of design shock spectra [2]. Normal mode theory [3] for linear lumped-parameter systems indicates that the shock spectrum values to be used for analysis correspond to the fixed-base natural frequencies of the equipment structure in place during the shock motion. The spectrum values tend to lie in the valleys of the spectrum curve, hence the term shock spectrum dip.

To construct satisfactory data from shock spectrum curves based on field tests, it is desirable to know something about the fixed-base natural frequencies of the equipment structure which is generally attached to a nonrigid foundation structure. Such information may be

obtained from analysis of the system or by experimental shaker tests [4]. By judiciously choosing the proper spectrum points, a design shock spectrum curve can be constructed [5] to check the adequacy of future equipment structures of similar design to withstand the shock environment. Present Navy specifications [6] use this approach to evaluate the design of heavy shipboard equipments to withstand shock.

The primary objective of this study is to determine how the shock spectrum, obtained when yielding occurs in an equipment structure, differs from the shock spectrum for the same equipment treated as a perfectly elastic system.

## ANALYSIS OF YIELDING STRUCTURE

Figure 1 shows the equipment and foundation structures represented as a two-degree-of-freedom system. The upper mass M and spring K form the equipment, while the lower mass $M_o$ and spring $K_o$ form the foundation. The equipment spring is allowed to yield in a perfectly plastic mode as depicted in Fig. 2. Figure 3 shows the shock input.

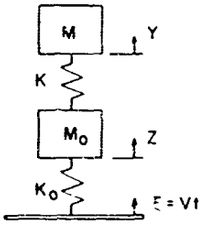


Fig. 1 - Equipment and foundation structures represented as a two-degree-of-freedom system

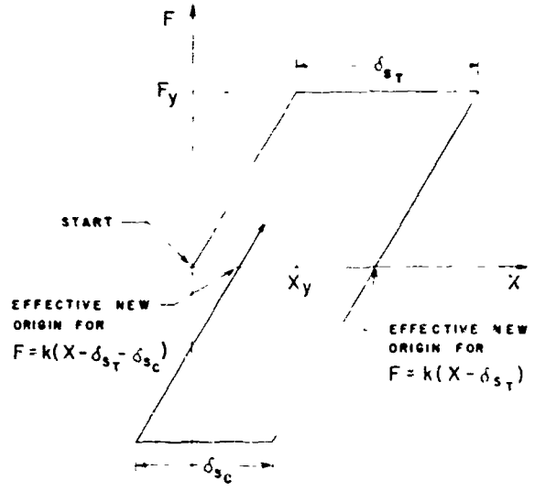


Fig. 2 - A representative force - displacement curve for a yielding spring

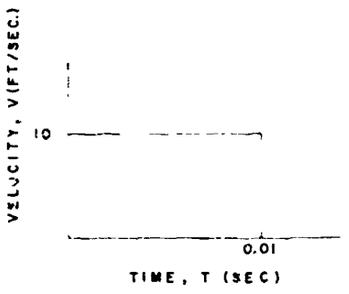


Fig. 3 - Shock input to the foundation structure

To determine the shock spectra for this situation, the response of the system to the applied shock must be examined in two modes: when the equipment support spring is operating in the elastic mode, and when the spring is undergoing yielding at a constant force. Since the expression for system foundation mass motion is developed from two sets of system equations, a simple expression for shock spectra cannot be obtained as is done in the perfectly elastic case [2]. For this reason, a digital computer is used to develop the base motion as a function of time, and then a numerical technique is used to solve for the shock spectrum data points.

In both modes of operation, exact solutions were found for the equations of motion. The solutions were developed in terms of the initial conditions so that the computer could step through the problem in small time increments, changing to the correct system mode of operation when the system dynamics indicated the time for switching.

The solutions to the equations of motion in both modes of operation are briefly discussed here. The detailed derivation of the expressions can be found elsewhere [7].

### Phase I. Response of a Perfectly Elastic System

The equations of motion for the system shown in Fig. 1 are as follows:

$$\ddot{Z} + (\omega^2 + \omega_o^2) Z - \omega_o^2 Y - \omega^2 \xi = 0, \qquad (1)$$

and

$$\ddot{Y} - \omega_o^2 Y - \omega_o^2 Z = 0, \qquad (2)$$

in which

$$\omega^2 \quad \frac{K_o}{M_o} ,$$

$$^2 \quad \frac{K}{M} ,$$

and

$$\quad - \frac{M}{M_o} .$$

Simultaneous solutions of Eqs. (1) and (2) can be found using Laplace transformations and by expressing the results in terms of the initial conditions. Since the objective is to determine shock spectra based on the response of the base, where the equipment is attached to the foundation, this expression is the only one of immediate concern. Expressing this response in the form of velocity yields

$$\dot{Z} \quad \frac{\omega_o^{\ 2}\ ^2}{(\ ^2_2 - \omega_1^2)} \left( \frac{1}{\omega_1} \sin \omega_1 t - \frac{1}{\omega_2} \sin \omega_2 t \right)$$

$$+ \frac{\omega_o^{\ 2}}{(\ ^2_2 - \ ^2_1)} (-\omega_1 \sin \ _1 t + \omega_2 \sin \omega_2 t) + V$$

$$+ \frac{V\omega_1^{\ 2}\ ^2}{(\omega_2^2 - \ ^2_1)} \left( - \frac{1}{\omega_1^2} \cos \ _1 t + \frac{1}{\omega_2^2} \cos \omega_2 t \right)$$

$$+ \frac{V\omega_1^{\ 2}}{(\ ^2_2 - \omega_1^2)} (\cos \omega_1 t - \cos \ _2 t)$$

$$+ \frac{Z_o(\omega_2^2 - \ ^2_1)}{(\omega_2^2 - \ ^2_1)} \left( - \omega_1 \sin \omega_1 t + \frac{\dot{Z}_o}{Z_o} \cos \omega_1 t \right)$$

$$- \frac{Z_o(\omega_2^2 - \ ^2_2)}{(\ ^2_2 - \omega_1^2)} \left( - \omega_2 \sin \ _2 t + \frac{\dot{Z}_o}{Z_o} \cos \omega_2 t \right)$$

$$+ \frac{Y_o\ ^2}{(\ ^2_2 - \ ^2_1)} \left( - \omega_1 \sin \omega_1 t + \frac{\dot{Y}_o}{Y_o} \cos \ _1 t \right)$$

$$- \frac{Y_o \omega_2^2}{(\ ^2_2 - \omega_1^2)} \left( - \omega_2 \sin \ _2 t + \frac{\dot{Y}_o}{Y_o} \cos \omega_2 t \right) . \quad (3)$$

in which

$$\omega_1^2{}_2 \quad \frac{1}{2} \left[ \omega^2 + (1 + \mu) \omega^2 \right]$$

$$= \frac{1}{2} \sqrt{\omega^2 + (1 + \mu)^{\ 2} \omega^2 - 4\omega^2 \ ^2} .$$

Termination of this mode of operation occurs when the force in the equipment support spring exceeds the yield strength. Since, in the elastic mode, the force is directly proportional to the spring displacement, the spring deflection must be determined. The relative position of the two masses is the measurement of the spring displacement from its initial state of rest; the only condition required is that both expansion and compression of the spring are possible.

The expression for the relative position of the masses is

$$X - Y - Z \quad (4)$$

where positive X indicates the spring is in tension. The value of $\dot{X}$ is required as an input to the second mode of operation. This is determined by differentiating Eq. (4).

Phase II. Response of a Yielding System

When the yield point of the equipment spring is reached, the system enters the second mode of operation. The equations of motion for this phase, where the equipment spring in Fig. 2 has been replaced by a constant force $F_y$, are as follows:

$$\ddot{Z} + \omega^2(Z - \xi) - \frac{F_y}{M_o} = 0 , \quad (5)$$

and

$$\ddot{Y} + \frac{F_y}{M_o} = 0 . \quad (6)$$

The response $\dot{Z}$ is again desired for shock spectrum computations; that is,

$$\dot{Z} = -Z_o \omega \sin \omega t + \dot{Z}_o \cos \omega t$$

$$+ \left( \omega Y_o + \frac{F_y}{\omega M_o} \right) \sin \omega t + V - V \cos \omega t . \quad (7)$$

This second mode is terminated when the relative velocity $\dot{X}$ is zero.

Should the applied shock cease before the predetermined computer processing interval is completed, the term V must disappear in the above equations.

With the relationships presented, a record can now be obtained of the base mass velocity as a function of time throughout both modes of system operation. It is possible to pass from one mode to the other, if the conditions for the

mode change have been met: $|F| > F_{yield}$ to go from elastic to plastic mode, or $\dot{X} = 0$ to go from plastic mode back to the elastic mode. The function $\dot{Z}$ is now the input to the equation of motion of the tunable oscillator to determine the shock spectra.

## Shock and Fourier Spectra

Figure 4 shows the tunable oscillator used to calculate shock spectra. The equation of motion is

$$\ddot{r} + \omega^2 r = -\ddot{Z}, \tag{8}$$

in which $r$ is the relative displacement between the mass and the moving base. The solution of Eq. (8) is

$$r = r_o \cos \omega t + \frac{\dot{r}_o}{\omega} \sin \omega t - \frac{1}{\omega} \int_0^t \ddot{Z}(T) \sin \omega (t - T)\, dT \tag{9}$$

Equation (9) and its derivative have been solved by a numerical method reported earlier [8]. This procedure solves the Duhamel integral in Eq. (9) when the base motion is expressed by $\dot{Z}(t)$. The numerical method calculates not only shock spectra but also, with little additional effort, Fourier spectra [8].

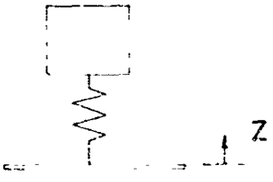


Fig. 4 - Tunable oscillator for calculating shock spectra

## THE COMPUTER PROGRAM

### Functions of the Program

The program performs two basic functions: it determines the system response to the shock input, and it develops the shock and Fourier spectra from the response data. The evaluation of the system response is done on a fixed time increment to facilitate the computation of shock spectra. The time increment $\Delta t$ must be small enough to attain the switching points between modes with as little error as possible. The constant time increment is introduced by replacing the term $t$ by $\Delta t$ in the response equations such as Eq. (3). This replacement reduces the program execution time since the trigonometric terms are computed only once for the problem.

The program has the capability of handling a constant velocity shock input of any duration. The memory storage is such that 2400 values of the dimensioned variables such as $\dot{Z}$ and , which are used for the shock spectra evaluation, can be stored; thus, system motion can be saved for a time duration up to 24,000 $\Delta t$, since data are stored only for every tenth computation of $\dot{Z}$. The Case 1 equations of motion are programmed in double precision to avoid loss of data in the terms of $1 - \omega_1^3$ and $1 - \omega_2^3$.

### Computation of Spring Length for the Elastic Mode

An interesting feature of the program is the means by which the force and spring length computations are kept within the limits of a perfectly elastic system for the purpose of controlling the switching between program modes while the system actually undergoes yielding. The spring length at any time is defined as

$$_s \quad (X - \quad), \tag{10}$$

in which

$_s$ = spring length in the perfectly elastic system,

$X$ = Y-Z, relative displacement of the masses, and

= permanent deflection.

The system starts from rest, so 0, and the test for reaching the yield point is simply

$$_s \quad X \quad 0.98\, X_{yield}$$

or (11)

$$_s \quad X \quad -0.98\, X_{yield}.$$

(The reason for using 98 percent of $X_{yield}$ is explained in the next section.) Upon exceeding 98 percent of the yield point, the value of the relative displacement of the masses is stored as $X_{start}$, and the computations in the plastic mode are started. At the termination of the plastic mode, the program computes the permanent stretch for that cycle of the plastic mode as

$$\quad X - X_{start} \tag{12}$$

and computes the total permanent deflection by the program statement

$$\cdot \quad {}_{s} \cdot \qquad (13)$$

in which the $\cdot$ on the right side of Eq. (13) is the previously computed . In Eqs. (12) and (13), the sign convention is always correct regardless of whether the system is subjected to tens..e or compressive yield. From Eq. (10), it is seen that $'_s$ can never exceed $0.98\ X_{yield}$. This, in effect, shifts the origin of the force versus displacement curve so that the force and displacement in the elastic mode are always computed on the basis of a perfectly elastic system. This is indicated in Fig. 2.

### Errors Present in the Program

In running the program on a constant time increment, which is desirable for determining shock spectra without interpolation, a main source of error is introduced. The yield point cutoff for the start of a plastic mode was taken as the first computed value of the spring length that exceeded 98 percent of the pr bed limit; that is, $(X - \cdot) \geq 0.98\ X_{yield}$. This meant that the magnitude of the spring force used in the plastic mode computations was

$$F = k(X - \cdot), \qquad (14)$$

which would be either slightly below or above the ideal yield force computed for $X = X_{yield}$ and $\cdot = 0$.

The program calculates the error each time it switches from Mode I to Mode II. For the cases to be presented in this paper, the average of these errors was never greater than $\pm 0.03$ percent, while the average of the absolute errors was never greater than 1.1 percent. The largest single individual error was 3.1 percent.

Because of the overrun which results from the constant time increment, a second problem was encountered when the program reentered the elastic mode after completing a computation cycle in the plastic mode. Since $X_{start} \geq 0.98\ X_{yield}$ at the start of the plastic mode, and $X = X_{start} \cdot \cdot$ at the end of the plastic mode, then $X - \cdot \cdot = X_{start} \cdot 0.98\ X_{yield}$ at the termination of the plastic mode. With the condition that $\dot{X} = 0$ at the termination of the plastic mode, the first calculation of $X$ in the elastic mode would be expected to be small. In some cases, the increment in $X$ resulting from the first computation in the elastic mode was so small that $(X - )$ remained greater than $0.98\ X_{yield}$, and the program was returned to the plastic mode from which it was unable to exit. This difficulty was eliminated by setting $0.98\ X_{yield}$ equal to $X_{start}$ on entering Case II and holding it at this value until Case II as well as ten computation cycles of Case I were completed. At this time $X_{yield}$ was restored to the value read in at the start of the problem.

## EXAMPLE PROBLEM

Figure 1 represents the system for which this investigation was made. This model was chosen because the exact solutions for the base motion in both the elastic and plastic modes were known. While this model appears simple, it does lend some insight into the yielding effects on shock spectra.

The equipment structure of mass $M$ and the spring constant $K$ were kept constant at values of 60 slugs and $1.5 \times 10^6$ lb/ft, respectively. The mass ratio $\mu = M/M_o$ was varied from 1.0 to 0.1 as shown in Table 1. Thus, the fixed-base natural frequency, $\omega = 25.16$, was held constant for each of the ten runs. A constant time increment of 0.05 msec was used throughout for the yielding spring computations.

The shock applied to the system is shown in Fig. 3. The short time duration of the disturbance was sufficient to disturb the system in each case so that the yield limit was always exceeded in the first cycle of the time response. The yield point for each system was taken as 50 percent of the maximum expected relative displacement $X$, computed from the expression developed in Eq. (2) for the perfectly elastic system; that is,

$$X_{max} \quad \frac{V_i^2}{\omega^2(1 + \mu)} \cdot \qquad (15)$$

Equation (15) assumes the shock input $V$ is applied over the length of time required to reach $X_{max}$. Generally, 15 cycles of record of $\dot{Z}$ were used for computing shock spectrum data.

Typical shock spectrum curves are shown in Fig. 5 for $\mu$ equal to 1.0, 0.5, and 0.1. The solid line represents the shock spectrum curve if the system were to remain perfectly elastic. Note the two peaks corresponding to the two system natural frequencies and the value at the fixed-base natural frequency in the valley. The dashed line represents the spectrum curve for the type of yielding already described.

As the mass ratio is decreased (while the base mass $M_o$ increases), the magnitude of the shock spectrum curves always decreases, as

TABLE 1
Summary of Computer Results

| | | | | Shock Spectrum Values | | | |
|---|---|---|---|---|---|---|---|
| | | | | Perfectly Elastic System | Yielding System | First Dip Value for Yielding System | |
| | (cps) | (cps) | (ft) | | | | Value |
| 1.0 | 20.98 | 52.07 | 0.08832 | 2.06 | 2.20 | 21 | 1.70 |
| 0.9 | 20.88 | 49.63 | 0.09060 | 2.15 | 2.31 | 20 | 1.77 |
| 0.8 | 20.75 | 47.08 | 0.09326 | 2.19 | 2.58 | 20 | 1.83 |
| 0.7 | 20.58 | 44.41 | 0.09641 | 2.26 | 2.78 | 20 | 1.89 |
| 0.6 | 20.34 | 41.60 | 0.10008 | 2.35 | 3.06 | 19 | 1.92 |
| 0.5 | 20.00 | 38.60 | 0.10415 | 2.63 | 3.64 | 19 | 2.01 |
| 0.4 | 19.45 | 35.53 | 0.10800 | 2.40 | 4.57 | 19 | 2.16 |
| 0.3 | 18.50 | 32.35 | 0.10858 | 2.30 | 8.43 | 19 | 2.19 |
| 0.2 | 16.67 | 29.31 | 0.09717 | 1.85 | 7.01 | 17 | 2.37 |
| 0.1 | 12.88 | 26.82 | 0.06233 | 1.00 | 2.28 | 12 | 3.04 |

one would expect. The spectrum curves for plastic yielding exhibit additional peaks. For the higher mass ratios the peaks occur at equal frequency intervals taken three at a time. For example, the frequency interval in Fig. 5b is approximately 20 cps for the first three peaks, followed by a 13-cps increment. The next three peaks are again separated by 20 cps, a 13-cps increment, etc. It is noted that the frequency increment for the perfectly elastic case is 18.6 cps, which is close to the 20-cps increment between successive third peaks. This phenomenon was also noted at the other mass ratios except at = 0.1 shown in Fig. 5c, since there are so many peaks for this case.

Another interesting observation of the spectrum curves is seen in a shifting to the left of the original peaks corresponding to and for the perfectly elastic case. Likewise, the spectrum value at the fixed base natural frequency of the equipment shifts to the left. In all cases tested, the shifted dip value occurred at approximately . As the mass ratio decreases, the magnitude of the shifted dip value increases. These observations appear to raise some interesting situations for proper interpretation of field data when the equipment has yielded, particularly if the analyst, unaware that yielding has taken place, wishes to compile data for a design shock spectrum curve.

## CONCLUSIONS

The computer results indicate that there are distinct differences between the shock spectrum for a perfectly elastic system and that for a similar system that undergoes yielding. It was found that the peaks and valleys of the shock spectrum for the perfectly elastic system shifted to lower frequency values for the yielding system. Also, for the systems that undergo yielding, several additional major peaks appeared in the shock spectrum curves occurring in multiples of three, separated approximately by ( ).

The dip spectrum value, which corresponds to the fixed-base natural frequency of the equipment in the elastic system, shifted to a lower frequency for all cases studied. This phenomenon raises some problems in formulating design shock spectrum curves from field data where the equipment structure yields.

It is suggested that further investigations are desirable to understand the difficulties in establishing design shock spectrum data from field measurements containing other types of nonlinearities, as well as damping effects.

## ACKNOWLEDGMENTS

The material herein is part of a thesis by William R. Mentzer, Jr., presented to the Department of Mechanical Engineering of the University of Maryland in July 1966, in partial fulfillment of the requirements for the Master of Science degree.

The computer time for this project was made available through the facilities of the Computer Science Center of the University of Maryland.

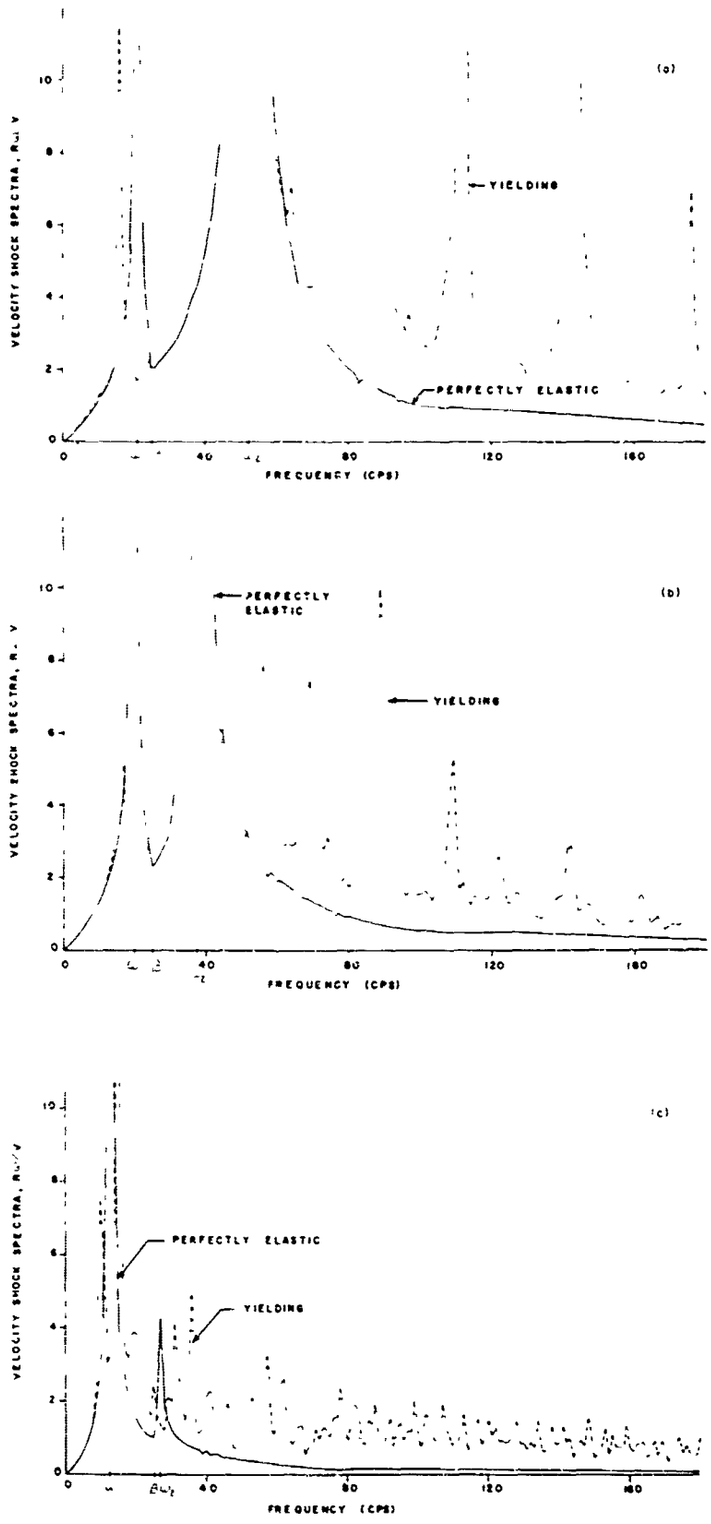


Fig. 5 - Scaled velocity shock spectrum curves: (a) .. = 1.0, (b) .. = 0.5, and (c) .. = 0.1

## REFERENCES


1. G. J. O'Hara, "Effect Upon Shock Spectra of the Dynamic Reaction of Structures," NRL Rept. 5236, Dec. 16, 1958

2. G. J. O'Hara, "Shock Spectra and Design Shock Spectra," NRL Rept. 5386, Nov. 12, 1959

3. G. J. O'Hara and P. F. Cunniff, "Elements of Normal Mode Theory," NRL Rept. 6002, Aug. 12, 1964

4. L. P. Petak and R. E. Kaplan, "Resonance Testing in the Determination of Fixed Base Natural Frequencies of Shipboard Equipment," NRL Rept. 6176, Dec. 15, 1964

5. "Shock Design of Shipboard Equipment, Part I," NAVSHIPS 250-423-30, May 1961

6. G. J. O'Hara and R. O. Belsheim, "Interim Design Values for Shock Design of Shipboard Equipment," NRL Memo. Rept. 1396, Feb. 1963

7. W. R. Mentzer, Jr., "Yielding Effects on Shock Spectra," M. S. Thesis, Dept. of Mech. Eng., Univ. of Maryland, June 1966

8. G. J. O'Hara, "A Numerical Procedure for Shock and Fourier Analysis," NRL Rept. 5772, June 5, 1962


* * *

# SHOCK SPECTRA OF PRACTICAL SHAKER SHOCK PULSES

John R. Fagan and Anthony S. Baran
Radio Corporation of America
Princeton, New Jersey

Shaker shock data are acquired using piezoelectric accelerometers and a wideband FM magnetic tape system for recording the pulses. Data reduction is accomplished with six relatively undamped galvanometers and tape speed translations effectively to produce a 1/3-octave shock spectrum analysis to 5 kHz. A method for selecting the four shock spectra (plus and minus initial, plus and minus residual) from a particular shock pulse is determined. Some consideration is given to expanding the system for on-line analysis.

The spectra of shock pulses used in shaker shock tests are compared to the theoretical specification pulse spectra. The spectra of transient inputs to test items due to fixturing parameters are determined, and their effects are discussed. Transients occurring during facility malfunctions or protective device operations are defined spectrally, and their effects on test items are determined.

A. S. Baran

## INTRODUCTION

The most common form of shock test specifies the desired waveform of the acceleration as a function of time. Recent requirements tend toward specifying the spectra of the shock pulse. For simple pulses defined in classical form, the associated spectra have been calculated.

Actual test pulses never completely fulfill the exact classical description, and their spectra remain unknown. The determination of the shock spectra has been a difficult task usually involving extensive computer programs. However, within the past two years, analog and simulative techniques were developed that permit on-line laboratory analysis of the shock transient.

## WAVEFORM SHOCK TESTING

Two common pulses are usually specified in "waveform demand" type of shock testing: the half-sine and the terminal peak sawtooth. Both pulses are specified as acceleration as a function of time. They both require a net change in velocity of the test item. The machines used to generate these pulses are quite varied in construction and design. The pulse generally is specified at the input of the test item. This, in effect, is a requirement for an infinite impedance of the test machine. When testing small items, the mass of the test machine is large enough to approach this condition. However, for very large test items, some loading of the test machine by the test item cannot be avoided. When this problem arises, the usual procedure is to obtain the specified pulse on the unloaded machine (or pure mass loaded), then mount the test item and accomplish the test.

A compromise between these two extremes is a pulse which, although not classical in shape, does fall within the liberal tolerances of the specification. The shock spectra of such pulses are often erroneously assumed to be those associated with and calculated from the classical mathematical representation of the shock pulse.

## INSTRUMENTATION

Because of the broad design of shock tests and the current techniques for obtaining shock spectra, instrumentation for the acquisition and reduction of shock data almost universally includes an accelerometer, suitable conditioning electronics, and a FM magnetic tape recorder. Analysis is accomplished by playback of the recorded tapes into a shock spectrum analyzer. Some analyzers require a single pulse to be replayed many times, while others essentially perform the complete analysis from a single pulse played back once (real-time analyzer). Tape speed translations (recording the data at one speed and playing them back at a different speed) can be utilized to expand the capability of the analyzer. A second method may be used whereby the shock pulse is recorded on an oscillogram or photograph and then compared with a specification pulse; however, to obtain the shock spectrum, additional work must be performed such as using an optical tracker or manually measuring the coordinates and supplying these data as input to a computer.

Many techniques for implementing shock spectrum analysis are available. The most common are simultaneous special low-pass filters, analog computers, digital computers, and mechanical analogs (reed gages, undamped galvanometers, etc.). Undamped galvanometers were selected for simplicity, completeness of analysis, ease of calibration, and relatively low initial cost (less than $2000 for special galvanometers). The idea for the basic shock spectrum analyzer was taken from a treatise by R. F. Karls [1].

A relatively undamped galvanometer has a frequency response of a linear second order mechanical system, allowing it to be used for shock spectrum analysis. A typical galvanometer adapted for such use is shown in Fig. 1.

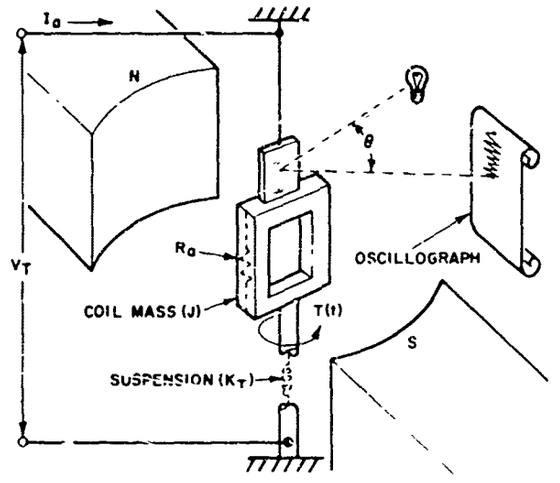


Fig. 1 - Galvanometer for detecting shock spectra

The voltage $V_T$ of the shock pulses is

$$V_T = I_a R_a . \qquad (1)$$

where $I_a$ is current in galvanometer (amp) and $R_a$ is galvanometer resistance. The instantaneous voltage $V_T(t)$ of the shock pulse as a function of time is

$$V_T(t) = I_a(t) R_a . \qquad (2)$$

The motion of the galvanometer is defined by

$$J \frac{d^2}{dt^2} + C \frac{d}{dt} + K_{TS} = T(t) \qquad (3)$$

where

J = moment of inertia of galvanometer (lb-in./sec$^2$),

C = mechanical viscous damping torque coefficient (lb-in./sec),

$K_{TS}$ = torsional spring constant of galvanometer suspension (lb-in./amp),

T = galvanometer driving torque (lb-in.), and

= coil angle of deflection (rad).

For a dc galvanometer, the driving torque T(t) is proportional to the current in the galvanometer coil [2]:

$$T(t) = K_T I_a(t) = \frac{K_T V_T(t)}{R_a} . \qquad (4)$$

where $K_T$ is the galvanometer torque constant (lb-in./amp). A velocity-dependent term, derived from the generated current $I_{EMF}$ in the galvanometer coil due to the angular velocity of the coil in the magnetic field (the back EMF), is defined by

$$\text{Velocity} = K_T I_{EMF} \frac{d}{dt} \qquad (5)$$

Combining equations yields

$$J \frac{d^2}{dt^2} + K_T I_{EMF} + C \frac{d}{dt} + K_{TS} = \frac{K_T V_T(t)}{R_a} \qquad (6)$$

The fundamental definition of shock spectra is identical to Eq. (6). A point of the shock spectrum is the peak response of a single-degree-of-freedom system excited by the pulse, as shown in Fig. 2.

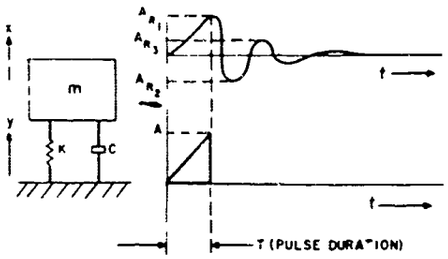


LEGEND:

A PEAK INPUT ACCELERATION

$A_{R_1}$ PEAK POSITIVE INITIAL RESPONSE ACCELERATION

$A_{R_2}$ PEAK NEGATIVE RESIDUAL RESPONSE ACCELERATION

$A_{R_3}$ PEAK POSITIVE RESIDUAL RESPONSE ACCELERATION

NOTE:

INITIAL NEGATIVE RESPONSE IS ZERO FOR SAWTOOTH SHOWN.

Fig. 2 - Shock spectra definition

The maximum shock spectra are obtained from the highest positive and the highest negative peak responses without considering the pulse time duration. Initial and residual spectrum points are obtained from their associated responses $(A_{R_1}, A_{R_2}, A_{R_3}, \ldots)$, $(f_1, f_2, f_3, \ldots)$. The equation of motion of the system shown in Fig. 2 is

$$m \frac{d^2x}{dt^2} + c \frac{dx}{dt} + kx = F(t) . \qquad (7)$$

where

$x$ = response displacement (in.),

$m$ = mass of system (lb-sec$^2$/in.),

$c$ = damping coefficient (lb-sec/in.),

$k$ = elastic spring constant, and

$F(t)$ = driving force (lb).

Equations (6) and (7) are both of the same form; therefore, Eq. (6) also describes a system that fits the definition of shock spectra.

The data acquisition system is shown in Fig 3. Data were recorded in the FM mode at 60 ips on magnetic tape. A tape synchronous signal, generated with the tape recorder, was also recorded for precision tape speed control. The data reduction system is shown in Fig. 4.

Some preliminary tests were performed in an attempt to reduce the natural frequencies of standard galvanometers by adding a shunt capacitor directly across the galvanometer coil [3]. Although significant changes in natural frequencies could be effected, the reduction in Q could not be tolerated and, therefore, this approach was abandoned. Additional tests were performed using a standard CEC Model 7-319 galvanometer with a natural frequency of 600 Hz. The lateral viscous damping was removed, and the Q was observed to have increased from 20 to 60. Six galvanometers with natural frequencies of 32, 40, 50, 400, 500, and 625 Hz and minimum Q's of 20 were obtained. The actual and desired frequency values of the six galvanometers are compared in Table 1.

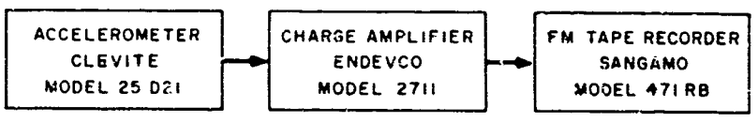


Fig. 3 - Shock data acquisition system, block diagram

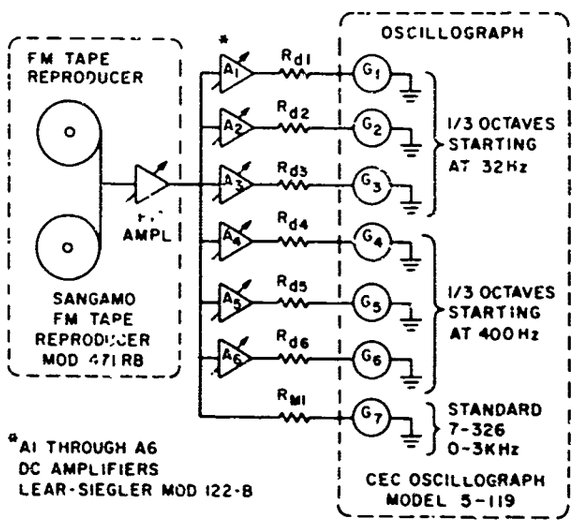


Fig. 4 - Shock data reduction system diagram

TABLE 1
Comparison of Actual and Desired
Galvanometer Frequencies

| CEC Galvanometer Model | Natural Frequency (Hz) | | Actual Q[a] |
|---|---|---|---|
| | Desired | Actual | |
| 7-351-0104 | 32 | 32 | 61 |
| 7-339-001 | 40 | 40 | 35 |
| 7-339-0103 | 50 | 50 | 41 |
| 7-343-0100 | 400 | 393 | 48 |
| 7-319-0100 | 500 | 494 | 41 |
| 7-319-0001 | 625 | 595 | 42 |

[a]With damping resistance of 1 megohm.

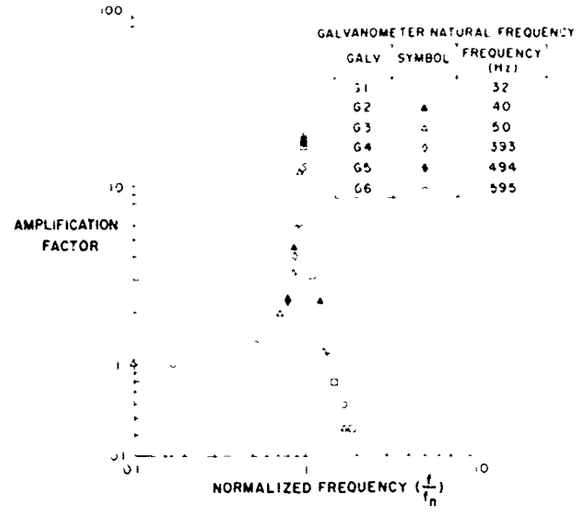


Fig. 5 - Shock galvanometer response

Magnetically damped galvanometers were chosen to permit ease of adjusting the Q's. The damping resistances ($R_{d1}$ through $R_{d6}$, Fig. 4) were T networks for changing the galvanometer Q's and normalizing the amplifiers for the different sensitivities of each galvanometer. Changing the damping resistance changes the middle term ($I_{EMF}$) of Eq. (6). All damping resistors were designed to obtain Q's of 20 (Fig. 5). Obviously, all Q's could have been raised to 35 if desired, and with a little special effort during galvanometer selection, perhaps even to 50. However, extremely high Q's may be more appealing in theory than in actual practice as even the slightest instrumentation noise (tape recorder, amplifier, etc.) may easily excite high-Q systems. This is especially noticeable when using extremes in tape speed translations (e.g., translations in excess of 8 to 1). Some preliminary investigations were made on tape speed translations up to 64 to 1 by re-recording the taped data and continuing to reduce the speed of playback (e.g., record original data at 60 ips and playback at 7-1/2 ips, re-record at 60 ips and playback at 30 ips, 15 ips, 7-1/2 ips, etc.). However, for this experiment, all data were recorded at 60 ips and played back at 60, 30, 15, and 7-1/2 ips only. The actual and desired 1/3-octave bands used for shock spectrum analysis are compared in Table 2.

After designing the damping resistance for each of the six galvanometers, a sinusoidal signal of 1 v rms and one-six the natural frequency of each galvanometer was connected individually to each of the amplifiers ($A_1$ through $A_6$) and the amplifier gain was trimmed to produce a 2-in. galvanometer trace deflection. The FM reproduce amplifier was calibrated by playing back a sinusoidal signal representing a known g level and adjusting the FM reproduce amplifier to a desired level to establish a voltage-g relationship. Galvanometer $G_7$ was also calibrated at this time for reproducing the actual pulse on the oscillograph. This galvanometer

TABLE 2
Comparison of Desired and Actual 1/3-Octave Frequencies for Analysis

| 1/3-Octave Frequency (Hz) | | | | | | | |
|---|---|---|---|---|---|---|---|
| At 60 ips | | At 30 ips | | At 15 ips | | At 7-1/2 ips | |
| Desired | Actual | Desired | Actual | Desired | Actual | Desired | Actual |
| 32 | 32 | 64 | 64 | 128 | 128 | 256 | 256 |
| 40 | 40 | 80 | 80 | 160 | 160 | 320 | 320 |
| 50 | 50 | 100 | 100 | 200 | 200 | 400 | 400 |
| 400 | 393 | 800 | 786 | 1600 | 1572 | 3200 | 3144 |
| 500 | 494 | 1000 | 988 | 2000 | 1976 | 4000 | 3952 |
| 625 | 595 | 1250 | 1190 | 2500 | 2380 | 5000 | 4760 |

was a standard CEC Model 7-326 with a frequency response from 0 to 3 kHz which permitted viewing the pulse wave shape. This galvanometer could also be used for normalizing the output and selecting the four shock spectra (initial positive, initial negative, residual positive, and residual negative).

With the oscillograph paper speed constant, and the tape speed reduced (from 60 to [illegible] ips or from 60 to 15 ips, etc.) the shock [illegible] dth from the standard galvanometer [illegible] increase. Since all of the galvanometers (shock as well as standard) will experience [illegible] ne change in time base, the shock pulse wave shape from the standard galvanometer may still be used for selecting the four shock spectra. Oscillograms made during an analysis of a terminal peak sawtooth are shown in Fig. 6. Prior to reducing actual shock data, several classical pulses [4] were created with an Exact Model 200 F waveform synthesizer and recorded on magnetic tape at 60 ips (Figs. 7 and 8). The tape was played back through the shock spectrum analyzer, and the resulting shock spectra were compared with the known calculated spectra of the classical pulses. Correlation was excellent. Because the galvanometer motion is in accordance with differential Eq. (6) that previously had been synthesized with computers or second order filters, it would be expected to produce the observed correlation.

## HALF-SINE SHOCK PULSES ON VIBRATION MACHINE

The use of electrodynamic vibration machines for shock testing has rapidly increased. The one great limitation of a vibration machine is its relatively small displacement capability. The half-sine and terminal peak sawtooth pulses are impulsive and require a net change in velocity of the test unit and a continually increasing displacement. The armature of a vibration machine cannot tolerate a net velocity change or a displacement change that is different from the equilibrium position of the armature. The above requirement dictates that the acceleration of the armature must vary about zero g so that the net area under the acceleration curve is zero.

The half-sine pulses and their spectra as obtained from a vibration machine are shown in Figs. 9, 10, and 11. The waveform shown in Fig. 11 is obviously far from the ideal and in fact it is possible to obtain shaker pulses which

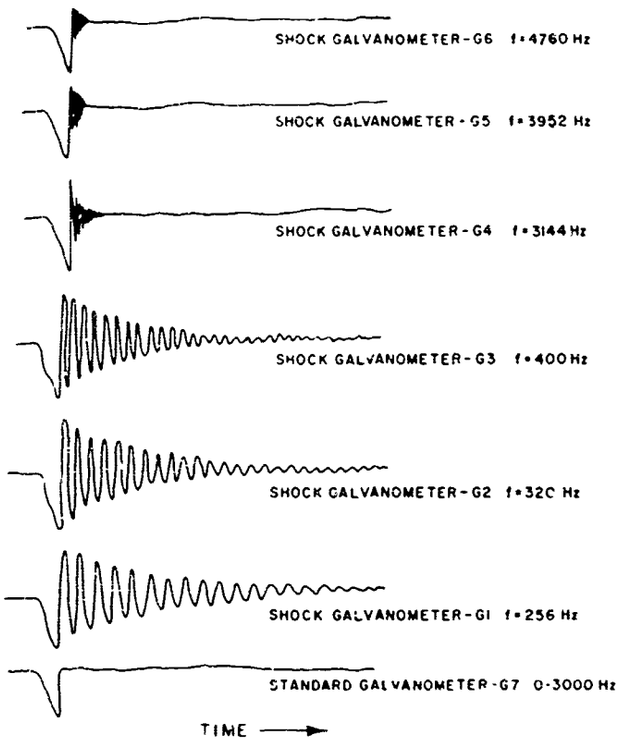


Fig. 6 - Shock spectrum oscillogram from tape played back at 7-1/2 ips

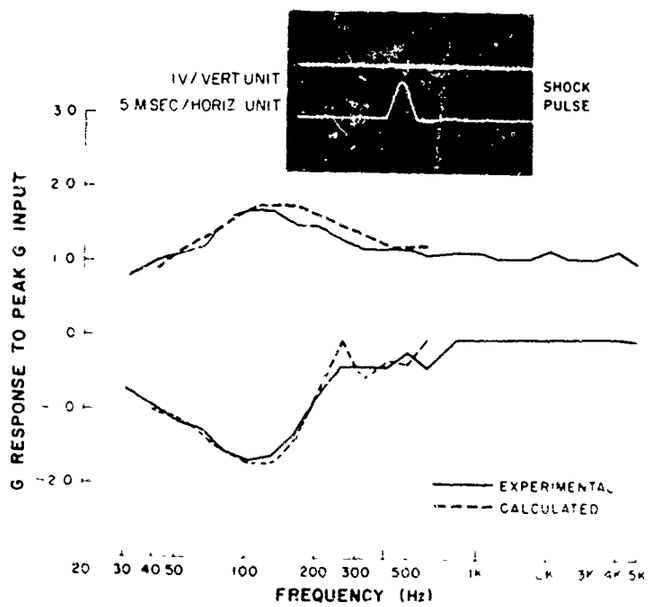


Fig. 7 - Shock spectrum for synthesized half-sine shaker shock pulse

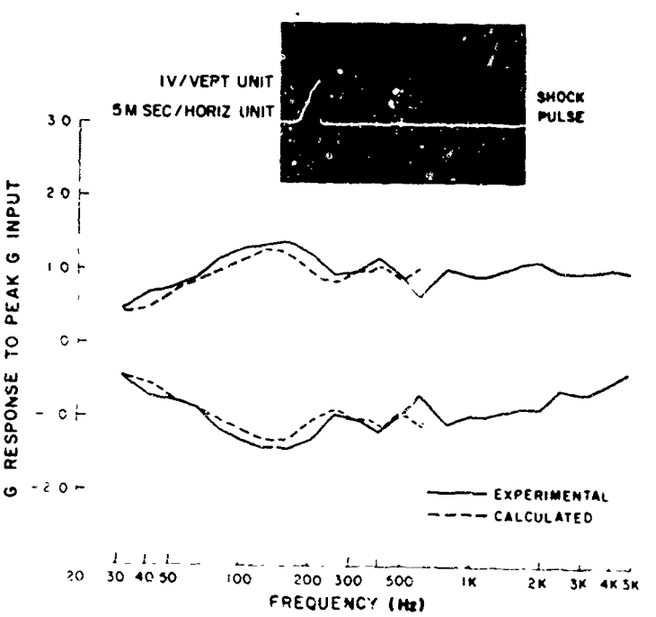


Fig. 8 - Shock spectrum for synthesized terminal peak sawtooth shaker shock pulse

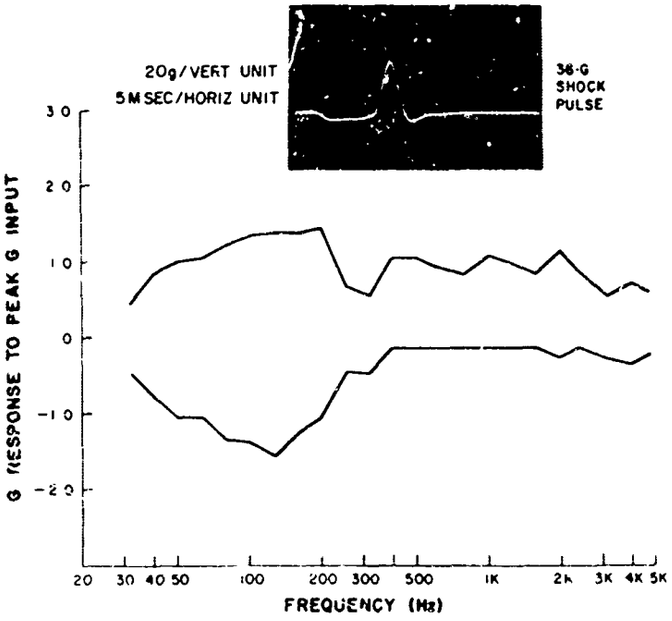


Fig. 9 - Shock spectrum for 36-g half-sine shaker shock pulse

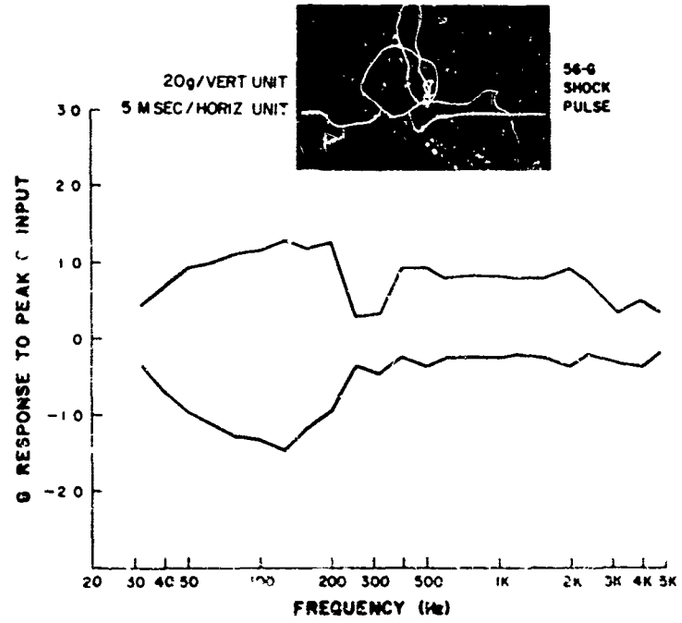


Fig. 10 - Shock spectrum for 56-g half-sine shaker shock pulse

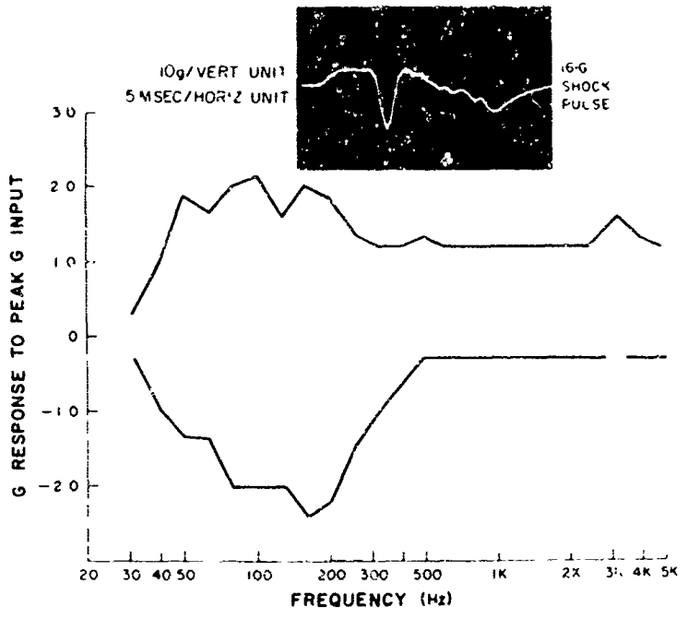


Fig. 11 - Shock spectrum for 16-g half-sine shaker shock pulse

are much more representative of the classical form shown in Figs. 7 and 8. Notice that there are significant accelerations on both sides of the zero g line in the trace shown in Fig. 11. It is the intent of the test engineer and the mechanics of the vibration machine to produce an acceleration-time history that has equal areas above and below the zero-g line. If these conditions are met, the armature of the machine will have zero initial and zero final conditions of both velocity and displacement. If the armature of the machine is not constrained as described above, it will impact with the stator. In comparing the spectra shown in Fig. 11 to the "intent spectra" shown in Fig. 7, the obvious difference is in the magnitude of the spectra. The actual pulse has an associated spectra of a higher magnitude in the region where the duration of the pulse corresponds to one-half the period of the frequency.

The spectra shown in Figs. 9 and 10 are good half-sine representations. The spectra also conform closely to the classical, with the exception of the notch that is demonstrated at 300 Hz. Without a spectral analysis, the spectral characteristics of these two pulses would have been assumed to be classical, and the existence of the 300-Hz notch would have remained undiscovered. Differences with respect to frequency are the result of slight variations in time duration of the pulses under consideration (the spectra plots are not normalized along the abscissa).

## GENERATION OF TERMINAL PEAK SAWTOOTH

The ideal terminal peak sawtooth has the associated spectra shown in Fig. 8. The pulse excites medium and high frequencies both positive and negative to the amplitude of the input. A practical sawtooth exhibits a somewhat attenuated spectrum at very high frequency due to the time duration required for the trailing edge of the pulse. The more triangular the pulse becomes, the less negative is the high-frequency spectral content [4].

Practical terminal peak sawtooth shock pulses present some difficulties generally not encountered with half-sine waveforms. The fixture and test machine are often excited by the test pulse. Both are limited to comparatively finite natural frequencies. A design dilemma is introduced involving the natural frequencies of the test system and the trailing edge of the sawtooth. If the test engineer strives for a classical shape (minimum time duration of the trailing edge), the fixture and the machine are more likely to respond to the pulse. As items of test become larger and larger the predominate test system natural frequencies will tend toward lower and lower values The point is soon reached where the sawtooth pulse cannot remain within specification because it either excessively "rings" the test system or becomes so shaped that it no longer resembles a terminal peak sawtooth. Therefore, many practical

terminal peak sawtooth pulses exhibit much "ringing" or "noise" after the pulse has been applied to the test item. Figure 4 shows this condition. Since ringing is on the input to the test item, it becomes a part of the test shock pulse.

The spectra of terminal peak sawtooth ringing pulses are shown in Figs. 12, 13, and 14. The effect of the ringing is displayed around the 2500-Hz point of the plot. This particular pulse was applied to a shaker slip plate by the shaker armature. The slip plate was "butted" to the

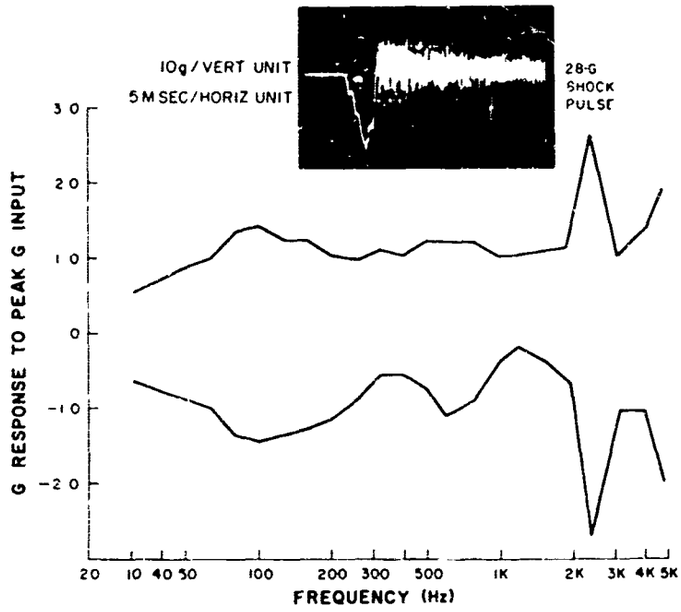


Fig. 12 - Shock spectrum for 28-g sawtooth shaker shock pulse

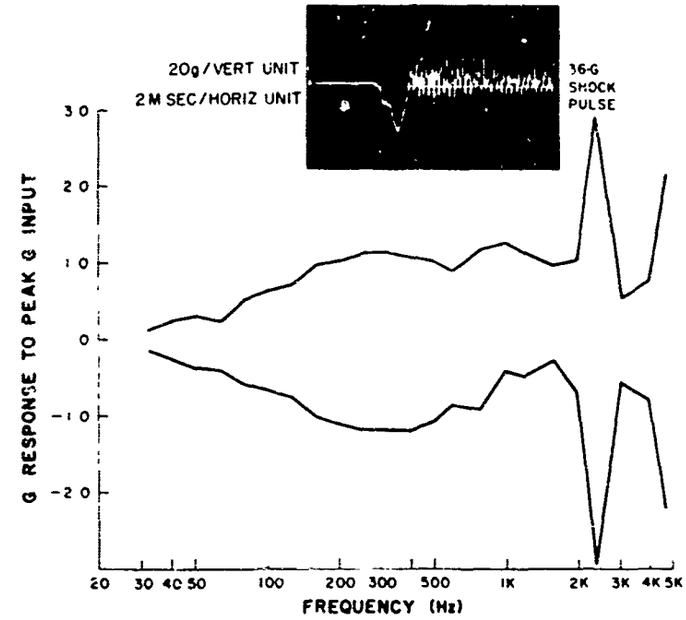


Fig. 13 - Shock spectrum for 36-g sawtooth shaker shock pulse

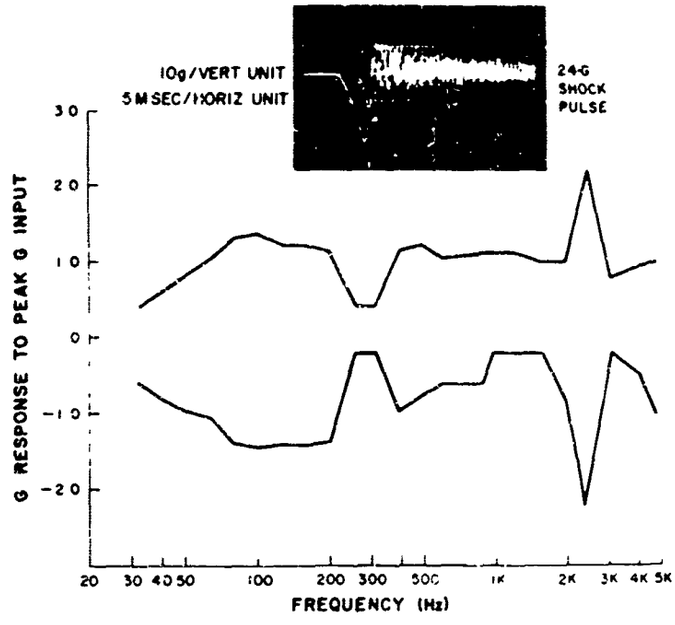


Fig. 14 - Shock spectrum for 24-g sawtooth shaker shock pulse

armature so that after driving the plate to the peak displacement, the plate disconnects and slides free. The slip plate natural frequency is 2490 Hz (see Appendix). Any test unit mounted to the slip plate will have as a shock input the oscillating component of the fixture natural frequency along with the intended pulse.

## FACILITY MALFUNCTION

Vibration systems, in general, have devices which protect the system from malfunctions and violent breakdowns. The system protection device is generally a dynamic braking device operating on the armature of the vibration exciter. "Amplitude protector" or "armature clamping" are terms used by the system manufacturers to describe the function of these devices. The reality of the operation of a protection device is a violent acceleration shock pulse that brakes or prevents the exciter armature from driving into the fixed or stator portion of the machine. During a vibration or shock test, if a malfunction arises, this braking or "blast" pulse is experienced by the test item. Techniques to determine what deleterious effect this pulse might have on a test item have previously been limited to discussions of the peak acceleration level. Frequency information either was not available or was so limited that it was useless.

A shock spectrum of the pulse would provide the information necessary to determine whether reliability has been compromised. The spectrum of a half-sine shock pulse and the operation of an exciter armature protector are shown in Figs. 15 and 16. The malfunction had little contribution to the overall spectrum of the intended pulse as shown in Fig. 15. The presence of high-frequency energy excited by the protection device is demonstrated by the spectrum shown in Fig. 16. With acceleration and frequency information available from the spectra of the transient, known frequency characteristics of the test item can be reviewed to determine if a significant response was probable.

## FUTURE CONSIDERATIONS

Waveform shock testing with an electrodynamic vibration machine is very limited in its application. Shock tests which require (or should require) no net change in velocity of the test item are well within the capabilities of a vibration machine. On-line shock spectrum analysis of an extremely fast sweeping sine acceleration waveform of an equalized exciter is a good approach [5]. One manufacturer has already marketed a shaker shock equalization system. A need still exists for rapid shock spectrum analysis. In this respect, the galvanometer

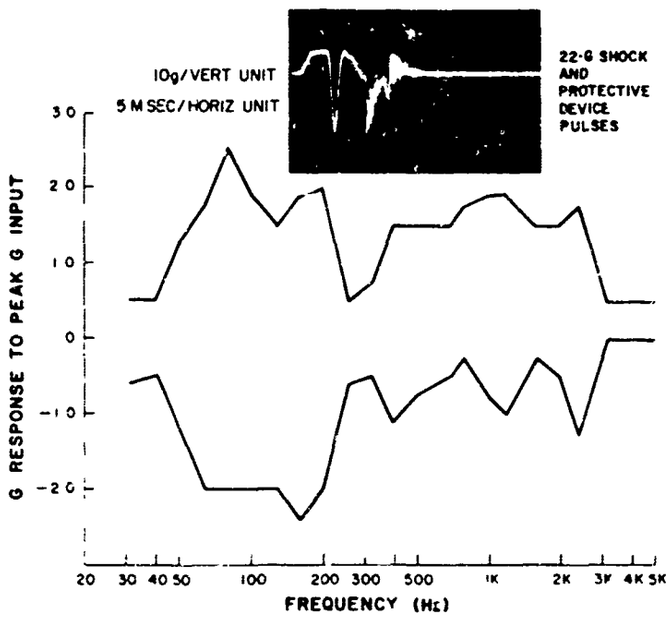


Fig. 15 - Shock spectrum for 22-g half-sine shaker shock pulse and protective device pulse

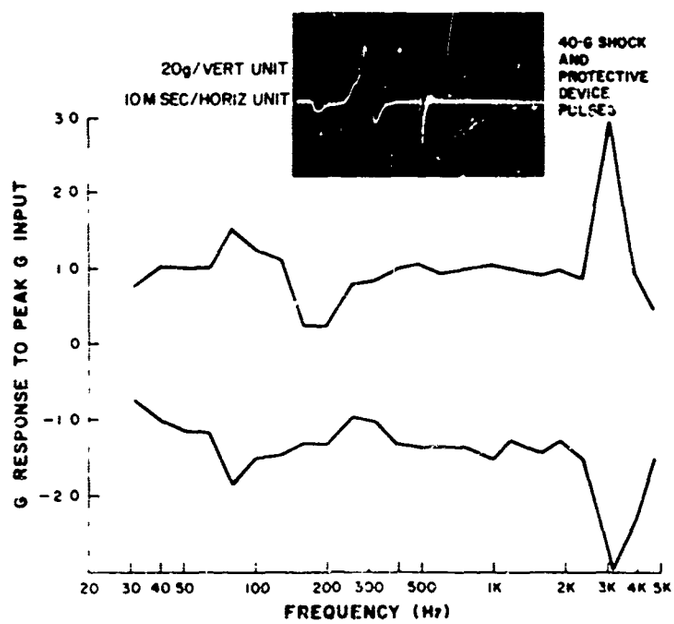


Fig. 16 - Shock spectrum for 40-g half-sine shaker shock pulse and protective device pulse

system warrants further development to eliminate the need for tape speed translations and the time-consuming task of reading the oscillograms and hand plotting the shock spectra. The need for tape speed translations would be eliminated if galvanometers of higher resonant frequencies were available, thus permitting the analyzer to be operated on a real-time basis. Hand plotting might be eliminated by an application of light-sensitive potentiometers with electronics to sense and hold the maximum excursions of each galvanometer. These outputs might be commutated and plotted directly in terms of shock spectra. The presently available simple, inexpensive laboratory shock spectrum analyzers (one of which is the galvanometer system) will do much to advance the state of the art of shock testing.

## CONCLUSION

The advent of inexpensive shock spectrum analysis should do much in furthering shock test standardization. Comparisons of spectra of test pulses with the theoretical specified pulse spectrum will give more information on the test deviation from the implied intent of the specification pulse spectrum. In general, supposedly similar pulses (within specification tolerances) exhibit wide spectral variations.

Half-sine shock testing with an electrodynamic vibration machine can be made to match the spectrum of the ideal half-sine pulse. This would require a compromised half-sine waveform of a level less than that of the specified pulse.

A good terminal peak sawtooth test shock pulse will invariably excite the fixture and test machine resonance. The spectrum of the practical sawtooth pulse will exhibit high levels at fixture and test machine resonant frequencies. The spectra, therefore, will be highly dependent on the fixture design and the characteristics of the test machine. The best approach to shock testing with an electrodynamic vibration machine is the sweeping sine wave input. The exciter can be equalized to account for fixture and machine resonances. The pulse requires no net velocity or displacement and essentially tests both attitudes of a direction [5].

## REFERENCES


1. R. F. Karls, "Shock Spectrum Analyzer for General Laboratory Use," IES Proc., p. 449, 1966
2. Del Toro and Parker, Control Systems Engineering, p. 215, McGraw-Hill, New York, 1960
3. H. S. Black, "Use of Shunt Condensers to Reduce the Effective Natural Frequency of Galvanometers," Consolidated Electrodynamics Corp., File 7-200-008, June 15, 1953
4. E. H. Schell, "Spectral Characteristics of Some Practical Variations in the Half-Sine and Saw-Tooth Pulses," Shock and Vibration Bull. No. 34, Part 3, pp. 223-251, Dec. 1964
5. G. A. Gallagher and A. W. Adkins, "Shock Testing a Spacecraft to Shock Response Spectrum by Means of an Electrodynamic Exciter," Shock and Vibration Bull. No. 35, Part 6, pp. 41-45, April 1966


## Appendix

## NATURAL FREQUENCIES OF SLIP PLATES

For a free-free end condition, the natural frequency $f_n$ of the slip plate is defined by:

$$f_n = \frac{1}{2\pi} \sqrt{\frac{E g}{\rho}}$$

where

$\ell$ = length of plate,

$E$ = modulus of elasticity,

$\rho$ = density, and

$g$ = acceleration of gravity.

For an aluminum plate with a length of 39.5 in. $E = 10 \times 10^6$ psi, $\rho = 0.1$ pci, and acceleration of 386 in. $sec^{-2}$, the natural frequency would be 2490 Hz.

## DISCUSSION

Mr. Rommel (Lockheed-California Co.): I want to congratulate you on your shock spectrum analyzer. I think it tends to answer the question that Mr. Schell brought up yesterday concerning the length of time it takes to perform a shock spectrum analysis after a test. The utilization of a standard galvanometer system to perform shock spectrum analysis should allow the analysis to be conducted almost as quickly as the shock test can be performed. How do you control the frequency on the galvanometers? Do you use a standard galvanometer frequency system?

Mr. Baran: I started to trim the frequencies by adding shunt capacity. This technique works all right but it lowers the Q so radically that it really cannot be used. One of the basic limitations is that galvanometers must be selected that have the different natural frequencies without adding shunt capacity; it is a "cut and try" method.

Mr. Rommel: My other question is in regard to the induced noise due to time scaling data with the tape speed playback.

Mr. Baran: That is a legitimate question. I ran a series of studies on time scaling or tape speed translation, and I completely obliterated the data at tape speed translations of 64 to 1. However, this is getting ridiculous because it would spread the spectrum out where you would never begin to use it. At tape speed translations of 4 to 1 or 8 to 1, there is not yet a severe problem.

* * *

# TRANSDUCER SHOCK STUDY

Arthur D. Carlson and Robert J. McGrattan
General Dynamics
Electric Boat Division
Groton, Connecticut

A sonar transducer was analyzed to determine the stresses induced in the ceramic drive element by an underwater explosion. Two explosive forces were considered: a hydraulic shock along the axis of the transducer, and a mechanical shock normal to this axis.

It was determined from the analysis that the peak stresses caused by these two loadings occur in different time periods and, therefore, the two types of shock motion are essentially independent of each other. Further analysis revealed that hydraulic shock is more damaging to the ceramic element than mechanical shock for a given standoff. The results of the analysis compared favorably with previously conducted experiments.

A parametric study was conducted to improve the transducer's resistance to both hydraulic and mechanical shock. The study showed that a significant increase in shock resistance is possible by minor redesign of the transducer.

R. J. McGrattan

## INTRODUCTION

A sonar transducer attached to a ship or platform subjected to an underwater explosion is affected by two types of shock: hydraulic shock on the face of the transducer head, and mechanical shock caused by movement of the ship or platform. This paper describes the analysis of a typical transducer and the modifications necessary to improve the transducer shock resistance. The data from this analysis and that from a previously conducted experiment for shock failure compared favorably at given standoffs.

For the mathematical model, the hydraulic shock was assumed to be in the direction of maximum input, i.e., along the longitudinal axis of the transducer, as shown in Fig. 1. The mechanical shock input was assumed to be in the direction of the transducer support brackets (staves), i.e., perpendicular to the longitudinal axis.

This paper describes the approach to the analysis, the results and the conclusions. The separate effects of the hydraulic and mechanical shocks are discussed quantitatively. The combined effect is discussed qualitatively. The details of the analysis, omitted from this paper for brevity, are contained in the original reports [1,2].

## NOMENCLATURE

- M Mass (lb-sec$^2$/in.)
- K Spring constant (lb/in.)
- Y Displacement (in.)
- C Damping (lb-sec/in.)
- E Modulus of elasticity (psi)
- L Length (in.)

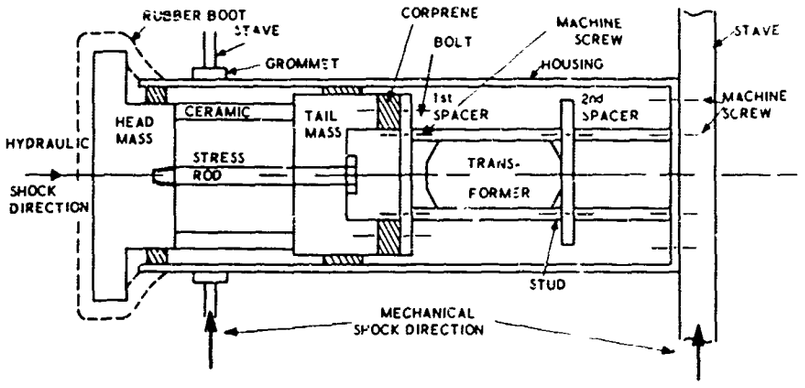


Fig. 1 - Typical transducer

A Cross-sectional area (sq in.)

F Load (lb)

P Pressure (lb/in.)

$P_o$ Maximum pressure

Mass density of sea water (lb/cu in./in./sec$^2$)

H Speed of sound in sea water (ips)

t Time (msec)

Time constant (msec)

Stress (psi)

$[\Psi]$ Reoriented eigenvectors

$\{q\}$ Generalized coordinates

$\bar{M}$ Generalized mass

Participation factor

R Response function

Dummy variable of integration

Ramp time (msec)

$V_o$ Peak velocity (ips)

$K_v$ Shear stress constant with respect to v loading (along vertical axis)

$K_w$ Shear stress constant with respect to w loading (transverse axis)

$I_w$ Moment of inertia about w-axis of cross section (transverse axis) (in.$^4$)

Moment of inertia about v-axis of cross section (vertical axis) (in.$^4$)

J Torsion constant (in.$^4$)

$\ddot{y}$ Acceleration (in./sec$^2$)

y Displacement (in.)

$\{D\}$ Directivity vector

$\{\Lambda\}$ Maximum displacement vector

Frequency (rad/sec)

Flexibility matrix (in./lb)

$\{\omega\}$ Displacement vector

Unoriented eigenvectors

Subscripts

1 2 3 4 5 6 On K denotes particular springs

1 2 3 4 On M denotes particular mass

E On K denotes elastic range

P On K denotes plastic range

Vector

Square matrix

Diagonal frequency matrix

terminal peak sawtooth pulses exhibit much "ringing" or "noise" after the pulse has been applied to the test item. Figure 4 shows this condition. Since ringing is on the input to the test item, it becomes a part of the test shock pulse.

The spectra of terminal peak sawtooth ringing pulses are shown in Figs. 12, 13, and 14. The effect of the ringing is displayed around the 2500-Hz point of the plot. This particular pulse was applied to a shaker slip plate by the shaker armature. The slip plate was "butted" to the

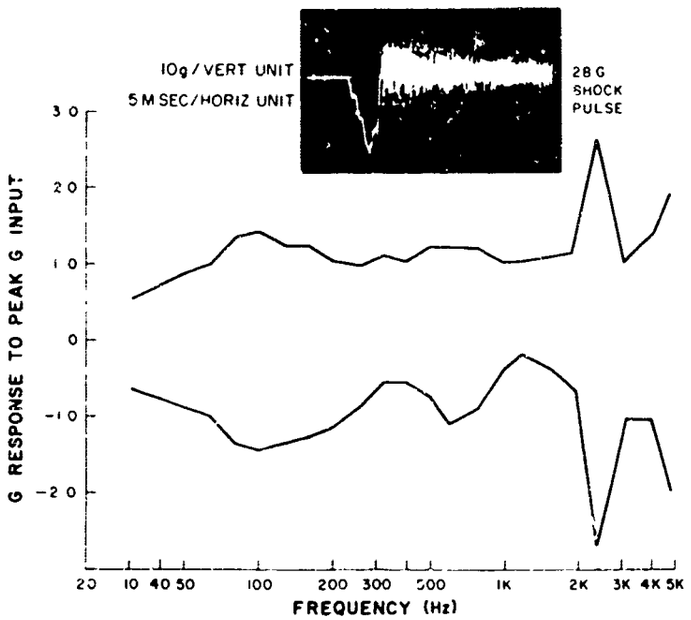


Fig. 12 - Shock spectrum for 28-g sawtooth shaker shock pulse

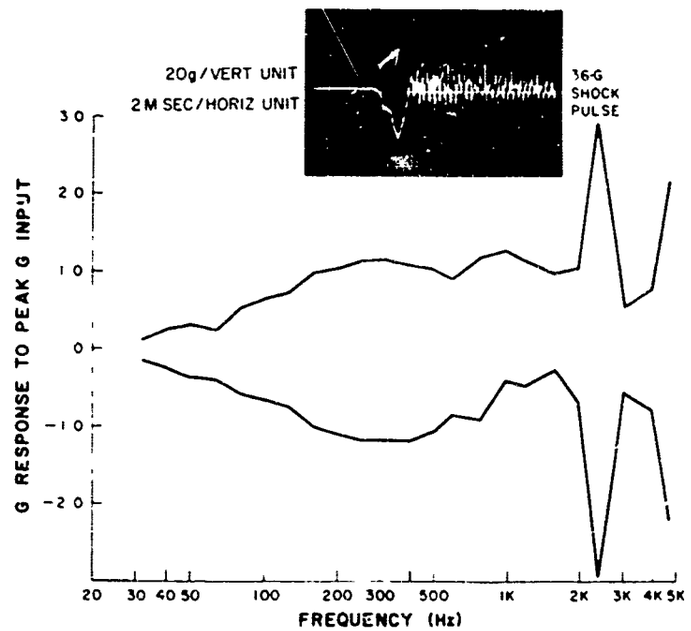


Fig. 13 - Shock spectrum for 36-g sawtooth shaker shock pulse

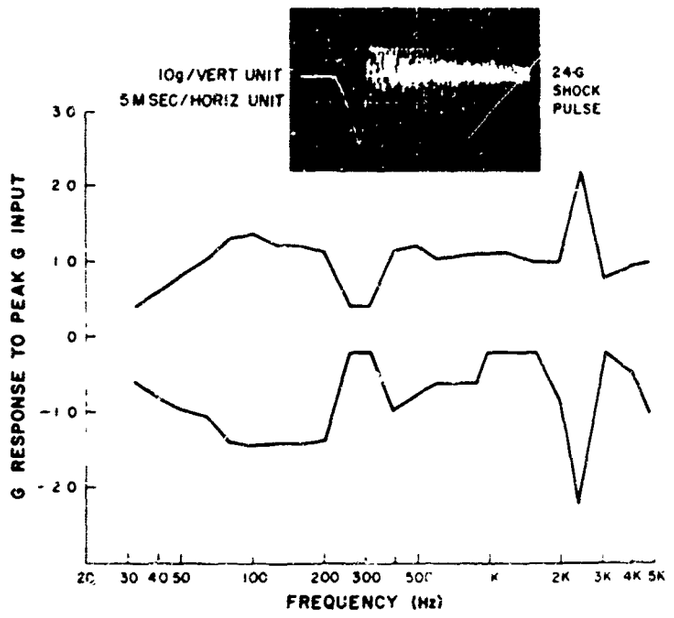


Fig. 14 - Shock spectrum for 24-g sawtooth shaker shock pulse

armature so that after driving the plate to the peak displacement, the plate disconnects and slides free. The slip plate natural frequency is 2490 Hz (see Appendix). Any test unit mounted to the slip plate will have as a shock input the oscillating component of the fixture natural frequency along with the intended pulse.

## FACILITY MALFUNCTION

Vibration systems, in general, have devices which protect the system from malfunctions and violent breakdowns. The system protection device is generally a dynamic braking device operating on the armature of the vibration exciter. "Amplitude protector" or "armature clamping" are terms used by the system manufacturers to describe the function of these devices. The reality of the operation of a protection device is a violent acceleration shock pulse that brakes or prevents the exciter armature from driving into the fixed or stator portion of the machine. During a vibration or shock test, if a malfunction arises, this braking or "blast" pulse is experienced by the test item. Techniques to determine what deleterious effect this pulse might have on a test item have previously been limited to discussions of the peak acceleration level. Frequency information either was not available or was so limited that it was useless.

A shock spectrum of the pulse would provide the information necessary to determine whether reliability has been compromised. The spectrum of a half-sine shock pulse and the operation of an exciter armature protector are shown in Figs. 15 and 16. The malfunction had little contribution to the overall spectrum of the intended pulse as shown in Fig. 15. The presence of high-frequency energy excited by the protection device is demonstrated by the spectrum shown in Fig. 16. With acceleration and frequency information available from the spectra of the transient, known frequency characteristics of the test item can be reviewed to determine if a significant response was probable.

## FUTURE CONSIDERATIONS

Waveform shock testing with an electrodynamic vibration machine is very limited in its application. Shock tests which require (or should require) no net change in velocity of the test item are well witnin the capabilities of a vibration machine. On-line shock spectrum analysis of an extremely fast sweeping sine acceleration waveform of an equalized exciter is a good approach [5]. One manufacturer has already marketed a shaker shock equalization system. A need still exists for rapid shock spectrum analysis. In this respect, the galvanometer

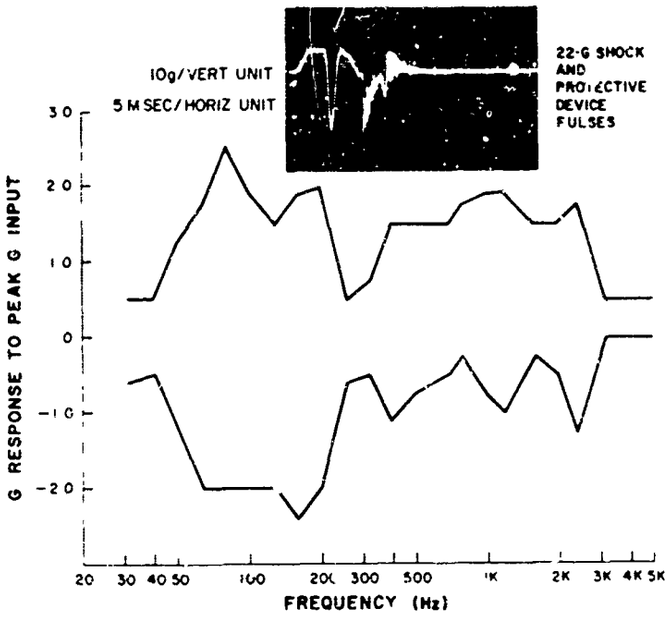


Fig. 15 - Shock spectrum for 22-g half-sine shaker shock pulse and protective device pulse

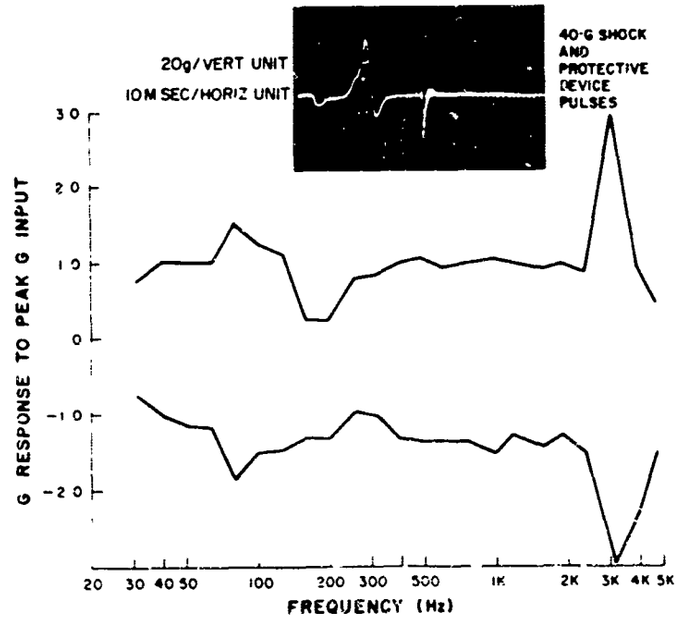


Fig. 16 - Shock spectrum for 40-g half-sine shaker shock pulse and protective device pulse

system warrants further development to eliminate the need for tape speed translations and the time-consuming task of reading the oscillograms and hand plotting the shock spectra. The need for tape speed translations would be eliminated if galvanometers of higher resonant frequencies were available, thus permitting the analyzer to be operated on a real-time basis. Hand plotting might be eliminated by an application of light-sensitive potentiometers with electronics to sense and hold the maximum excursions of each galvanometer. These outputs might be commutated and plotted directly in terms of shock spectra. The presently available simple, inexpensive laboratory shock spectrum analyzers (one of which is the galvanometer system) will do much to advance the state of the art of shock testing.

## CONCLUSION

The advent of inexpensive shock spectrum analysis should do much in furthering shock test standardization. Comparisons of spectra of test pulses with the theoretical specified pulse spectrum will give more information on the test deviation from the implied intent of the specification pulse spectrum. In general, supposedly similar pulses (within specification tolerances) exhibit wide spectral variations.

Half-sine shock testing with an electrodynamic vibration machine can be made to match the spectrum of the ideal half-sine pulse. This would require a compromised half-sine waveform of a level less than that of the specified pulse.

A good terminal peak sawtooth test shock pulse will invariably excite the fixture and test machine resonance. The spectrum of the practical sawtooth pulse will exhibit high levels at fixture and test machine resonant frequencies. The spectra, therefore, will be highly dependent on the fixture design and the characteristics of the test machine The best approach to shock testing with an electrodynamic vibration machine is the sweeping sine wave input. The exciter can be equalized to account for fixture and machine resonances. The pulse requires no net velocity or displacement and essentially tests both attitudes of a direction [5].

## REFERENCES


1. R. F. Karls, "Shock Spectrum Analyzer for General Laboratory Use," IES Proc., p. 449, 1966
2. Del Toro and Parker, Control Systems Engineering, p. 215, McGraw-Hill, New York, 1960
3. H. S. Black, "Use of Shunt Condensers to Reduce the Effective Natural Frequency of Galvanometers," Consolidated Electrodynamics Corp., File 7-200-008, June 15, 1953
4. E. H. Schell, "Spectral Characteristics of Some Practical Variations in the Half-Sine and Saw-Tooth Pulses," Shock and Vibration Bull. No. 34, Part 3, pp. 223-251, Dec. 1964
5. G. A. Gallagher and A. W. Adkins, "Shock Testing a Spacecraft to Shock Response Spectrum by Means of an Electrodynamic Exciter," Shock and Vibration Bull. No. 35, Part 6, pp. 41-45, April 1966


## Appendix

## NATURAL FREQUENCIES OF SLIP PLATES

For a free-free end condition, the natural frequency $f_n$ of the slip plate is defined by:

$$f_n = \frac{1}{2\ell}\sqrt{\frac{Eg}{\rho}},$$

where

$\ell$ = length of plate,

$E$ = modulus of elasticity,

$\rho$ = density, and

$g$ = acceleration of gravity.

For an aluminum plate with a length of 39.5 in. $E = 10 \times 10^6$ psi, $\rho = 0.1$ pci, and acceleration of 386 in./sec$^2$, the natural frequency would be 2490 Hz.

Mr. Rommel (Lockheed-California Co.): I want to congratulate you on your shock spectrum analyzer. I think it tends to answer the question that Mr. Schell brought up yesterday concerning the length of time it takes to perform a shock spectrum analysis after a test. The utilization of a standard galvanometer system to perform shock spectrum analysis should allow the analysis to be conducted almost as quickly as the shock test can be performed. How do you control the frequency on the galvanometers? Do you use a standard galvanometer frequency system?

Mr. Baran: I started to trim the frequencies by adding shunt capacity. This technique works all right but it lowers the Q so radically that it really cannot be used. One of the basic limitations is that galvanometers must be selected that have the different natural frequencies without adding shunt capacity; it is a "cut and try" method.

Mr. Rommel: My other question is in regard to the induced noise due to time scaling data with the tape speed playback.

Mr. Baran: That is a legitimate question. I ran a series of studies on time scaling or tape speed translation, and I completely obliterated the data at tape speed translations of 64 to 1. However, this is getting ridiculous because it would spread the spectrum out where you would never begin to use it. At tape speed translations of 4 to 1 or 8 to 1, there is not yet a severe problem.

* * *

# TRANSDUCER SHOCK STUDY

Arthur D. Carlson and Robert J. McGrattan
General Dynamics
Electric Boat Division
Groton, Connecticut

A sonar transducer was analyzed to determine the stresses induced in the ceramic drive element by an underwater explosion. Two explosive forces were considered: a hydraulic shock along the axis of the transducer, and a mechanical shock normal to this axis.

It was determined from the analysis that the peak stresses caused by these two loadings occur in different time periods and, therefore, the two types of shock motion are essentially independent of each other. Further analysis revealed that hydraulic shock is more damaging to the ceramic element than mechanical shock for a given standoff. The results of the analysis compared favorably with previously conducted experiments.

A parametric study was conducted to improve the transducer's resistance to both hydraulic and mechanical shock. The study showed that a significant increase in shock resistance is possible by minor redesign of the transducer.

R. J. McGrattan

## INTRODUCTION

A sonar transducer attached to a ship or platform subjected to an underwater explosion is affected by two types of shock: hydraulic shock on the face of the transducer head, and mechanical shock caused by movement of the ship or platform. This paper describes the analysis of a typical transducer and the modifications necessary to improve the transducer shock resistance. The data from this analysis and that from a previously conducted experiment for shock failure compared favorably at given standoffs.

For the mathematical model, the hydraulic shock was assumed to be in the direction of maximum input, i.e., along the longitudinal axis of the transducer, as shown in Fig. 1. The mechanical shock input was assumed to be in the direction of the transducer support brackets (staves), i.e., perpendicular to the longitudinal axis.

This paper describes the approach to the analysis, the results and the conclusions. The separate effects of the hydraulic and mechanical shocks are discussed quantitatively. The combined effect is discussed qualitatively. The details of the analysis, omitted from this paper for brevity, are contained in the original reports [1,2].

## NOMENCLATURE

- M Mass (lb-sec$^2$/in.)
- K Spring constant (lb/in.)
- X Displacement (in.)
- C Damping (lb-sec/in.)
- E Modulus of elasticity (psi)
- L Length (in.)

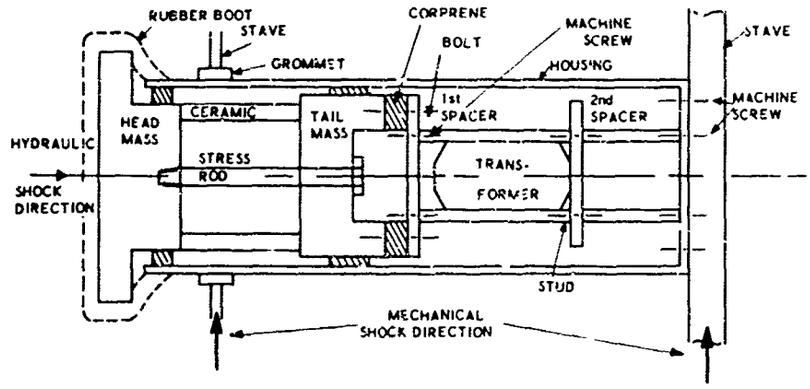


Fig. 1 - Typical transducer

A Cross-sectional area (sq in.)

F Load (lb)

P Pressure (lb/in.)

$P_o$ Maximum pressure

$\rho$ Mass density of sea water (lb/cu in. / in./sec$^2$)

H Speed of sound in sea water (ips)

t Time (msec)

$\tau$ Time constant (msec)

$\sigma$ Stress (psi)

$\{\Psi\}$ Reoriented eigenvectors

$\{q\}$ Generalized coordinates

$\bar{M}$ Generalized mass

$\Gamma_r$ Participation factor

R Response function

$\lambda$ Dummy variable of integration

$t_r$ Ramp time (msec)

$V_o$ Peak velocity (ips)

$K_v$ Shear stress constant with respect to v loading (along vertical axis)

$K_u$ Shear stress constant with respect to u loading (transverse axis)

$I_u$ Moment of inertia about u-axis of cross section (transverse axis) (in.$^4$)

$I_v$ Moment of inertia about v-axis of cross section (vertical axis) (in.$^4$)

J Torsion constant (in.$^4$)

$\ddot{y}$ Acceleration (in./sec$^2$)

y Displacement (in.)

$\{D\}$ Directivity vector

$\{Y\}$ Maximum displacement vector

$\omega$ Frequency (rad/sec)

$[f_{ij}]$ Flexibility matrix (in./lb)

$\{u\}$ Displacement vector

$[\phi]$ Unoriented eigenvectors

Subscripts

1, 2, 3, 4, 5, 6 On K denotes particular springs

1, 2, 3, 4 On M denotes particular mass

E On K denotes elastic range

P On K denotes plastic range

$\{\ \}$ Vector

$[\ ]$ Square matrix

$[\omega_j^2]$ Diagonal frequency matrix

## HYDRAULIC SHOCK

### Problem Approach

A mathematical model was developed that described the motion of the transducer system. Using this model, the equations of motion were written. An analog computer was used to solve these equations because several of the springs in the model were nonlinear and it was desired to vary several of the system parameters. Nonlinear spring elements were not used for the hydraulic shock optimization part of the analysis because plastic deformation of the transducer elements is not desirable. Different spring constants and spring combinations were tried until a significant stress reduction in the ceramic element was made. Only those springs that did not affect the acoustic characteristics were changed. The hydraulic shock input considered both the head mass face velocity and the shock load area reduction. To find the stress level in any component, the elongation of the component was multiplied by its spring constant to give the force from which the axial stress was found.

### Model

Using the transducer shown in Fig. 1 as a reference, the model shown in Fig. 2 was developed.

For any mathematical model, the number and magnitude of the masses are dependent on the mass distribution of the system and the desired accuracy. A mass point is usually located in the model at a corresponding mass concentration in the real system. Therefore, this transducer system was approximated with four masses. Mass $M_1$ represented the head mass, its rubber boot, and part of the stress rod and ceramic. Mass $M_2$ represented the tail mass and part of the stress rod and ceramic element. The next major mass concentration was located in the transformer area. Accordingly, mass $M_3$ represented the transformer and the adjacent spacer and disc assembly. Because the housing was essentially independent of the internal components of the transducer, it was also considered as a model mass point $M_4$. The electrical cables were included in this mass.

When the mass points had been determined, it was necessary to find the type and stiffness of the springs connecting them. The transducer contained all of the three types most often found in mechanical systems: linear, softening, and hardening springs. The materials of these springs were ceramic, metal, and a cork-rubber compound (corprene), respectively. The unit measure for stiffness was pounds per inch.

The ceramic element was considered linear because it was a brittle material and, for all practical purposes, its elastic limit, yield point, and ultimate strength coincided. The metal elements were described as softening because as the yield point was passed, and the metal went from the elastic into the plastic zone, the stiffness in each range was considered linear. It was assumed that the plastic spring constant could be reasonably approximated as being equal to 1/20 of the elastic spring constant. The corprene was a nonlinear hardening spring. It hardened at such a rate that it could be approximated with two linear curves. Table 1 shows the transducer elements represented by springs $K_1$ through $K_6$.

It should be noted that $K_6$ only became effective after the 90-mil clearance was reduced to zero (Fig. 2). As an example, the model for determining spring $K_3$ is shown in Fig. 3.

The disc was effective in compression and the spacer assembly in tension because of several sliding connections and the very large difference in stiffness between the corprene disc and the spacer assembly. The spring constant

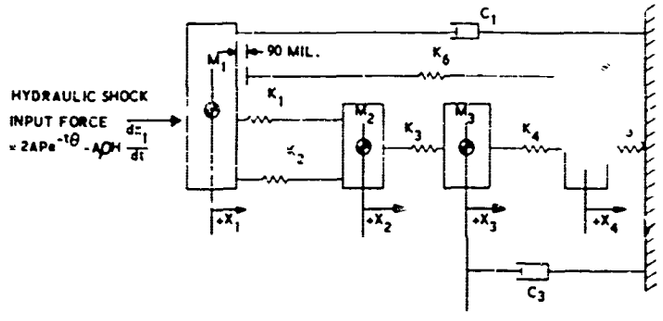


Fig. 2 - Mathematical model--hydraulic shock

TABLE 1
Transducer Spring–Hydraulic Shock Model

| | |
|---|---|
| $K_1$ | Stress rod |
| $K_2$ | Ceramic |
| $K_3$ | Corprene disc and first spacer assembly |
| $K_4$ | Second spacer assembly |
| $K_5$ | Stave (mounting bracket for transducer) |
| $K_6$ | Transducer housing |

of the corprene disc was found experimentally by loading it and measuring the deflection under each load increment. The resultant load-deflection curve was approximated as a bilinear hardening spring. The spacer assembly was modeled as a series of spring elements made up of springs $K_B$, $K_{SC}$, $K_{SP}$, and $K_{ST}$. These values were found analytically. This equivalent series spring was extended into the plastic region by assuming the force deflection curve was 1/20 of the value in the elastic range. This value was based on the stress-strain properties of the spacer assembly material. The force deflection curve for $K_3$ is shown in Fig. 4a. The spring constant curves for the shock optimization analysis were made linear. In general, the range was between 10 times stiffer and 10 times softer than the original spring values. Springs $K_3$, $K_4$, and $K_5$ were the only parameters changed because the other springs, particularly $K_1$ and $K_2$, could seriously affect the acoustic characteristics of the transducer. The only major change in a spring design was the replacement of the soft corprene disc by a much stiffer nonmetallic disc. The other spring changes were simple increases or decreases in stiffness that could be accomplished with stock material and size changes. Figures 4, 5, and 6 show the original values and the range of the new spring configurations considered.

The major damping of this system was considered to occur on the head mass. Although each component in the transducer provided some damping, it was assumed that most of the damping was provided by the rubber boot which covered the head mass and connected to the housing and the water which surrounded the

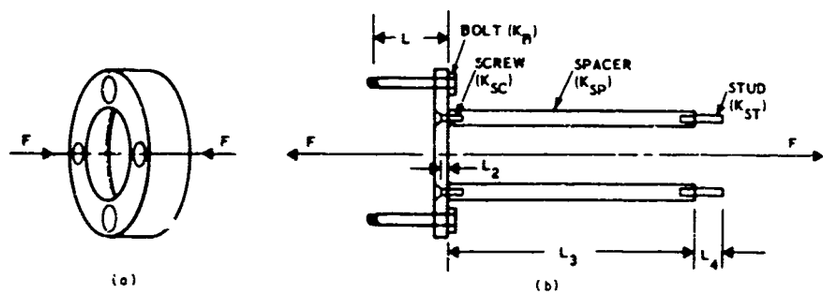


Fig. 3 - (a) Corprene disc, and (b) first mechanical spacer assembly

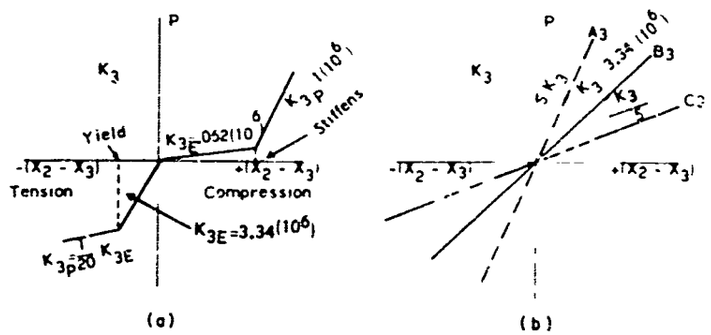


Fig. 4 - Force deflection curves: (a) original spring, and (b) optimized spring

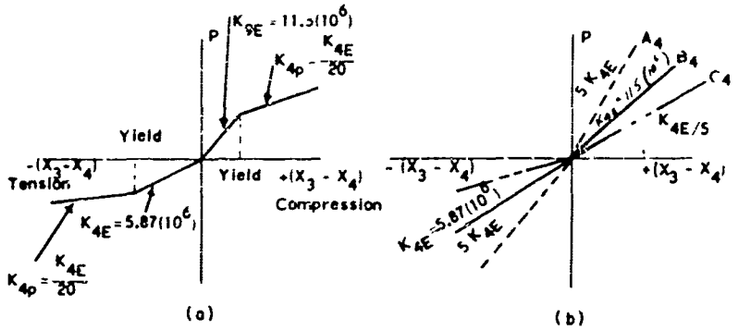


Fig. 5 - Forge deflection curves: (a) original spring, and (b) optimized spring

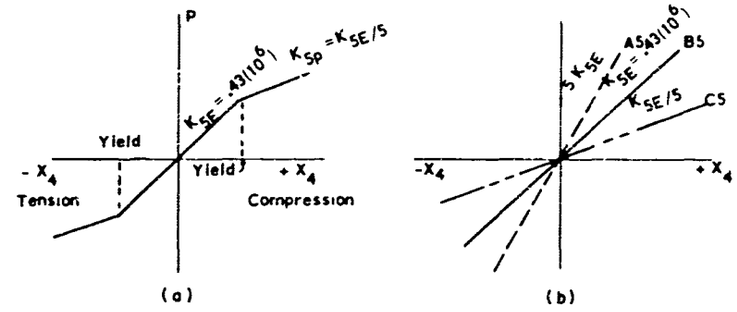


Fig. 6 - Forge deflection curves: (a) original spring, and (b) optimized spring

face of the head mass. This damping was assumed to be velocity dependent. There was some experimental data available for this transducer which showed the decay rate of the ceramic vibration. The damping coefficient $C_1$ was adjusted in the analog computer circuit to make the ceramic vibration decay at the experimentally determined rate. A very small amount of damping $C_3$ was used on mass $M_3$ to make this mass and mass $M_4$ decay.

## Input Force

The input force to the transducer was caused by the shock wave of the underwater explosion impacting the face of the head mass. The resultant input force was influenced by the angle of incidence of the shock wave. For most standoffs, however, this angle was relatively small.

Before impact, the shape of the shock wave was described as a decaying exponential, but after impact it changed drastically. The shape before impact is described by

$$P = P_0 e^{-t/\theta} . \qquad (1)$$

If the shock wave impacted a rigid wall, Eq. (1) would still apply, but with $P_0$ doubled. Because the face of the head mass was not rigid, the pressure on the face was described by Eq. (2), which was more accurate than Eq. (1) [3]:

$$P = 2P_0 e^{-t/\theta} - \rho H \frac{dx_1}{dt} . \qquad (2)$$

The term $\rho H(dx_1/dt)$ considered the motion of the head mass. To calculate the total force applied to the transducer from the shock wave, the pressure was multiplied by the area it affected. In this case, however, the area was not constant. The rear face was affected approximately 0.024 msec after the shock wave impacted the front face of the head mass. The force on this surface acted in the opposite direction, thereby effectively cancelling out part of the initial input (Fig. 7).

A typical input force plot is shown in Fig. 8. Area cancellation caused the decrease in the force at 0.024 msec and transducer velocity

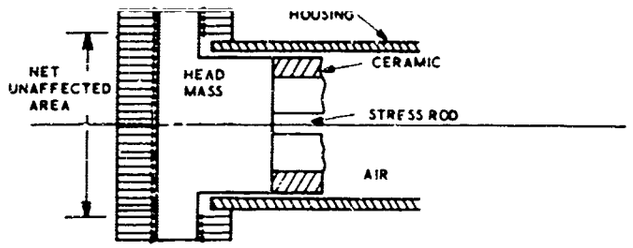


Fig. 7 - Net unaffected area for hydraulic shock

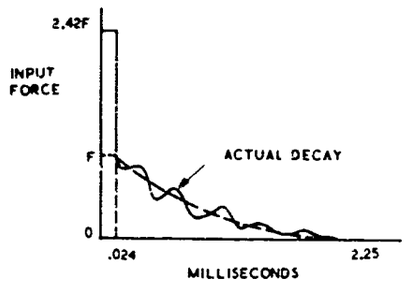


Fig. 8 - Input force vs time for hydraulic shock

caused the nonexponential decay. The input was essentially zero after 2.25 msec.

## Equations of Motion

The equations of motion of the modeled system were as follows:

$$M_1 \frac{d^2X_1}{dt^2} + C_1 \frac{dX_1}{dt} + K_6(X_1 - X_4) + K_1(X_1 - X_2) - 2AP_0 e^{-t} + A \cdot H \frac{dX_1}{dt} = 0 . \quad (3)$$

$$M_2 \frac{d^2X_2}{dt^2} + K_3(X_2 - X_3) - K_1(X_1 - X_2) - K_2(X_1 - X_2) \quad 0 \quad (4)$$

$$M_3 \frac{d^2X_3}{dt^2} + K_4(X_3 - X_4) - K_3(X_2 - X_3) - 0. \quad (5)$$

and

$$M_4 \frac{d^2X_4}{dt^2} + K_5(X_4) + K_6(X_1 - X_4) - K_4(X_3 - X_4) - 0. \quad (6)$$

## Analog Computer Shock Inputs

Computer runs were made at 13 different standoffs. Standoff was defined as the horizontal distance between the charge and the transducer. Standoffs used in this analysis were at 600, 400, 350, 300, 250, 200, 150, 100, 75, 50, 30, 25, and 20 ft. The simulated explosive charge was the standard underwater charge used to conduct transducer shock tests.

## Results and Discussion of Original Model and Optimization Study

The relative motion between $M_1$ and $M_2$ caused the stress in the ceramic. Equation (7) was developed to calculate this stress and considered the type of ceramic, its size, the direction of loading and ceramic prestress:

$$\sigma = 2100 (X_1 - X_2) - 1500 . \quad (7)$$

The nominal breaking stress of the ceramic was assumed to be 2500 psi in tension and 50,000 psi in compression. As shown in Table 2, the peak tensile and compressive stresses in the ceramic occurred within the first millisecond. Assuming the nominal ceramic breaking stresses mentioned above, the data in this table shows that failure from hydraulic shock alone can be expected at the 50-ft standoff.

A typical analog computer output for the transducer (the nonoptimized design) is shown in Fig. 9. The charge was at a standoff of 30 ft. Figure 9a shows a plot of the relative displacement of the ceramic. The first two cycles show the expected decay. Figure 9b shows that the back of the head mass contacted the housing twice, causing the ceramic to extend to 5 mils and later to 2.7 mils; i.e., the 90-mil clearance shown in Fig. 2 was twice reduced to zero. Figure 9c shows spring $K_3$ becoming effective in its tensile direction, thereby causing small extensions of the ceramic at 7.4, 9.8, and 12 msec. (These extensions are shown in Fig. 9a.)

TABLE 2
Ceramic Stress Levels

| Standoff (ft) | Compression | | Tension | | | Does Head Mass Hit Housing? |
|---|---|---|---|---|---|---|
| | Max. Compressive Stress (psi) | Time Max. Stress Occurs (msec) | Min. Time for Tensile Stress to Reach 2500 psi | Max. Tensile Stress | Time Max. Tensile Stress Occurs (msec) | |
| 600 | 2,400 | 0.1 | Never reaches it | Always compressive | — | No |
| 400 | 2,730 | | | | — | |
| 350 | 3,180 | | | | — | |
| 300 | 3,490 | | | | — | |
| 250 | 4,020 | | | | — | |
| 200 | 4,540 | | | | — | |
| 150 | 5,640 | | | | — | |
| 100 | 8,210 | | | 1,020 | 0.23 | |
| 75 | 10,310 | | | 1,780 | 0.22 | No |
| 50 | 15,150 | | 0.16 | 3,750 | 0.20 | Yes |
| 30 | 22,900 | | 0.20 | 9,000 | 0.75 | |
| 25 | 26,700 | | 0.19 | 10,050 | 0.24 | |
| 20 | 30,900 | 0.1 | 0.18 | 12,600 | 0.50 | Yes |

The extensions of the ceramic occurred at these times because $K_3$, being much softer in the compressive direction, experienced a large initial compression and then, when it went into tension, a sudden increase in stiffness. Figure 9d is a plot of the displacement of $K_4$.

The spring combinations and values used in the optimization study that showed significant ceramic stress reduction at the most severe shock condition, i.e., at a 20-ft standoff, are shown in Table 3. The data in this table show that when the stiffnesses of $K_3$, $K_4$, and $K_5$ are of the same order of magnitude, the stress in the ceramic will be significantly less. Spring $K_6$ did not act, as shown by the data for $X_1 - X_4$, because the relative displacement was less than 90 mils. This spring was made to act in some of the tests, but it did not improve the system. The tests showed that regardless of the spring combinations used, the basic dynamic characteristics of the transducer remained essentially the same.

## MECHANICAL SHOCK

### The Model

To determine the effects of mechanical shock, the physical model of the transducer (Fig. 1) was idealized as a discrete mass system. Figures 10 and 11 show how the physical model was converted to the mathematical model. The total mass of the transducer was idealized as 19 discrete masses with 21 dynamic degrees of freedom, 19 translational and 2 rotational. The flexibility of the system was represented by 29 members. Each member had flexibility in six directions. The details of the mass-elastic system are presented in the Appendix.

The accuracy of the solution depends on the accuracy of the mathematical model. However, the proper formulation of the mathematical model is not simple. Experience and experimental checks are essential. Most of the differences between the theoretical and the

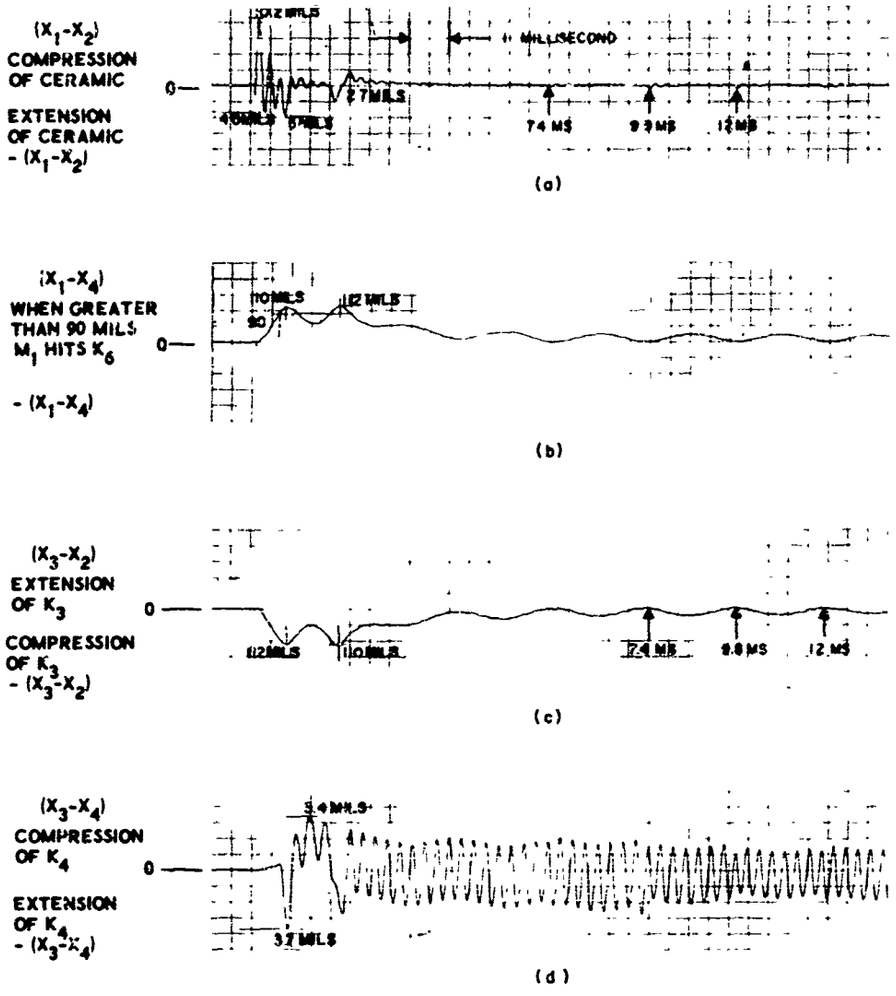


Fig. 9 - Relative displacement of masses: (a) $M_1$ and $M_2$, (b) $M_1$ and $M_4$, (c) $M_2$ and $M_4$, and (d) $M_3$ and $M_4$

TABLE 3
Results of Optimization Study

| Spring | | | Max. Ceramic Compressive Stress (psi) | Max. Ceramic Tensile Stress (psi) | $X_4$ (mils) | $X_3 - X_2$ (mils) | $X_1 - X_4$ (mils) | $X_3 - X_4$ (mils) |
|---|---|---|---|---|---|---|---|---|
| $K_3$[a] | $K_4$[b] | $K_5$[c] | | | | | | |
| Orig. | Orig. | Orig. | 30,900 | 12,600 | 125 | 125 | 120 | 38 |
| $B_3$ | $C_4$ | $B_5$ | 30,900 | 5,850 | 58 | 8 | 56 | 4 |
| $B_3$ | $B_4$ | $A_5$ | 30,900 | 3,960 | 65 | 35 | 48 | 12 |
| $B_3$ | $B_4$ | $2A_5$ | 30,900 | 3,960 | 40 | 34 | 50 | 14 |

[a]See Fig. 4.
[b]See Fig. 5.
[c]See Fig. 6.

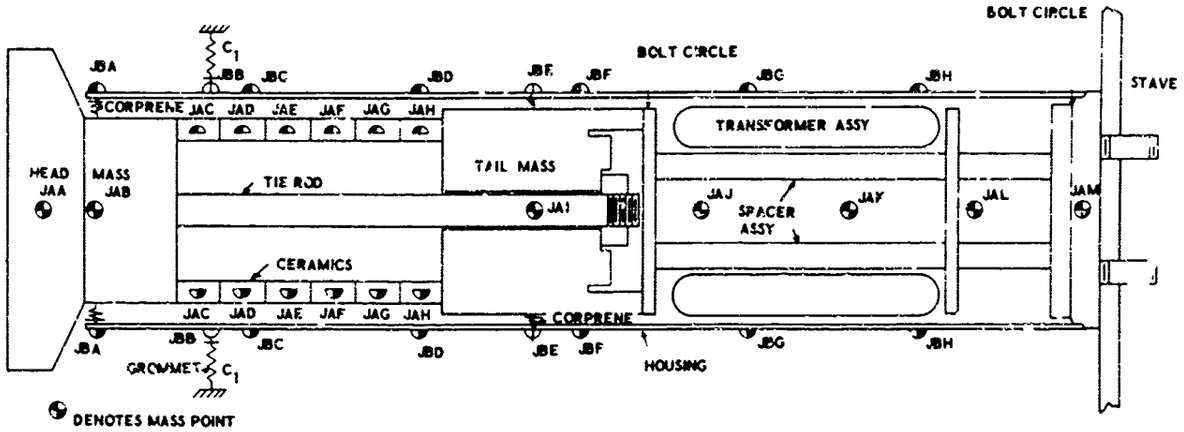


Fig. 10 - Transducer assembly sketch mass point location mechanical shock model

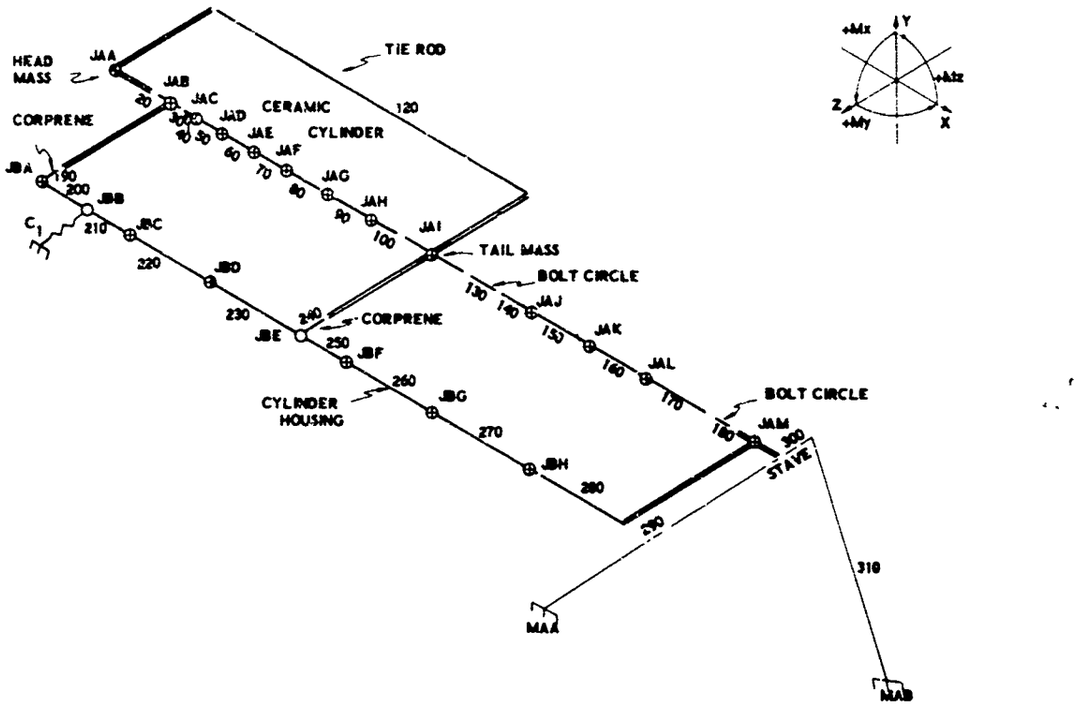


Fig. 11 - Transducer mathematical model for mechanical shock

observed behaviors of the transducer can be attributed to the differences between the physical and the mathematical models. Moreover, if the analysis is to be valid, the input data must represent the physical shock problem. For the mechanical shock, a triangular velocity versus time curve (Fig. 12) was used to represent the vertical motion of the shock platform. If the ramp time (time to reach peak velocity $V_0$) and the decay time (time to reach zero velocity) are the same for all tests, the results can be scaled by the ratios of the peak velocities for each test.

Theoretical Development

The mathematical model for mechanical shock was represented by a system of linear elastic springs and discrete masses as shown in Fig. 11. The equation of motion for this system in matrix form is:

$$[m]\{\ddot{y}\} + [K]\{y\} = -\ddot{y}_o[m]\{D\} \qquad (8)$$

Since this system had 21 degrees of freedom, Eq. (8) represented 21 simultaneous, second

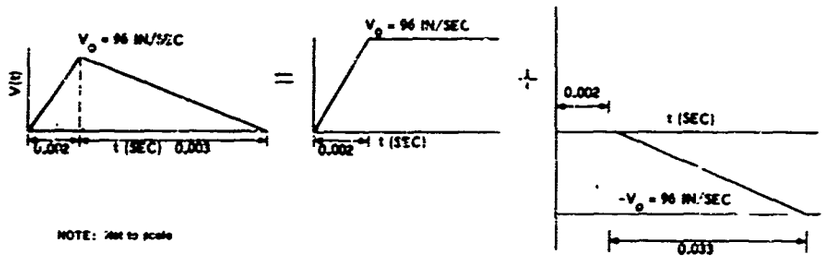


Fig. 12 - Shock input

order, ordinary differential equations of motion. From the homogeneous form of this equation (considering $\ddot{y}_o = 0$), the frequency equation for free vibrations was formed by stipulating periodic motion:

$$\{y\} = \{A\} \sin \omega t . \tag{9}$$

Equation (9) was substituted into Eq. (8) to obtain the frequency Eq. (10),

$$\left| \frac{1}{\omega^2} [\,] - [\delta][m] \right| = 0 \tag{10}$$

where

$$[\delta] = [K]^{-1} .$$

A more expedient form of Eq. (10) was obtained when mass matrix [m] was factored to give

$$[m] = [\beta]^T [\beta] . \tag{11}$$

Equations (11) and (9) were substituted into Eq. (8) and the result was premultiplied by $[\beta]$ to give

$$[\beta]\{y\} = -[\beta][\delta][\beta]^T[\beta]\{\ddot{y}\} . \tag{12}$$

This procedure was equivalent to a change in coordinates from $\{y\}$ to $\{u\}$:

$$\{u\} = [\beta]\{y\} = -[\beta][\delta][\beta]^T\{\ddot{u}\} . \tag{13}$$

Again stipulating periodic motion,

$$\{u\} = \{\theta\} \sin \omega t . \tag{14}$$

the alternate form of the frequency equation became

$$\left| \frac{1}{\omega^2} [I] - [\beta][\delta][\beta]^T \right| = 0 . \tag{15}$$

This form was advantageous since $[\beta][\delta][\beta]^T$ was a symmetrical matrix and computer storage was required for only half of the nondiagonal terms. However, the mode shapes obtained, $[\phi]$, had to be reoriented to the original coordinate

$$[\,] = [\beta]^{-1}[\phi] . \tag{16}$$

The frequency equation, Eq. (15), was tridiagonalized by Householder's method [4] and the eigenvalues were calculated by using the method of Sturm sequences [5]. Finally, the eigenvectors were calculated [6] and reoriented to the original coordinate system by Eq. (16). Once the natural frequencies ($\omega$'s) and mode shapes [ ] were determined, the time-dependent shock problem could be considered. Equation (8) was converted to a more general form by letting

$$\{y\} = [\,]\{q\} . \tag{17}$$

and premultiplying Eq. (8) by $[\,]^T$:

$$[\,]^T[m][\,]\{\ddot{q}\} + [\,]^T[K][\,]\{q\} = -\ddot{v}_o[\,]^T[m]\{D\} . \tag{18}$$

Since the orthogonality and normalization equations could be written

$$[\,]^T[m][\,] = \bar{M}[I] \tag{19}$$

and

$$[\,]^T[K][\,] = \bar{M}[\omega_j^2] . \tag{20}$$

Eq. (18) became

$$\{\ddot{q}\} + [\omega_j^2]q = -\ddot{y}_o\{\gamma\} , \tag{21}$$

where

$$\{\gamma\} = \frac{[\,]^T[m]\{D\}}{\bar{M}} . \tag{22}$$

Considering the system at rest, i.e., $\dot{y}_o = \dot{y}_o = 0$, at the initial time of the shock,

$$\{q\} = [R]\{\gamma\} , \tag{23}$$

where

$$\{R\} = \begin{bmatrix} -\frac{1}{\omega_1}\int_0^t \ddot{y}_o(\lambda)\sin\omega_1(t-\lambda)d\lambda \\ -\frac{1}{\omega_j}\int_0^t \ddot{y}_o(\lambda)\sin\omega_j(t-\lambda)d\lambda \\ \vdots \\ -\frac{1}{\omega_n}\int_0^t \ddot{y}_o(\lambda)\sin\omega_n(t-\lambda)d\lambda \end{bmatrix}. \quad (24)$$

Since $\{y\} = [\phi]\{q\}$, the dynamic deflection with respect to the stave was

$$\{y\} = [\phi][R]\{\gamma\}. \quad (25)$$

In terms of forces,

$$\{F\} = [K]\{y\} = [K][\phi]\{q\}. \quad (26)$$

Premultiplying Eq. (26) by $[\phi]^T$ and using Eqs. (17), (19) and (20) gave

$$\{F\} = [m][\phi][\omega_i^2]\{\gamma\}. \quad (27)$$

The triangular shock pulse was considered a combination of two ramp pulses (Fig. 12). For a ramp pulse, the convolution integrals in the [R] matrix were

$$R_j = -\frac{1}{\omega_j}\int_0^t \ddot{y}_o(\cdot)\sin\omega_j(t-\lambda)d\lambda$$

$$= -\frac{V_o}{\omega_j^2\epsilon}\{1-\cos\omega_j t\}, \quad t \le \epsilon$$

$$= -\frac{V_o}{\omega_j^2\epsilon}\{\cos\omega_j(t-\epsilon)-\cos\omega_j t\}, \quad t \ge \epsilon. \quad (28)$$

Considering one mass point (i) and one natural frequency (j) gave the displacement and force from Eqs. (25) and (26):

$$y_{ij} = \frac{R_j}{\bar{M}}\phi_{ij}\sum_{k=1}^{n}\phi_{kj}m_k D_k \quad (29)$$

and

$$F_{ij} = \frac{\omega_j^2 m_i}{\bar{M}}R_j\phi_{ij}\sum_{k=1}^{n}\phi_{kj}m_k D_k. \quad (30)$$

The total displacement and forces for all frequencies were the sum of Eqs. (29) and (30), respectively, for all the natural frequencies:

$$y_i = \sum_{j=1}^{n} y_{ij} \quad (31)$$

and

$$F_i = \sum_{j=1}^{n} F_{ij}. \quad (32)$$

From these equations, the deflection, shear, and moment diagrams were developed [1,2].

## Results for Original Model

The first step in the analysis was to determine the natural frequencies and mode shapes of the system. Since there were 21 dynamic degrees of freedom, the idealized system had a corresponding number of natural frequencies and mode shapes. The first three mode shapes were plotted in Fig. 13. The higher modes were plotted in Ref. 1. The mathematical procedures used to determine the natural frequencies and mode shapes have been explained in the theoretical development section and in the Appendix.

The dynamic displacements and forces were calculated from Eqs. (29) and (30), using the calculated natural frequencies and mode shapes in conjunction with the mass and velocity input data. The displacements (relative to the shock platform) are shown in Fig. 14. Since the head mass was a major contributor to the stresses in the ceramic, the dynamic forces at the head mass are shown in Fig. 15. The shear and moment diagrams for the ceramic stack are given in Ref. 1.

For a peak velocity ($V_o$) of 8 fps, the maximum bending moment in the ceramic was $M$ = 4300 in./lb. The maximum shear force was 530 lb. Converting the maximum moment in the ceramic to bending stress gave $\sigma$ = 865 psi. Converting the maximum shear in the ceramic at the tail mass to shear stress gave $\tau$ = 175 psi.

## Optimization Study

To improve the mechanical shock resistance of the original model, the effects of a systematic increase in mount and bolt circle stiffness were studied. The basic geometry, location of mounts, and mass distribution of the transducer

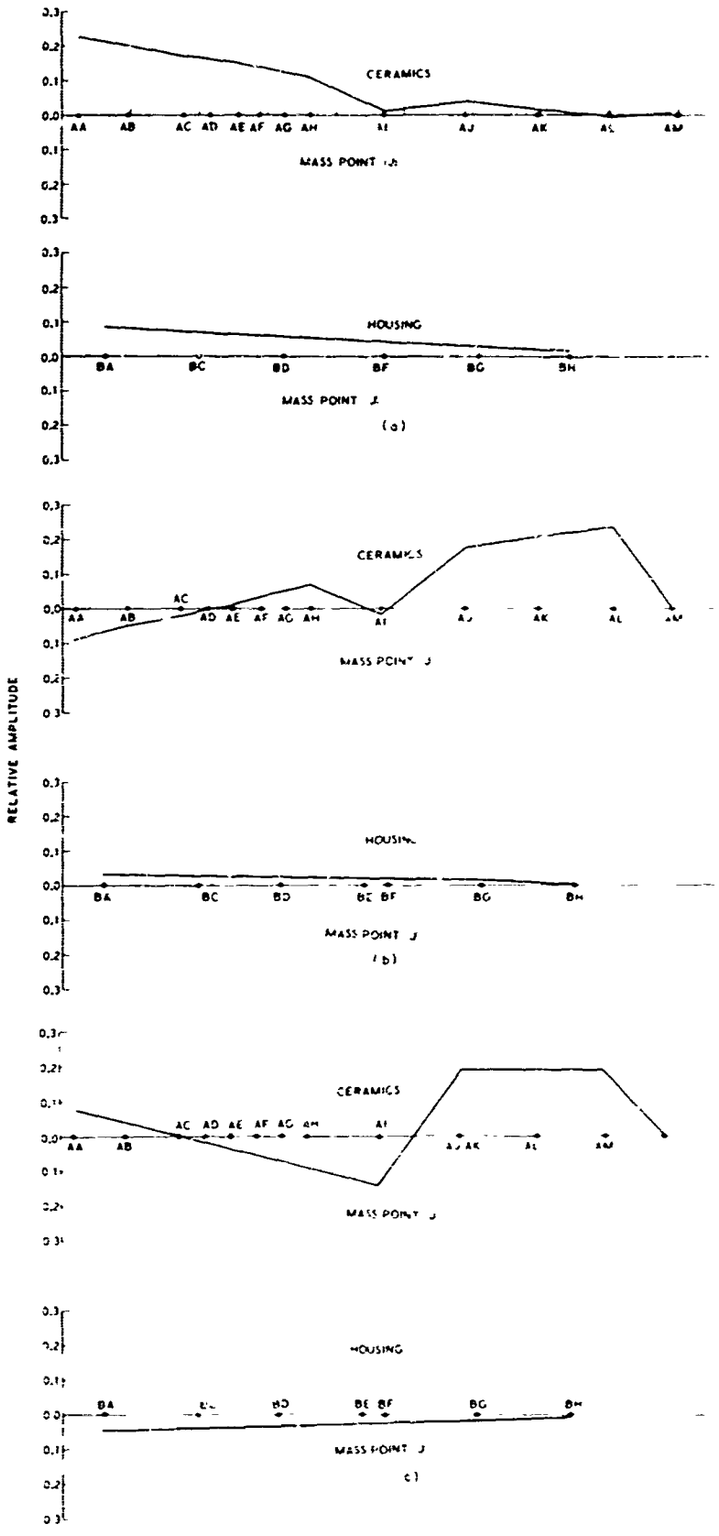


Fig. 13 - Head mass. ceramics, tail mass, and transformer assembly: (a) mode 1, frequency 42.81 cps, (b) mode 2, frequency 67.05 cps; and (c) mode 3, frequency 131.62 cps

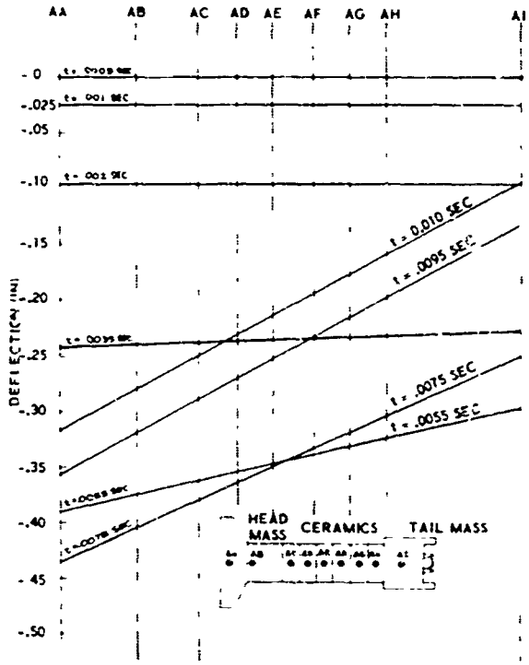


Fig. 14 - Deflections for head mass, ceramics, and tail mass

a factor of 10. Figure A-4 indicates a stiffness of 2500 lb/in. for member $C_1$. The stiffness ($C_1$) was changed to 25,000 lb/in.

Model 3 — The stiffness of the corprene mount at the head mass (piece 190 of Fig. 11) was increased by a factor of 10.

Model 4 — The stiffness of the tail mass bolt circle (piece 130 of Fig. 11) was increased by a factor of 10.

Model 5 — The stiffness of the rear stave members was increased by a factor of 10.

Model 6 — The stiffness of the bolt circle (piece 180 of Fig. 11) at the foundation end was increased by a factor of 10.

Results of Optimization Study

Only the first four mode shapes were used to calculate stresses because the original analysis indicated that the stresses in the ceramic due to the higher modes were negligible. Table 4 lists the natural frequencies for the models studied.

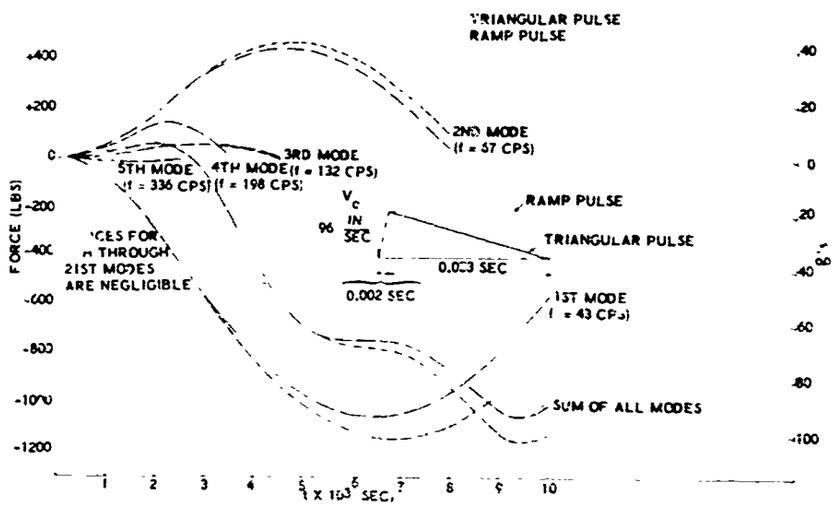


Fig. 15 - Head mass (joint JAA) forces

were maintained. The various changes in the original model are indicated below.

Model 1 — The tail mass stiffness of the corprene piece number 240 (Fig. 11) was increased by a factor of 10.

Model 2 — The stiffness of the stave grommet (member $C_1$ of Fig. 11) was increased by

The results of the original analysis indicated that the first mode obviously controlled the stresses in the ceramic. Therefore, an examination of the mode shapes for the first frequency [2] indicates that model 3 should cause the largest change in stresses in the ceramic. This conclusion was based on two facts. this change caused the largest increase

TABLE 4
Summary of Frequencies

| Mode No. | Frequencies (cps) | | | | | | |
|---|---|---|---|---|---|---|---|
| | Orig. | Model 1 | Model 2 | Model 3 | Model 4 | Model 5 | Model 6 |
| 1 | 42.81 | 45.47 | 49.13 | 53.49 | 43.61 | 50.96 | 44.22 |
| 2 | 67.05 | 80.21 | 68.17 | 79.15 | 69.47 | 69.44 | 101.2 |
| 3 | 131.6 | 141.2 | 132.3 | 135.3 | 198.2 | 132.5 | 182.1 |
| 4 | 198.7 | 335.5 | 259.4 | 335.9 | 352.2 | 302.9 | 236.7 |
| 5 | 336.7 | 375.6 | 337.0 | 348.4 | 747.6 | 336.7 | 643.6 |
| 6 | 1051 | 1071 | 1051 | 1075 | 1951 | 1369 | 1067 |
| 7 | 1713 | 1715 | 1715 | 1715 | 1734 | 1715 | 1715 |
| 8 | 1952 | 1969 | 1954 | 1961 | 1952 | 2995 | 1960 |
| 9 | 3298 | 3302 | 3298 | 3305 | 3298 | —[a] | 3303 |
| 10 | 3691 | 3691 | 3691 | 3691 | 3735 | 3691 | —[a] |
| 11 | 3769 | 3786 | 3785 | 3786 | 3813 | 3785 | 3782 |

[a]Frequency for this mode is greater than 4000 cps.

in the first resonance, i.e., 25 percent, and the mode shape indicated a drastic reduction in rotation in the ceramic (Fig. 16).

The dynamic displacements were calculated using the first four frequencies and the mode shapes for model 3 (Fig. 17). The corresponding forces and moments are plotted in Ref. 2. The dynamic displacements are relative to the shock platform. Since the head mass response is a major contributor to the stresses in the ceramic, the head mass forces are plotted in Fig. 18.

For a peak velocity ($V_o$) of 8 fps the maximum bending moment in the ceramic was $M$ = 4000 in.-lb. The maximum shear force was 515 lb [2]. Converting the maximum moment in the ceramic to bending stresses gave $\sigma$ = 810 psi. Converting the maximum shear in the ceramic to shear stress gave $\tau$ = 173 psi. This indicated only a slight reduction in maximum ceramic stresses from the original models ($\sigma$ = 865 psi, $\tau$ = 175 psi). However, an important result was that the mounts could be stiffened to prevent bottoming without an increase in ceramic stresses. An increase of each mount by a factor of 5 was sufficient to prevent bottoming and keep the ceramic stresses below ultimate (2500 psi) at a 20-ft standoff [2].

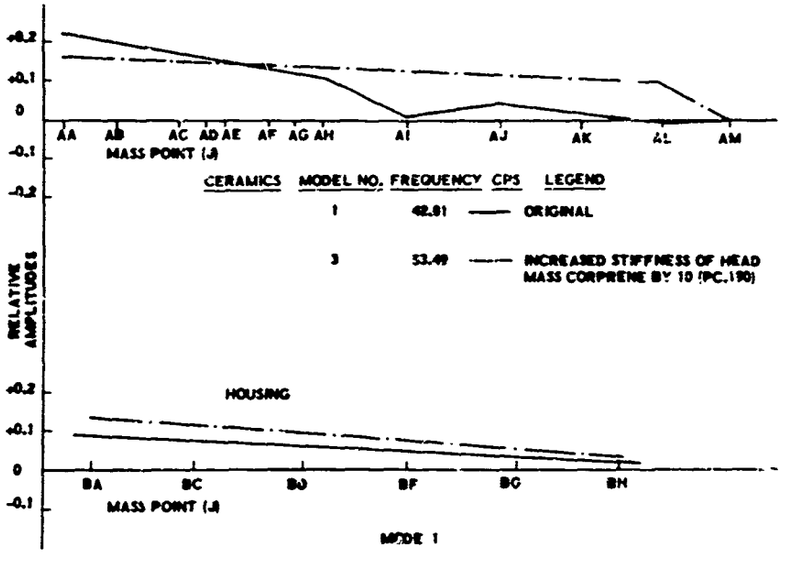


Fig. 16 - Fundamental mode shapes

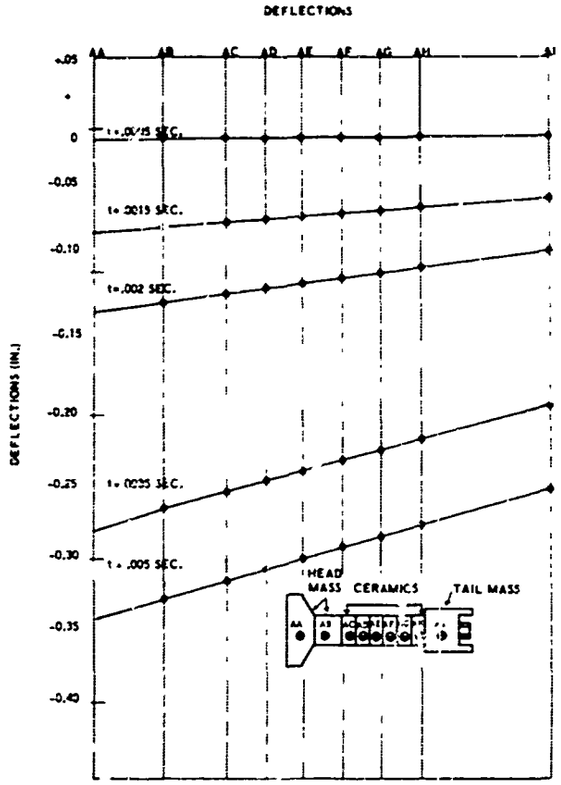


Fig. 17 - Dynamic displacements

Discussion for Original Model

The stresses induced by mechanical shock for the case of an 8-fps peak velocity were less than the ultimate stress in tension (2500 psi). However, the results showed that the head mass mount and stave grommet would bottom out at a velocity of about 8 fps. The tail mass mount would bottom out at about 4 fps, but the effect of the tail mass mount on the stress in the ceramic is small and the bottoming of this mount would not cause major changes. However, this was not true of the head mass mounts and stave grommet. Once these mounts bottomed, the stresses in the ceramic would be seriously altered.

The peak stresses due to mechanical shock occurred at 7.5 msec. Since the peak stresses in the ceramic occurred at less than 1 msec, there was a negligible interaction between the two shock effects. Therefore, the a priori assumption of separately treating the two shock analyses is correct.

There are many possible ways of reducing the peak stresses in the ceramics. The most direct ways involve the mounts. Since the motion of the head mass induces most of the bending stresses in the ceramic, decreasing the

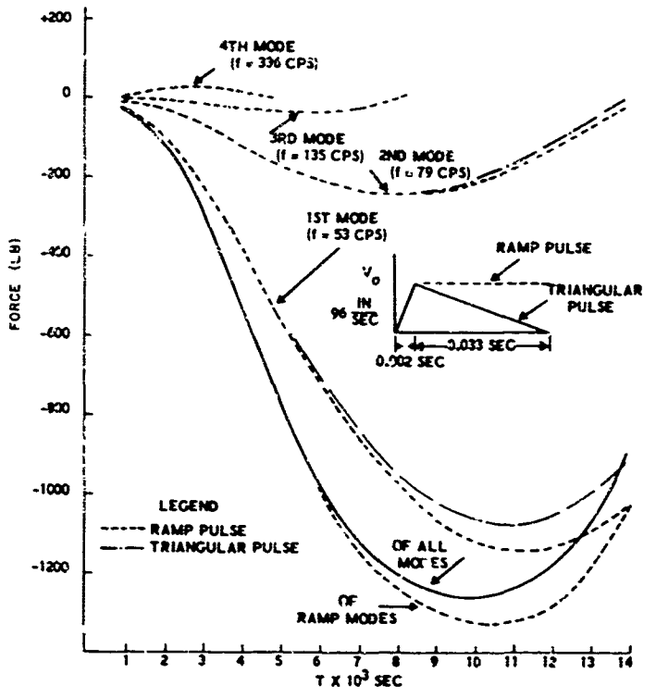


Fig. 18 - Head mass (joint AA) forces

distance from the center of gravity of the head to the middle of the head mount would help. Also, an increase in the stiffness of the head mount and stave grommet would decrease the deflection and rotation of the head mass and reduce the stresses in the ceramic. If it were possible to increase the depth of the mounts, bottoming might be prevented, thus increasing the resistance to failure by mechanical shock.

The flexural modes of vibration for the ceramic cylinder contribute very little to the stress in the ceramic because the first flexural resonance is at 1714 cps compared to the first resonance of the system of 43 cps. Since the deflections in the ceramic cylinder are inversely proportional to the squares of the natural frequencies, the amplitudes of the flexural modes are nil. The corresponding forces are small compared to the forces induced by the lower modes.

### Discussion of Optimization Study

It was learned from this study that if the mounts can be stiffened to avoid bottoming, the stresses in the ceramic stack can be kept below ultimate (2500 psi) at a 20-ft standoff. Since this stiffening may affect the acoustic behavior, the total effect of the stiffer mounts on the system should be studied.

The stiffness of the nonstructural members (mounts and bolt circles) and stave supports were systematically varied to determine which members seriously affected the ceramic stresses. The head mass mount was the critical member. The most favorable change would be to position the head mass mount in line with the center of gravity of the head mass. If this change is not feasible, the alternate change would be to stiffen all the mounts to prevent bottoming.

The deflection across the mounts was proportional to the stiffness of the mount. The conclusion from this analysis is that an increase of stiffness in each mount by a factor of 5 will prevent bottoming and keep the ceramic stresses below the ultimate (2500 psi) at a 20-ft standoff.

## CONCLUSIONS

### Original Model

1. It was learned from the analysis that hydraulic shock stresses occur within 1 msec, whereas the high stresses due to mechanical shock occur at 7.5 msec. Therefore, these types of shock act independently.

2. For any given standoff, hydraulic shock causes higher stresses in the ceramic cylinder than does mechanical shock.

3. For the hydraulic shock, the ceramic first fails at a 50-ft standoff. All failures in the ceramic, regardless of the standoff distance, are tension failures.

4. For the mechanical shock, a peak velocity of 8 fps does not cause a failure in the ceramic, but it does cause incipient bottoming of the head mass and stave mounts.

5. The flexural modes of vibration of the ceramic cylinder caused by mechanical shock contribute very little to the total dynamic stress. This condition exists because the first flexural mode of the ceramic stack occurs at 1714 cps, whereas the first resonance of the system occurs at 43 cps.

### Optimization Study

1. The tensile stress in the ceramic caused by hydraulic shock can be significantly reduced by varying several of the spring elements. The analysis indicated that the tensile stress at a 20-ft standoff can be reduced from 13,000 to 4000 psi. The compressive stress was essentially constant for any of the spring combinations investigated.

2. For mechanical shock, an increase in the stiffness of each mount by a factor of 5 will prevent bottoming and keep the ceramic stresses below the ultimate (2500 psi) at a 20-ft standoff.

3. An order of magnitude change in mount stiffness does not appreciably change the stress in the ceramic.

4. A stiffness change on the head mass mount causes the most significant change in the fundamental frequency of the transducer.

## REFERENCES


1. A. D. Carlson and R. J. McGrattan, "Transducer Shock Study," Electric Boat Div., General Dynamics, DDC Rept. AD631 344, Oct. 1965

2. A. D. Carlson and R. J. McGrattan, "Transducer Shock Study Phase II," Electric Boat Div., General Dynamics, Rept. U411-66-031, May 23, 1966

3. D. S. Cohen, "Shock-Wave Transmission at a Water-Backed Plate," UERD, Norfolk Naval Shipyard, Rept. No. F-32-51

4. J. H. Wilkinson, "Householder's Method for the Solution of the Algebraic Eigenproblem," Computer J., pp. 23-27, April 1960

5. J. M. Ortega, "On Sturm Sequences for Tridiagonal Matrices," Stanford Univ. Appl. Math. and Statistics Lab. Tech. Rept. No. 4, 1960

6. J. H. Wilkinson, "The Calculation of the Eigenvectors of Codiagonal Matrices," Computer J., pp. 90-96, July 1958

## Appendix

## STIFFNESS MATRIX FOR MECHANICAL SHOCK MODEL

The initial operation in the solution of a mass elastic system is to idealize the structure as a system of masses and massless elastic springs (Fig. 11). The only parameters required to find the natural frequencies of the system are the mass distribution, the spring geometry (to determine the stiffness of the system), and the boundary conditions. To determine further the time-dependent deflections and forces, a time-dependent input at the boundaries is also required.

To determine the stiffness of the structure, the total stiffness at each joint is required, e.g., joint JBE in Fig. 11. The joint stiffness is a function of all the members (p) between the joint in question and the adjoining joints. The flexibility of each structural member (p) is first calculated at its own center and is represented as a $6 \times 6$ flexibility matrix.

$$p = \begin{bmatrix} \delta_{11} & 0 & \cdots & 0 \\ 0 & \delta_{22} & & \vdots \\ & & \delta_{33} & \\ & & & \delta_{44} \\ & & & & \delta_{55} & 0 \\ 0 & \cdots & & & 0 & \delta_{66} \end{bmatrix} \qquad \text{(A-1)}$$

where

$$\delta_{11} = \frac{L}{AF} ,$$

$$\delta_{22} = \frac{L^3}{12EI_w} + \frac{K_v L}{AG} ,$$

$$\delta_{33} = \frac{L^3}{12EI_v} + \frac{K_w L}{AG} ,$$

$$\delta_{44} = \frac{L}{IG} ,$$

$$\delta_{55} = \frac{L}{EI_v} ,$$

and

$$\delta_{66} = \frac{L}{EI_w} .$$

This flexibility matrix applies to all beams whose shear centers coincide with the centroid. Additional off-diagonal terms are required for members with shear centers eccentrically located with respect to the centroid. The flexibility of each member includes axial, bending, shear and torsional deformations. The flexibilities for the structural members of Fig. 11 are given in Ref. 1.

There were several nonlinear springs in the system that were considered linear for the purpose of this analysis. Therefore, the solution was only valid for the range of deformation in which these springs were nearly linear. These springs included the bolt circles (Figs. A-1 and A-2) and the mounts (Figs. A-3 and A-4).

The stiffnesses of the bolt circles were determined experimentally by applying unit forces and moments to the bolt circle members. Transformation equations (Eq. A-2) were used to determine the flexibilities of the bolt circles at their centroids. Since the transformer and bolt circle configurations had different stiffnesses about the horizontal and vertical axes, one set of values was chosen, i.e., the ones in the more flexible (or soft) direction. The flexibilities used in the mathematical model are reported in Ref. 1. The stiffnesses of the mounts were also determined experimentally, as shown in Figs. A-3, A-4, and A-5. Flexibility for these numbers was considered in one direction only. They also are given in Ref. 1.

After the flexibilities of each member were computed, each flexibility matrix was rotated from its own coordinate system (u, v, w) to a

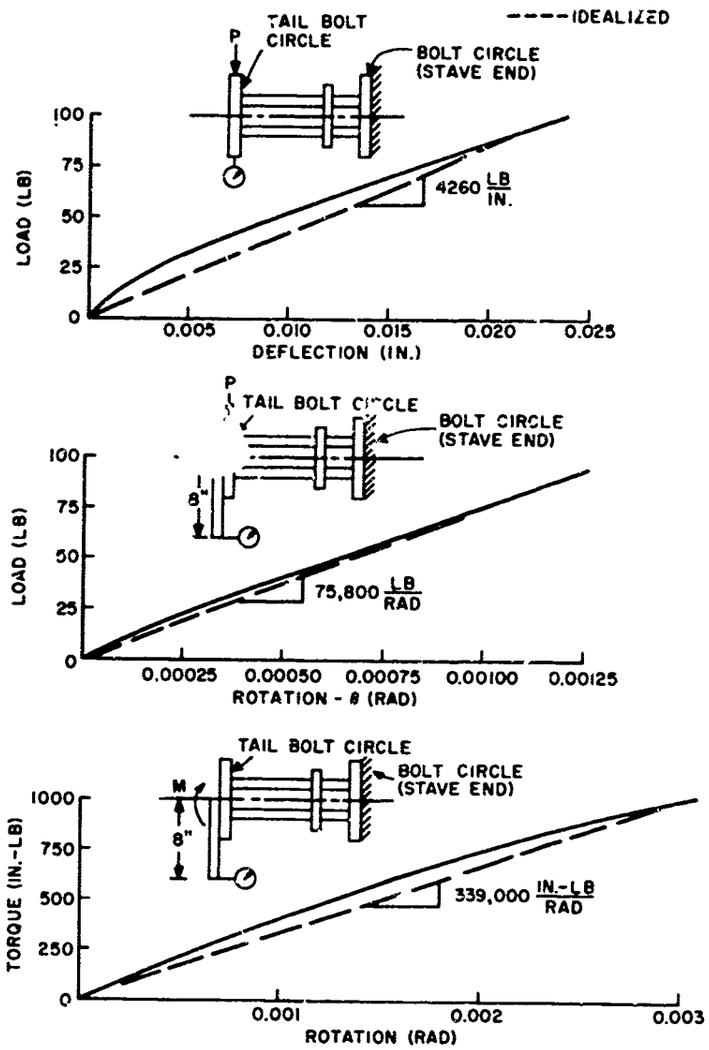


Fig. A-1 - Bolt circle and spacer assembly load deflection curves

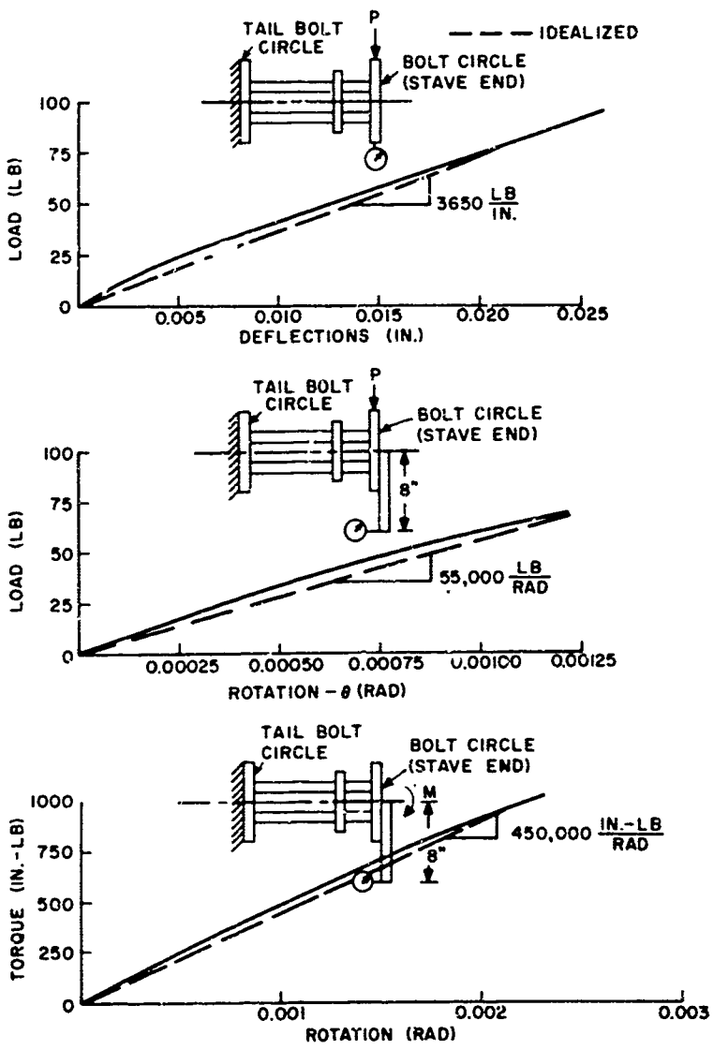


Fig. A-2 - Bolt circle and spacer assembly load deflection curves

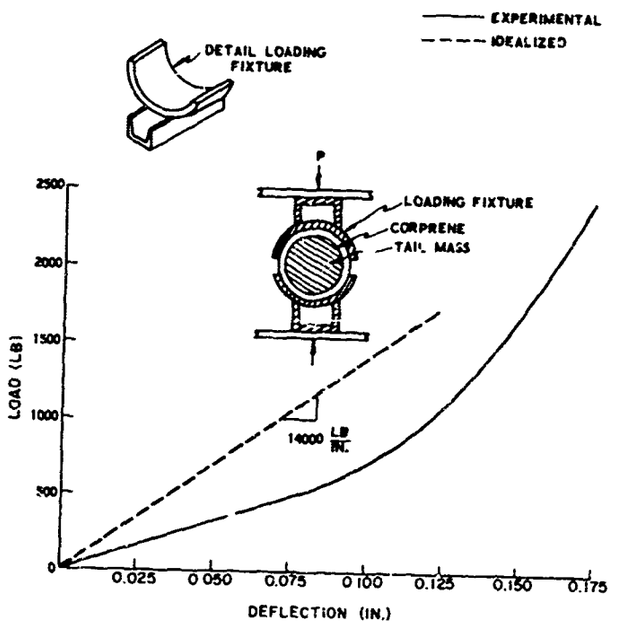


NOTE: Deflections plotted here are twice that which would occur from inertial loading of mass. Dotted line shows actual stiffness used.

Fig. A-3 - Corprene band around tail mass load deflection curve

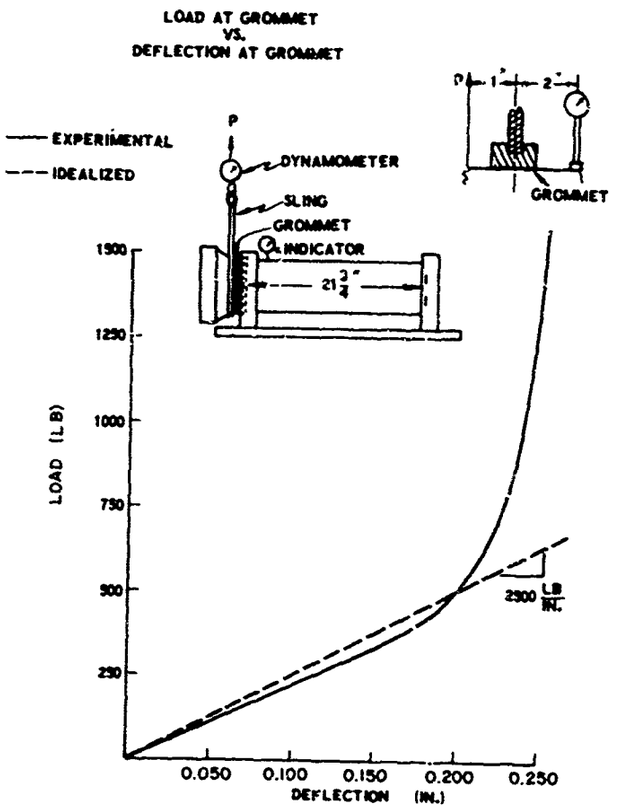


Fig. A-4 - Neoprene stave grommet $C_1$

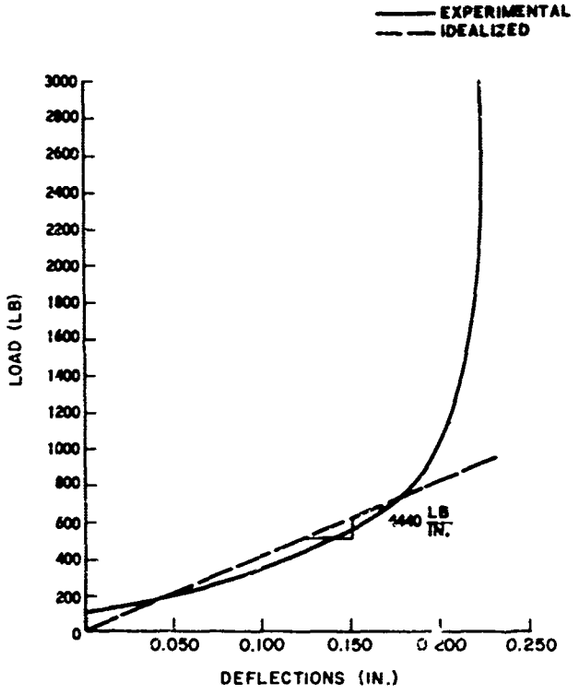


Fig. A-5 - Load deflection curve for head mass mounts

common coordinate system (x, y, z) and translated from the center of the member (p) to the appropriate joints (j and k). This was accomplished by

$$[\delta_p^i] = [B]^T[L]^T[\delta][L][B] , \qquad \text{(A-2)}$$

where i = j and k,

$$[L] = \begin{bmatrix} \cos ux & \cos uy & \cos uz & 0 & 0 & 0 \\ \cos vx & \cos vy & \cos vz & 0 & 0 & 0 \\ \cos wx & \cos wy & \cos wz & 0 & 0 & 0 \\ 0 & 0 & 0 & \cos ux & \cos uy & \cos uz \\ 0 & 0 & 0 & \cos vx & \cos vy & \cos vz \\ 0 & 0 & 0 & \cos wx & \cos wy & \cos wz \end{bmatrix} .$$

and

$$[B] = \begin{bmatrix} 1 & 0 & \cdots & & & 0 \\ 0 & 1 & & & & \vdots \\ 0 & 0 & 1 & & & \vdots \\ 0 & (z_i - z_p) & (y_p - y_i) & 1 & & \vdots \\ (z_p - z_i) & 0 & (x_i - x_p) & 0 & 1 & 0 \\ (y_i - y_p) & (x_p - x_i) & 0 & 0 & 0 & 1 \end{bmatrix} .$$

The flexibilities of each member (p) between joints (e.g., members 170 and 180 between joints JAL and JAM) were summed in the x, y, z coordinate system and inverted to form a stiffness matrix [1]. This stiffness matrix was added to all the other stiffnesses of members contributing to the joint stiffness. The stiffness matrix for the mathematical model was given in Ref. 1. The square root method [A-1] was used to determine the flexibility matrix [δ].

## REFERENCE

A-1. V. N. Faddeva, Computational Methods of Linear Algebra. Dover Publications, New York, 1959

* * *

# DIRECT MEASUREMENT OF 5"/54 GUN SETBACK ACCELERATION

Peter S. Hughes and Luigi A. Vagnoni
Naval Ordnance Laboratory
Silver Spring, Maryland

Recording of a significant portion of setback shock for six rounds, fired in a shortened 5"/54 naval gun, was successfully accomplished with piezoelectric transducers and hardwire instrumentation. Several rounds were also fired to investigate correlation between chamber pressure and projectile acceleration. The recorded pulses had superimposed oscillations with frequencies up to 11 kHz and amplitudes estimated at 1-1/2 times the faired peak value. Initial portions of the projectile acceleration recordings were of complex shape, lagged pressure by a significant amount, and the high-frequency peaks varied widely from shot to shot. Shock spectra were compiled in the high-frequency region for the pulses. Test apparatus and instrumentation are described.

P. S. Hughes

## INTRODUCTION

This report presents the results of an investigation undertaken to determine the feasibility of recording projectile setback shock in 5"/54 guns using present state-of-the-art instrumentation. Past attempts to record artillery shock directly have met with limited success. Although displacement-time measurements using the Doppler method have been successful, the data generated, when differentiated twice, can neither show the high-frequency content of the shock nor the erratic projectile motion. Peak shock measurements also have been made in a number of projectile firings using peak-reading accelerometers; however, until such time that the frequency content of gun shock is known, it is not possible to interpret these measurements meaningfully. Gun shock information was sought primarily to interpret VT fuze anomalies that cannot be explained on the basis of current shock theory and to provide shock criteria for future fuze designs.

The investigation consisted of firing several instrumented rounds from a 5"/54 gun with a shortened barrel. The projectile instrumentation consisted of a piezoelectric shock transducer mounted in a VT fuze, and a coaxial transmission cable (hardwire). The recording instrumentation consisted of a charge amplifier and a magnetic tape recorder. The shortened gun barrel was used instead of the full-length barrel to permit photographic coverage of the initial phase of projectile motion and to prevent transmission cable pile-up in the barrel during firings. The short barrel also reduced the chances of barrel slap, a major problem in piezoelectric transducer recording. Because previous studies indicated that the shock peak was reached in a few feet of barrel length, use of the shortened gun barrel was justified for purposes of determining gun shock effects on fuzes.

## SHOCK AND PRESSURE MEASUREMENTS

Nine instrumented rounds were fired in the shortened 5-in. gun shown in Fig. 1. Projectile travel in the barrel was about 29 in., compared

Fig. 1 - Sawed-off 5"/54 gun showing attachment of accelerometer cable

with about 19 ft in a standard 5"/54 barrel. Shock transients were successfully recorded for six out of the nine rounds. Table 1 summarizes the results for test rounds fired with and without obturators (see the Appendix for a discussion of obturators). Both acceleration and breech pressure were monitored on round 9. The velocity of each round was determined from the projectile flight time between two induction coils located at 81.60 and 172.84 ft ahead of the gun mount trunnion. A sketch of the test setup is shown in Fig. 2.

Two shock signatures are shown in Figs. 3 and 4. Figure 3 shows a shock signature for a shot with an obturator; this signature was typical of all shots fired with obturators. With an obturator, the shock pulse is characterized by superimposed oscillations with frequencies up to 11 kHz and with amplitudes of 1-1/2 times

TABLE 1
Summary of Test Conditions and Shock Parameters

| Round No. | Test Conditions | Projectile Velocity (fps) | Peak Acceleration[a] | |
|---|---|---|---|---|
| | | | Faired (g) | Unfaired (g) |
| 1 | Cup obturator; cork plug removed | 1238 | b | b |
| 2 | Cup obturator | 1250 | b | b |
| 3 | Same as round 1 | 1231 | 6760 | 8900 |
| 4 | Same as round 1 | 1245 | c | c |
| 5 | Same as round 1 | 1252 | c | c |
| 6 | Same as round 1 | 1241 | c | c |
| 7 | Ring obturator; cork plug removed | 1236 | 6680 | 9450 |
| 8 | Service round | 1234 | b | b |
| 9 | Service round | --- | 6060 | 7050 |

[a]Parameters are for partial shocks recorded.
[b]Signal distorted due to cable strain or barrel slap.
[c]No signal due to instrumentation failure.

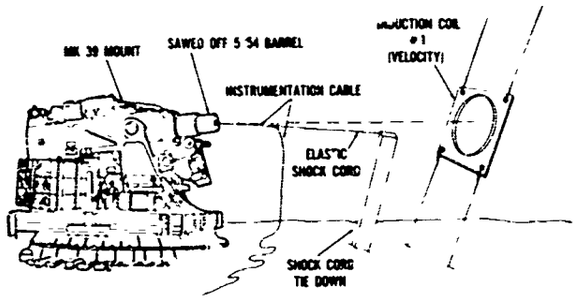


Fig. 2 - Sketch of test setup at Naval Weapons Laboratory, Dahlgren, Va.

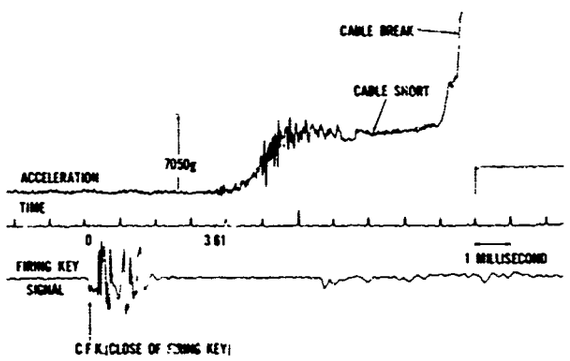


Fig. 3 - Typical shock signature, shot 9

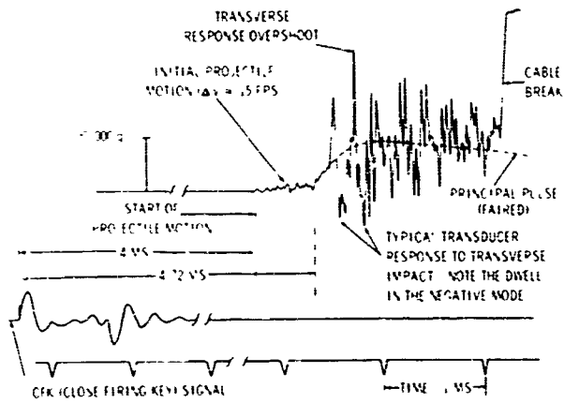


Fig. 4 - Shock signature showing transverse impact, shot 8 without obturator

the faired peak value. Figure 4 shows the shock signature of one of the two shots made without an obturator. The projectile experienced severe transverse impacts against the barrel during its travel. Because of the transverse sensitivity of the accelerometer, it was impossible to monitor the true axial shock. The large negative velocity change in the shock transient made integration invalid and precluded meaningful shock spectra. The shock signature of the other non-obturated shot was similar to Fig. 3.

A close of firing key signal (CFK) was recorded from an induction coil around the electrical cable to the cartridge case igniter, and was used as the time reference point. The records show a delay of approximately 3 msec between CFK and the first perceivable acceleration. A delay of 3 to 4 msec is typical of the time for burning to commence and the pressure to act on the projectile.

## DATA ANALYSIS

### Velocity-Time History

The FM taped shock signatures were played into an electronic integrator to yield velocity-time signatures. Figure 5 shows the acceleration-time signature for shot 7 and its accompanying velocity-time signature. As indicated, when the cable shorted out, the instantaneous velocity was 500 fps with a corresponding displacement of 7.5 in. A previously established pressure-distance curve for the 5"/54 barrel showed the pressure peak occurs after approximately 2 ft of projectile travel. Since pressure and acceleration are assumed to peak simultaneously, it was concluded that recording was terminated before the acceleration peak was reached. The cable appears to have shorted just as the first plateau in the shock signature was reached.

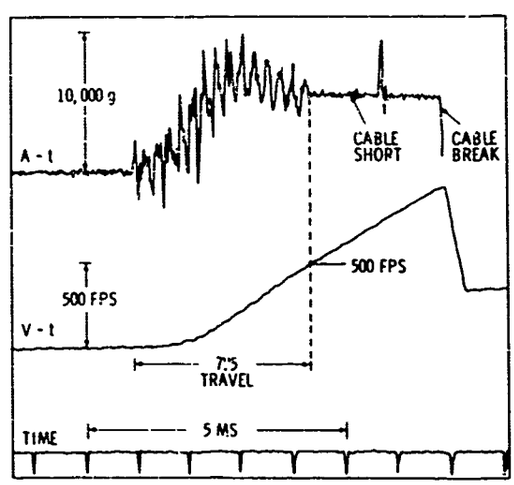


Fig. 5 - Integration of shock transient, shot 7

## Synthesized Pulse

An attempt has been made to synthesize electronically the entire shock signature for a full-length barrel by utilizing the interior ballistics data recorded to date. The parameters utilized were the known velocity change of 2600 fps and the nominal time from CFK to projectile exit of 16 msec. The high-frequency oscillations are typical of the recorded partial shocks; however, the faired pulse shape is only an educated guess and represents a median condition. A sketch of this signature is shown in Fig. 6.

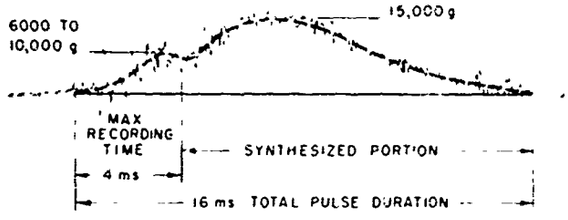


Fig. 6 - Synthesized shock for full 5"/54 barrel

## Response Spectra

Shocks as complex as those described above, even when the whole shock picture is known, do not necessarily identify the shock stresses which fuze components experience during gun setback. Only by determining the effect of complex shock on mechanical structures can meaningful use be made of any setback shock data. Shock (response) spectra, for five of the six recorded shots, were compiled using analog computer circuitry. As previously mentioned, the spectrum for shot 8 was not valid because of the severe transverse impact on the projectile. All the spectra were computed using 2 percent critical damping in a linear single-degree-of-freedom system. Figure 7 shows the response spectra for shots 3 and 7. Analysis of the partial shocks was limited to the high-frequency range between 4 and 20 kHz because of the limited recording durations. All the spectra bear out the predominance of the 11-kHz frequency and the lack of appreciable frequency content beyond 11 kHz.

## Pressure-Time Histories

One of the significant findings in these tests was the relationship between the chamber pressure and the projectile acceleration;

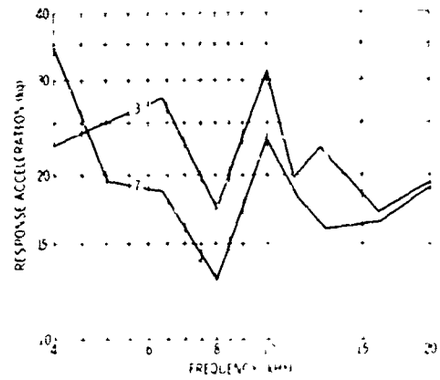


Fig. 7 - Response spectra of partial 5"/54 gun shock, computed at 2 percent critical damping on analog computer

projectile acceleration was not proportional to the chamber pressure. The forces resisting projectile motion (engraving and angular acceleration) were, apparently, sufficiently high at first to cause the chamber pressure to build up sharply and erratically. Unfortunately, recording time was too short to determine when the projectile acceleration finally approaches the thrust indicated by the pressure-time history.

Figure 8 compares thrust (in gravity units), calculated from pressure measurements, with projectile acceleration:

$$a(t) = P(t) \times \text{bore area/projectile weight}$$

The chamber pressure was recorded with a piezoelectric gage in the base of the cartridge

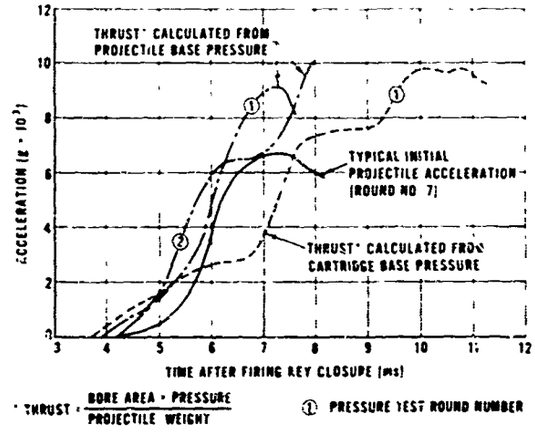


Fig. 8 - Correlation between thrust and projectile acceleration

case; pressure signatures were nearly identical for the test rounds fired. The pressure acting on the base of the projectile was recorded with a piezoelectric transducer in the projectile base.

## CONCLUSIONS

Projectile acceleration is not directly proportional to pressure, at least during the initial phase of projectile motion. Moreover, pressure measured directly behind the projectile has a much shorter rise time than pressure measured at the base of the cartridge case. Use of pressure data to compute acceleration-time signatures for artillery projectiles could result in considerable error. However, under normal firing conditions, peak acceleration may be proportional to peak pressure.

Projectile setback shock is much more complex in character than was previously thought. In addition to high-frequency high-g ringing, there is an unusually abrupt change in acceleration during the first few milliseconds of projectile travel. The effect of shock of this character on simple mechanical systems can be extremely severe. Spectra of the portions of the shock measured show that responses to projectile setback shock can range as high as three to four times the principal pulse peaks. In addition, examination of the response spectra of the five shock signatures analyzed, i.e., Nos. 1, 2, 3, 7, and 9, bears out the lack of significant frequency content beyond 11 kHz.

The apparatus and instrumentation used to record gun shock proved successful enough to provide a significant amount of information on the character of projectile setback shock. By ruggedizing the instrumentation cable, there is little doubt that longer recording time can be achieved and that a more complete study can be made of this obviously complex shock. Barrel slap for one out of six rounds monitored was severe enough to affect transducer response adversely and to obscure most of the shock transient. This may pose a serious problem in monitoring shock in full-length guns.

## ACKNOWLEDGMENTS

The invaluable suggestions of those persons who reviewed this paper are gratefully acknowledged. A special measure of gratitude is extended to David Sloan and the personnel of the Naval Weapons Laboratory, Dahlgren, Va., without whom this interior ballistics investigation would have been impossible.

## Appendix

## TEST EQUIPMENT

The principal problems associated with hardwire methods for recording artillery projectile shock were known when the 5"/54 shock investigation was started. These were instrumentation cable separation, high transverse shock, the inability to photograph accurately the initial phase of projectile motion, and high electrical noise. The 5"/54 test barrel was shortened in an attempt to solve the first three problems. The electrical noise problem was solved by potting the shock transducers in hard epoxy. The succeeding paragraphs describe the test apparatus and discuss the techniques used to remedy the above problems.

### SHORTENED BARREL

The decision to cut off the barrel, which is normally more than 22 ft long, to a length of 72 in. was primarily based on three considerations. The first consideration was the pressure-distance curve for the Mk 18 barrel. This curve shows that the peak chamber pressure occurs within 72 in. from the breech.

The second consideration was that of preserving the integrity of the instrumentation cable. By using the shortened barrel, the cable was unconfined and allowed to fall away as the projectile moved out of the barrel, thereby improving significantly the odds of cable survival.

The third consideration involved the accompanying transverse shock known as barrel slap. It was concluded that the chance of incurring barrel slap would be greatly reduced if the projectile travel were reduced. The projectile orientation after ramming and just prior to firing is shown in Fig. A-1. Using this barrel, the total travel of the projectile was 28.70 in.

Fig. A-1 - Cross section of barrel showing projectile prior to firing

## OBTURATORS

An obturator is a device designed to prevent the escape of propellant gases between the projectile and the barrel. In this investigation it was essential that any leakage be reduced to a minimum to prevent damage to the instrumentation cable. It was found that both the heat and the pressure blast reduce the life of the cable. Since cable life is the limiting factor in the acceleration recording process, it is imperative that an obturator be used with each instrumented round. In addition, the use of an obturator allows better camera coverage of the projectile motion.

The first attempt at constructing an obturator resulted in the high Durometer nitrile rubber (US-19D) cup shown in Fig. A-2. This cup was epoxied to the base of the projectile and was designed to expand against the barrel as the propellent gases filled the cup. High-speed motion pictures revealed that the cup remained attached to the projectile as it exited the barrel; however, the propellent gases could be seen escaping ahead of the projectile. In fact, the gases led the projectile for approximately 8 ft before falling behind. In addition, it was felt that the 0.3-in. thick rubber base of the obturator cup was possibly attenuating some of the higher frequency components of the shock. Consequently, an obturator which leaves the base of the projectile bare was desired.

The second obturator consisted of a ring of nylon plastic, type FM 101, molded in the form of a rotating band. This obturator ring was epoxied directly behind the copper rotating band as shown in Fig. A-3. The nylon creates a good gas seal and is easily engraved by the rifling. Motion pictures taken at 8000 frames per second showed no perceptible gas leakage past the obturator ring until it cleared the muzzle (Fig. A-4). These obturators led to a considerable increase in the duration of the recorded setback transient, i.e., 2 msec of data without the obturator versus 4 to 5 msec with the obturator. In addition, the new obturator appears to have significantly reduced barrel slap.

## ACCELEROMETERS

The projectile acceleration was measured with an 80-kHz natural frequency, undamped, piezoelectric crystal accelerometer with linear response to 50,000 g. To eliminate ground loops, the accelerometer had to be electrically isolated from the projectile ground. The accelerometer was isolated by potting it with a rigid

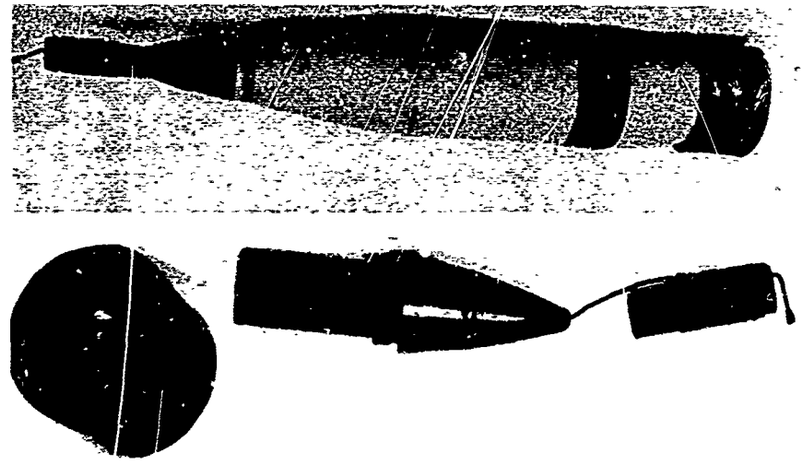

Fig. A-2 - Obturator cup, instrumented fuze, and Mk 41 Mod 0 projectile with cup and fuze attached

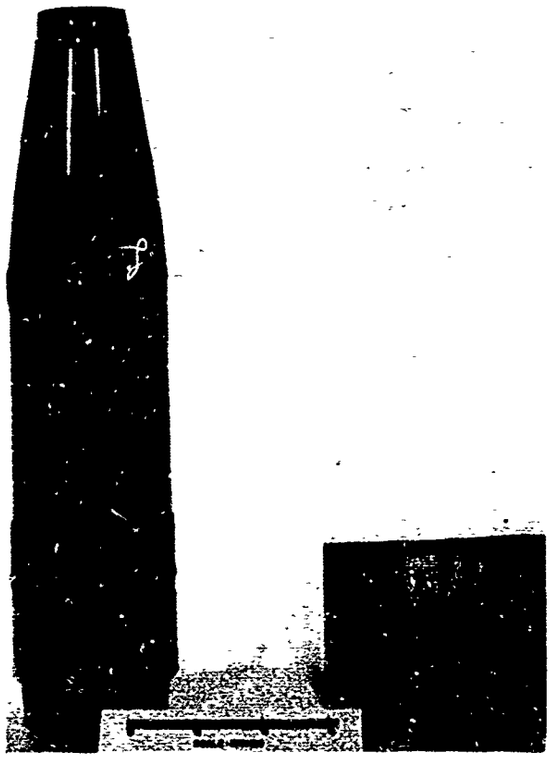

Fig. A-3 - Nylon obturator ring, projectile with ring attached

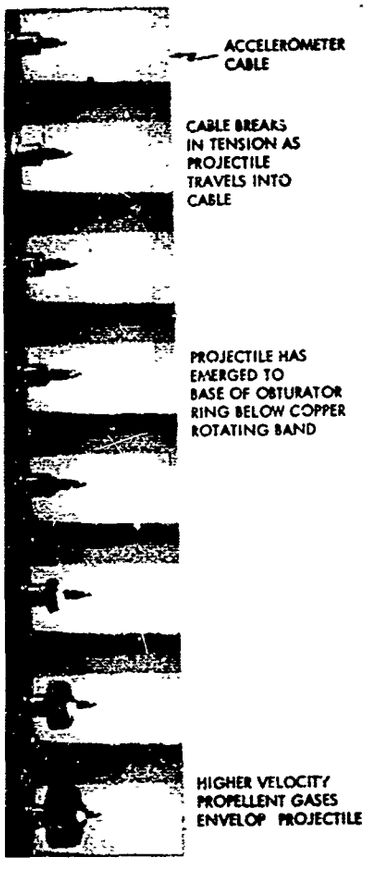


Fig. A-4 - Pictures at 8000 frames/sec showing projectile exciting barrel and obturator ring preventing blow-by

epoxy in an aluminum housing that replaced a component in the fuze sleeve. This location in the fuze was a point of principal interest and was considered to be the location where the shock would be most complex. As expected, the accelerometer in this location experienced the fundamental longitudinal natural frequency of the steel fuze sleeve. Figure A-5 shows the orientation of the accelerometer assembly. Drop tests in the laboratory showed that the potting caused negligible degradation of the accelerometer response.

## INSTRUMENTATION CABLE

The accelerometer output was hardwired to a recording system in the instrumentation van located 175 ft behind the gun. The cable used to transmit the signal was a low noise

Fig. A-5 - Cross section of fuze and potted accelerometer

coaxial type designed to be insensitive to shock and to withstand temperatures up to 500°F. To protect the first 2 ft of cable from any propellent gases that might leak by the obturator, the cable was fed through a 1/2-in. O.D. aluminum tube attached to the nose of the fuze. This stinger, when capped with a rubber tip, cushioned the load on the cable as the projectile overtook it upon firing.

In an attempt to accelerate the cable along with the projectile and thus increase the time before the projectile breaks the cable in tension, the cable was preloaded to a 15-lb tensile load using elastic shock cord. Tests in the laboratory were made to insure that the 15-lb load on the cable would not plastically deform it.

## RECORDING AND DATA ANALYSIS EQUIPMENT

The transducer output was fed into a charge amplifier used to condition the signal before going into a magnetic tape recorder. The charge amplifier has a frequency response flat from dc to 100 kHz. The magnetic tape recorder, operating in the FM mode, has a frequency response from dc to 20 kHz. A tape recording of the data was desired to perform additional data analysis such as electronic integration and shock spectrum analysis. To be sure that the recording system had a high enough frequency response, the shock pulse for shot 8 was also recorded on an oscilloscope (frequency response dc to 10 MHz). Figure A-6 is a picture of the oscilloscope recording and shows no frequency content much beyond 11 kHz. It is evident that a 20-kHz flat recording system should faithfully record the shock signature.

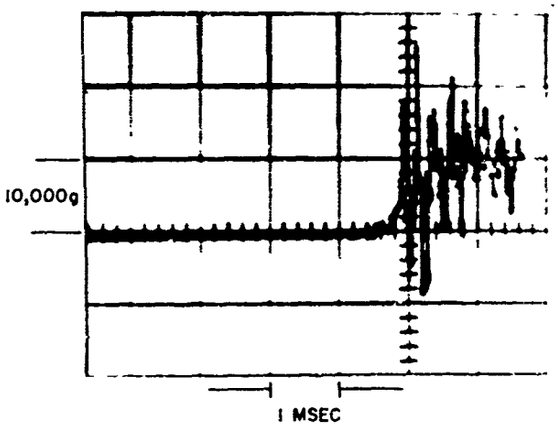


Fig. A-6 - Oscilloscope record of shock signature, shot 8 without obturator

Analysis of the data consisted of obtaining a shock spectrum for the shock transient, electronically integrating, and electronically fairing the pulses.

Briefly, a shock spectrum is a plot of the maximum absolute values of the response of a set of single-degree-of-freedom (s-d-o-f) oscillators which have been subjected to the shock transient. The values are plotted as a function of the natural frequency of the s-d-o-f oscillators. An analog computer was used to simulate electrically the s-d-o-f oscillators. The shock spectra for data recorded during these tests were obtained by playing back the recorded shock transients into a series of oscillators from 4 to 20 kHz.

Integration of the shock transient was desired to determine the projectile's velocity at the instant the cable shorted. Integration was performed electronically by reducing the recorder playback speed and feeding the signal into an operational amplifier wired as an integrator. The velocity-time curve was a very smooth transient; therefore, a second integration to find the displacement could be easily performed graphically. Figure A-7 shows a schematic of the integration circuit.

To identify the principal parameters of the partial shock measured, the pulses were faired

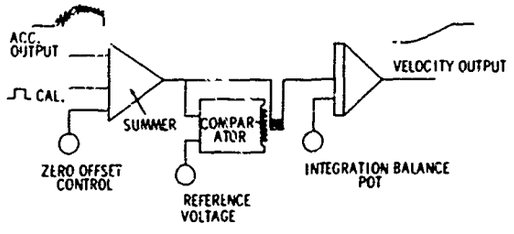


Fig. A-7 - Schematic of integration circuit

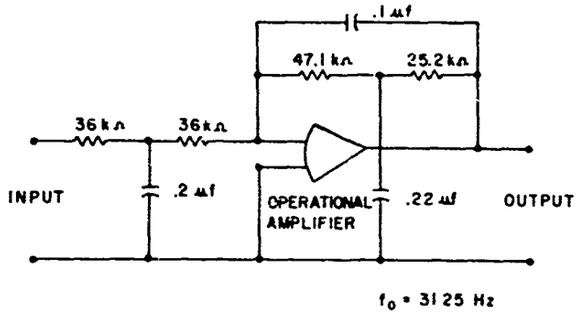


Fig. A-8 - Active low-pass filter

electronically. Fairing was accomplished by playing back the tape recorded pulses into an active low-pass filter. The cutoff frequency was set for 31.25 Hz; this is equivalent to using a 1000-Hz low-pass filter since the data are slowed down by a factor of 32 during playback. Figure A-8 is the circuit used for the filter.

## DISCUSSION

Mr. Hanks (NASA Langley Research Ctr.): I used Microdot cable with accelerometers in measuring the impact of projectiles and found accelerations and times similar to those you had. We discovered that cable whip affected the data. Did you have any similar problems in your work?

Mr. Hughes: Initially we used the standard orange Microdot cable which is very sensitive to jerking. An accelerometer signal would wobble all over an oscilloscope when the cable was jerked. But the new cables by Endevco and Kistler, the red and blue cables, are very insensitive to this sort of thing. You can jerk them until they break, and the accelerometer shows little drift. That is what we used here. In addition, the cable is stable at 500°F.

Mr. Schell (AF Flight Dynamics Lab.): You mentioned that you got 2600 fps. Did that apply to the velocity at the end of the unsawed-off barrel?

Mr. Hughes: That is correct.

Mr. Schell: And your exit velocity was about 1200 fps in this particular test. What accelerations did you have coming out of the barrel on this test?

Mr. Hughes: We got faired values. In other words, you fair electronically through the high frequency between 6 and 10,000 g with a high-frequency ringing of about 50 percent over this.

Mr. Arnold (Honeywell, Inc.): With 300 ft of cable, did you consider the other electrical characteristics of the cable, such as inductance and capacitance between the wires at 10,000 Hz? I think that could be a significant portion of the data that you are reading, and you would not even realize that you have quite a filter in the system.

Mr. Hughes: I do not think that the length of the cable would have any effect up to 10,000 Hz. You may have a point, but I don't think our electronics people have experienced this sort of thing.

Mr. Arnold: We had those problems, so you might look into it.

* * *

# SIMULATION OF HEAT SHIELD PYROTECHNIC SHOCK IMPEDANCE

Norris J. Huffington, Jr., and Robert L. Goldman
The Martin Company
Baltimore, Maryland

It frequently occurs that dynamics experiments must be conducted on a test article which differs in some respect from its prototype. An example of this situation arose when pyrotechnic shock tests had to be made on a reentry vehicle before the production heat shield became available. It was necessary to assess in advance whether dynamic simulation of an actual heat shield was feasible and whether tests performed with such a simulation could be used to develop prototype design criteria. These objectives were satisfied by formulating a theory for the motion of a strip of two-layered surface and using this theory to compare the wave propagation characteristics of a simulated heat shield with those of the actual heat shield. The feasibility of accomplishing a practical match of phase velocities and attenuation factors over a wide range of frequencies was explored in detail before concluding that an adequate simulation could be achieved.

N. J Huffington, Jr.

## INTRODUCTION

The damaging potential of stress waves caused by pyrotechnic shock is often a critical consideration in the design of an aerospace vehicle. These shocks may give rise to equipment acceleration levels far exceeding design capability. Prediction of shock environment is, therefore, a primary problem in establishing equipment qualification levels. The actual analytical prediction of pyrotechnic shock environment, however, is usually so difficult that the designer must base his predictions on a tenuous extrapolation of previous experimental experience. This prediction can often be improved by performing ground tests on a suitable simulation of the actual hardware. The basis for the simulation, however, must take into consideration the mechanical impedance properties of the structural paths between the pyrotechnic device and the critical components. Recent experience with such a test article for simulation of a "lifting body" reentry vehicle has led to an analytical procedure that proved to be most useful in design. In this application the basic structural body of the reentry vehicle is a conventional arrangement of aluminum skin, stringers and frames covered with a low-density silicon elastomer ablator. Pyrotechnic devices are used for vehicle separation, drogue chute deployment, drogue chute release and hatch ejection. For the pyrotechnic shock tests, a full-scale instrumented dynamic test article was planned which would be structurally identical to the flight vehicle except for the heat shield. The application of this heat shield to doubly curved portions is a tedious procedure, entailing an extended thermal curing cycle. In the interest of avoiding undue delays and costs, it was preferred to use a substitute layer of an easily applied viscoelastic material which would simulate the dynamic characteristics of the actual heat shield.

This paper is concerned with the establishment of criteria for equivalence between the mechanical impedance properties of the actual and substitute heat shields. The approach utilized, believed unique, entails comparison of stress wave propagation properties of analytical models for the heat shields and their substructure.

## DEFINITION OF SYMBOLS

$A, B, C$ Amplitude coefficients

$E_1, E_2$ Young's moduli of layers 1 and 2, respectively

$F_1, F_2$ Axial force resultants

$G_{xy}$ Shear modulus of heat shield

$H_{xy}$ Damping modulus of heat shield

$M_1, M_2$ Bending moments

$S_1, S_2$ Transverse shear forces

$c_j$ Phase velocity ($j$th branch)

$f_j$ Frequency (cps)

$h_1, h_2$ Thicknesses of layers 1 and 2, respectively

$k$ Shear coefficient

$n$ Wave number ($= 2\pi/\lambda$)

$t$ Time

$u$ Axial displacement

$u_a$ Uniform portion of axial displacement

$v$ Transverse displacement

$v_b, v_s$ Transverse displacements in bending and shear, respectively

$x, y$ Axial and transverse position coordinates, respectively

$\Omega_j$ Real circular frequency ($j$th branch)

$\alpha$ Attenuation coefficient

$\gamma_{xy}$ Shearing strain

$\epsilon_x$ Dilatational strain

$\lambda$ Wavelength

$\rho_1, \rho_2$ Mass densities of layers 1 and 2, respectively

$\sigma$ Normal stress at interface between layers

$\sigma_x$ Normal stress in axial direction

$\tau$ Shearing stress at interface between layers

$\tau_{xy}$ Shearing stress acting in $xy$-plane

$\psi$ Angle of rotation of cross section of layer 2

$\omega$ Circular frequency

## MATHEMATICAL MODEL

A simple model for the heat shield coated structure, which appears adequate for the purpose of comparing wave propagation characteristics, is a two-layered beam (Fig. 1) which may be regarded as a strip of the shell structure having unit width. Layer 1 represents the metallic substructure, which is composed of an isotropic material having Young's modulus $E_1$. It is assumed that this layer deforms by elongation and flexure but not by transverse shear. Consequently, its displacements may be expressed as

$$u = u_a(x,t) - y\frac{\partial v}{\partial x} \quad \text{and} \quad v = v(x,t), \tag{1}$$

and its strain components as

$$\epsilon_x = \frac{\partial u_a}{\partial x} - y\frac{\partial^2 v}{\partial x^2}, \qquad \gamma_{xy} = 0. \tag{2}$$

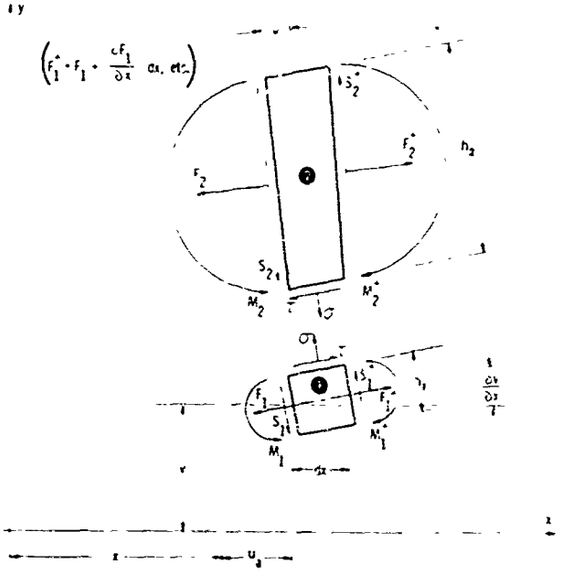

Fig. 1 - Exploded view of element of beam model

The corresponding axial force and bending moment are

$$F_1 = E_1 h_1 \frac{\partial u_a}{\partial x} \tag{3}$$

and

$$M_1 = -\frac{E_1 h_1^3}{12} \frac{\partial^2 v}{\partial x^2} \tag{4}$$

Layer 2 is the heat shield, composed of a relatively weak material, that is anisotropic, mainly due to the presence of ribbons of glass laminate which serve to retain the char. However, only those properties associated with deformation in the xy-plane are required for this analysis. The material dissipates a significant amount of energy by the mechanism of transverse shear deformation. The simplest constitutive function which describes this behavior and is in reasonable agreement with physical evidence may be expressed as

$$\begin{aligned} \sigma_x &= E_2 \epsilon_x , \\ \tau_{xy} &= G_{xy} \gamma_{xy} + \frac{H_{xy}}{\omega} \frac{\partial \gamma_{xy}}{\partial t} . \end{aligned} \tag{5}$$

This form of damping, in which the damping coefficient $H_{xy}$ is divided by the circular frequency $\omega$ to remove the linear frequency dependence of the energy dissipation, is usually termed "hysteretic damping" [1]. While transverse sections of layer 2 do not actually remain plane during deformation, the displacements are expressed in this manner on the basis that a Timoshenko-type beam theory will result. On this basis the displacements in layer 2 may be expressed as

$$\begin{aligned} u &= u_a(x,t) - \frac{h_1}{2} \frac{\partial v}{\partial x} - \left(y - \frac{h_1}{2}\right) \psi(x,t) \\ &\text{and} \\ v &= v_b(x,t) + v_s(x,t) . \end{aligned} \tag{6}$$

These expressions also provide for continuity of displacements at the interface between layers 1 and 2. The strain-displacement relations for layer 2 become

$$\epsilon_x = \frac{\partial u_a}{\partial x} - \frac{h_1}{2} \frac{\partial^2 v}{\partial x^2} - \left(y - \frac{h_1}{2}\right) \frac{\partial \psi}{\partial x}$$

and (7)

$$\gamma_{xy} = \frac{\partial v_s}{\partial x} = \frac{\partial v}{\partial x} - \psi .$$

The associated relations for the axial force, bending moment, and transverse shear force acting on a cross section of the heat shield are:

$$F_2 = E_2 h_2 \left( \frac{\partial u_a}{\partial x} - \frac{h_1}{2} \frac{\partial^2 v}{\partial x^2} - \frac{h_2}{2} \frac{\partial \psi}{\partial x} \right) . \tag{8}$$

$$M_2 = -\frac{E_2 h_2^3}{12} \frac{\partial \psi}{\partial x} . \tag{9}$$

and

$$S_2 = k h_2 \left[ G_{xy} \left( \frac{\partial v}{\partial x} - \psi \right) + \frac{H_{xy}}{\omega} \left( \frac{\partial^2 v}{\partial x \partial t} - \frac{\partial \psi}{\partial t} \right) \right] . \tag{10}$$

In Eq. (10), k is the Timoshenko shear coefficient which accounts for the variation of the shearing stresses over the cross section (and the accompanying distortion of the section). From considerations discussed in Appendix A of Ref. 2, the value k = 5/6 has been selected for use in subsequent numerical analyses.

## EQUATIONS OF MOTION

The differential equations of motion for the beam elements shown in Fig. 1, obtainable by summation of forces in the longitudinal and transverse directions and summation of moments about the mass centers, are for layer 1

$$\frac{\partial F_1}{\partial x} + \tau = \rho_1 h_1 \frac{\partial^2 u_a}{\partial t^2} . \tag{11}$$

$$\frac{\partial S_1}{\partial x} + \sigma = \rho_1 h_1 \frac{\partial^2 v}{\partial t^2} , \tag{12}$$

and

$$S_1 - \frac{\partial M_1}{\partial x} - \frac{h_1}{2} \tau = \frac{\rho_1 h_1^3}{12} \frac{\partial^3 v}{\partial x \partial t^2} . \tag{13}$$

and for layer 2

$$\frac{\partial F_2}{\partial x} - \tau = \rho_2 h_2 \left( \frac{\partial^2 u_a}{\partial t^2} - \frac{h_1}{2} \frac{\partial^3 v}{\partial x \partial t^2} - \frac{h_2}{2} \frac{\partial^2 \psi}{\partial t^2} \right) . \tag{14}$$

$$\frac{\partial S_2}{\partial x} - \sigma = \rho_2 h_2 \frac{\partial^2 v}{\partial t^2} . \tag{15}$$

and

$$S_2 - \frac{\partial M_2}{\partial x} - \frac{h_2}{2} \tau = \frac{\rho_2 h_2^3}{12} \frac{\partial^2 \psi}{\partial t^2} . \tag{16}$$

In the formulation of these equations, certain nonlinear coupling terms were omitted on the premise that a small deflection, linearly elasti analysis would be adequate. This assumption

appears reasonable since it was known in advance that the permanent deformation would be limited to the immediate neighborhood of the pyrotechnic detonation. Thus, the analysis will serve to answer the question as to whether the use of a simulated heat shield would significantly affect the elastic wave transmission characteristics of the structure while the test program will determine whether elastic stress waves of sufficient intensity to damage delicate equipment will reach the equipment locations.

The relations of the preceding formulation may be readily combined to obtain the three partial differential equations for the dependent variables $u_a$, $v$, and $\psi$. Substituting the values of $F_1$ and $F_2$ from Eqs. (3) and (8) into Eqs. (11) and (14) and adding the latter equations gives:

$$(E_1h_1 + E_2h_2)\frac{\partial^2 u_a}{\partial x^2} - \frac{E_2h_2}{2}\left(h_1\frac{\partial^3 v}{\partial x^3} + h_2\frac{\partial^2 \psi}{\partial x^2}\right)$$

$$= (\rho_1h_1 + \rho_2h_2)\frac{\partial^2 u_a}{\partial t^2} - \frac{\rho_2h_2}{2}\left(h_1\frac{\partial^3 v}{\partial x \partial t^2} + h_2\frac{\partial^2 \psi}{\partial t^2}\right). \tag{17}$$

The second equation of motion can be derived by using Eqs. (13) and (16) to eliminate $\tau$, solving the result for $S_1$. This expression plus the one for $S_2$ given by Eq. (10) may then be introduced into the relation obtained by adding Eqs. (12) and (15). The desired equation may then be expressed as:

$$E_1h_1^3\frac{\partial^4 v}{\partial x^4} + 12(\rho_1h_1 + \rho_2h_2)\frac{\partial^2 v}{\partial t^2} - \rho_1h_1^3\frac{\partial^4 v}{\partial x^2 \partial t^2}$$

$$= h_1h_2^2\left(E_2\frac{\partial^3 \psi}{\partial x^3} - \rho_2\frac{\partial^3 \psi}{\partial x \partial t^2}\right) + 12k(h_1 + h_2)$$

$$\times\left\{G_{xy}\left(\frac{\partial^2 v}{\partial x^2} - \frac{\partial \psi}{\partial x}\right) + \frac{H_{xy}}{\omega}\left(\frac{\partial^3 v}{\partial x^2 \partial t} - \frac{\partial^2 \psi}{\partial x \partial t}\right)\right\}. \tag{18}$$

The third equation of motion may be obtained by subtracting Eq. (14) from Eq. (11) and introducing the resulting expression for $\tau$ into Eq. (16) along with the preceding relations for $F_1$, $F_2$, $M_1$, $M_2$, and $S_2$. This manipulation yields:

$$5E_2h_2^3\frac{\partial^2 \psi}{\partial x^2} + 3E_2h_1h_2^2\frac{\partial^3 v}{\partial x^3} + 6h_2(E_1h_1 - E_2h_2)\frac{\partial^2 u_a}{\partial x^2}$$

$$+ 24kh_2\left\{G_{xy}\left(\frac{\partial v}{\partial x} - \psi\right) + \frac{H_{xy}}{\omega}\left(\frac{\partial^2 v}{\partial x \partial t} - \frac{\partial \psi}{\partial t}\right)\right\}$$

$$= 5\rho_2h_2^3\frac{\partial^2 \psi}{\partial t^2} + 3\rho_1h_1h_2^2\frac{\partial^3 v}{\partial x \partial t^2} + 6h_2(\rho_1h_1 - \rho_2h_2)\frac{\partial^2 u_a}{\partial t^2}. \tag{19}$$

The latter three equations, which are of hyperbolic type, are suitable for investigating both standing and traveling wave motions of the layered structure.* It may be readily verified that these equations approach the proper limiting forms as the thickness of either layer approaches zero.

## TRAVELING WAVE SOLUTIONS

To compare the wave transmission characteristics of the actual and simulated heat shields, the problem of traveling waves in an unbounded specimen has been treated. Consider the infinite train of sinusoidal waves, progressing in the positive sense, represented by the displacements

$$u_a = Ah_1e^{i(nx-\omega t)},$$

$$\psi = Be^{i(nx-\omega t)}, \tag{20}$$

and

$$v = Ch_1e^{i(nx-\omega t)},$$

where $n$ is the wave number. Since the beam is unbounded, $n$ may be prescribed as a continuous parameter. When these displacements are substituted into the equations of motion, three homogeneous equations in the amplitudes A, B, C are obtained and the frequencies are determined as eigenvalues of this set of equations. After some manipulation, the frequency equation may be represented as the bi-cubic

$$e_6\omega^6 + e_4\omega^4 + e_2\omega^2 + e_0 = 0, \tag{21}$$

where

$$e_6 = \rho_2h_2^2(\rho_1h_1 + \rho_2h_2)\left\{\rho_1h_1^3n^2 + 3(4\rho_1h_1 + \rho_2h_2)\right\}$$

$$e_4 = -\Big[h_1^3h_2^2\left\{(E_1\rho_2 + E_2\rho_1)(\rho_1h_1 + \rho_2h_2)\right.$$

$$\left. + \rho_1\rho_2(E_1h_1 + E_2h_2)\right\}n^4$$

$$+ 3\left\{2h_2^2(2E_1\rho_2h_1 + 2E_2\rho_1h_1 + E_2\rho_2h_2)(\rho_1h_1 + \rho_2h_2)\right.$$

$$+ k(\rho_1^2h_1^4 + 2\rho_1\rho_2h_1h_2[2h_1^2 + 3h_1h_2 + 2h_2^2]$$

$$\left. + \rho_2^2h_2^4)(G_{xy} - iH_{xy})\right\}n^2$$

$$+ 36k(\rho_1h_1 + \rho_2h_2)^2(G_{xy} - iH_{xy})\Big].$$

*After completion of this analysis, the authors became aware of a report [3] in which a rather general formulation for the vibration of two-layered plates is derived by the variational method. However, Ren and Yu introduced damping in a somewhat different manner and were not concerned with the application of this theory made in the present paper.

$$e_2 = h_1^3 h_2^2 \left\{ F_1^2 \rho_2 h_1 + 2E_1 E_2 (\rho_1 h_1 + \rho_2 h_2) + E_2^2 \rho_1 h_2 \right\} n^6$$

$$+ 3\left\{ E_2 h_2^2 (4E_1 h_1 + E_2 h_2)(\rho_1 h_1 + \rho_2 h_2) \right.$$

$$+ 2k\left[ E_1 \rho_1 h_1^4 + (E_1 \rho_2 + E_2 \rho_1)(2h_1^2 + 3h_1 h_2 \right.$$

$$\left. \left. + 2h_2^2) h_1 h_2 + E_2 \rho_2 h_2^4 \right] (G_{xy} + iH_{xy}) \right\} n^4$$

$$+ 36k(E_1 h_1 + E_2 h_2)(\rho_1 h_1 + \rho_2 h_2)(G_{xy} + iH_{xy}) n^2 ,$$

and

$$e_0 = -\left\{ E_1 E_2 h_1^3 h_2^2 (F_1 h_1 + E_2 h_2) n^8 \right.$$

$$+ 3k\left\{ F_1^2 h_1^4 + 2F_1 F_2 h_1 h_2 (2h_1^2 + 3h_1 h_2 + 2h_2^2) \right.$$

$$\left. \left. + E_2^2 h_2^4 \right\} (G_{xy} + iH_{xy}) n^6 \right]$$

Equation (21) provides three roots for $c^2$ for each assigned value of $n$. These roots are complex numbers except where $H_{xy} = 0$. Letting

$$\omega_j(n) = \alpha_j + i\beta_j \qquad (j = 1,2,3) , \qquad (22)$$

a typical displacement may be expressed in the forms

$$u_a = A_j h_1 e^{\beta_j t} e^{i(nx - \Omega_j t)} = A_j h_1 e^{\beta_j t} e^{\frac{2\pi i}{\lambda}(x - c_j t)} , \qquad (23)$$

where the phase velocity $c_j = \Omega_j / n$. It is seen that the sinusoidal wave train is subjected to the attenuating factor $e^{\beta_j t}$ (for negative $\beta_j$). The space-wise attenuation factor per unit length of beam is, therefore, $e^{\beta_j / c_j}$.

## RESULTS OF CALCULATIONS

Although it is conventional to plot phase velocity versus wave number, it is more convenient for the present application to display the phase velocity as a function of frequency, as shown in Fig. 2. The solid lines in this figure represent the three-phase velocity branches associated with the three roots of Eq. (21) for a layered structure consisting of 0.063 in. of aluminum alloy plus 0.875 in. of partially charred heat shield. The dashed lines are the corresponding curves for the same substructure plus a 1.00-in. thick layer of a candidate substitute for the actual heat shield (Type 300 material). The material properties employed in the construction of these curves are listed in Table 1. The values of elastic moduli were obtained from static tests on small specimens, while the values of the damping modulus were determined from decay measurements. The Type 300 material is similar to the ablator in the heat shield

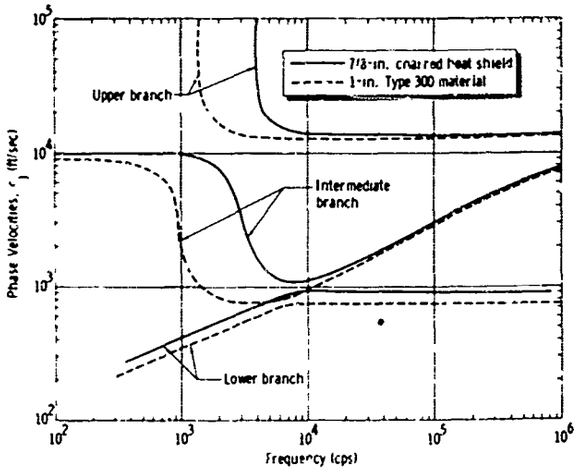


Fig. 2 - Phase velocity spectrum for surface layer

TABLE 1
Heat Shield Material Properties

| Material | $E_2$ (psi) | $G_{xy}$ (psi) | $H_{xy}$ (psi) | $\rho_2$ (pcf) |
|---|---|---|---|---|
| Partially charred heat shield | 4000 | 3065 | 800 | 22.0 |
| Type 300 | 3100 | 600 | 168 | 24.5 |

but could be applied with a trowel at room temperature and was easy to remove. It is relatively weak in shear due to the absence of any cellular reinforcement.

Although the evaluation of intermediate points on the phase velocity curves is a tedious procedure best performed on a computer, certain limiting properties of these curves can be expressed in closed form. The lower branch ($j = 1$) begins at $f_1 = 0$, $c_1 = 0$ corresponding to $n = 0$, where the mode is purely lateral oscillation ($A = B = 0$). This mode is also predominantly lateral motion for frequencies up to 1000 cps, then becomes coupled motion involving all three displacement variables for intermediate frequencies (1000-7500 cps), and finally becomes principally motion in the $\psi$ variable at higher frequencies. This lower branch asymptotically approaches the phase velocity $c_1 = \sqrt{E_2/\rho_2}$ as $n \to \infty$.

For the intermediate branch ($j = 2$) at $n = 0$, $f_2 = 0$ and

$$c_2 = \sqrt{E_1 h_1 + E_2 h_2 / \rho_1 h_1 + \rho_2 h_2} . \qquad (24)$$

At this limit the mode is purely longitudinal oscillation ($B = C = 0$) and the same is preponderantly true at low frequencies. In the intermediate frequency range, the mode involves all three variables, while at higher frequencies $u_a$ again becomes dominant. The asymptotic phase velocity for this branch as $n \to \infty$ is also given by Eq. (24).

The higher branch ($j = 3$) commences at a cutoff frequency given by

$$\omega_3 = \sqrt{\frac{12k(\rho_1 h_1 + \rho_2 h_2)(G_{xy} - iH_{xy})}{\rho_2 h_2^2 (4\rho_1 h_1 + \rho_2 h_2)}} \qquad (25)$$

corresponding to $n = 0$. At this limit the phase velocity $c_3$ is unbounded and the vibratory mode is a combination of the $u_a$ and $\psi$ variables; i.e., $B/A = 2n_1(\rho_1 h_1 + \rho_2 h_2)/\rho_2 h_2^2$, $C = 0$. For the intermediate frequency range the eigenvector is principally composed of the same variables. This branch approaches the phase velocity $c_3 = \sqrt{E_1/\rho_1}$ as $n \to \infty$.

## APPLICATION OF THEORY

A perfect simulation cannot be achieved unless all the relevant material properties are matched. However, the preceding analysis can be used to determine whether a moderate mismatch of certain properties has any serious effect on the simulation. Calculations were made for different thicknesses of the heat shield, in both the uncharred and partially charred condition, and for several substitute materials. For simplicity, only results corresponding to the data of Table 1 will be presented but these may be regarded as representative.

It may be seen from Fig. 2 that the lower branch curve for the Type 300 material is somewhat below that for the heat shield throughout the frequency spectrum. This is almost entirely due to the disparity in the values of the ratio $E_2/\rho_2$ for these materials. If this ratio were the only criterion, it would not be difficult to obtain a satisfactory substitute material. Turning to the second branch, it may be noted that the agreement between curves is good up to about 500 cps. This is because the thickness of the substitute material was selected to provide a match of the intermediate branch phase velocities given by Eq. (24). The thickness for the substitute material was actually calculated using properties of the uncharred heat shield but the match is still good for the charred case. Since $E_2 h_2 \ll E_1 h_1$, this procedure amounts to matching the masses per unit area.

The only other significant differences in the phase velocity curves are for branches 2 and 3 in the frequency range from 1 to 10 kc. These differences result from the sizable discrepancy in the shear moduli (Table 1). It seems unlikely that the shear modulus of the Type 300 material could be increased significantly without providing a honeycomb core bonded to the substructure, similar to the actual heat shield. Of course, resort to the latter would defeat the purpose of the simulation. That this predicament is not too serious can be seen by observing Fig. 3, which shows the frequency dependence of the spatial attenuation coefficient $\beta_j/c_j$ for both materials. As might be anticipated, in the frequency range of concern, where the shear deformation is significant, the damping in both actual and substitute heat shields is appreciable. Consequently, even though modes in this range may not be faithfully matched, excitation of the surface structure in this frequency band will be rapidly attenuated and will not contribute to the vibration level which is subsequently experienced at the internal locations of sensitive equipment. (It would have been possible also to introduce damping proportional to the dilatation. This added complexity was avoided since this mechanism is believed to be relatively ineffective in comparison to shear deformation. However, had this effect been included, the principal modification to the present results would have been an increase in the attenuation in the low-frequency range.) It should be noted that Fig. 3 shows the spectrum of the spatial attenuation factor $\beta_j/c_j$, whereas the temporal factor $\beta_j$ is a much larger number. This observation is particularly significant when assessing the damping in the third branch modes.

Although the possibility of matching the phase velocities and attenuation factors has been considered for the complete frequency spectrum, it is only necessary that a reasonable match be achieved for the range of frequencies in which practically important modes occur. In the present application, the fundamental structural frequency is in the neighborhood of 12 cps, with about 20 modes below 100 cps and many more below 1 kc. From this it may be inferred that even the Type 300 material would provide an adequate simulation for modes up to and beyond those for which meaningful calculations can be made.

## CONCLUDING REMARKS

A procedure has been presented whereby the structural impedances of a prototype vehicle

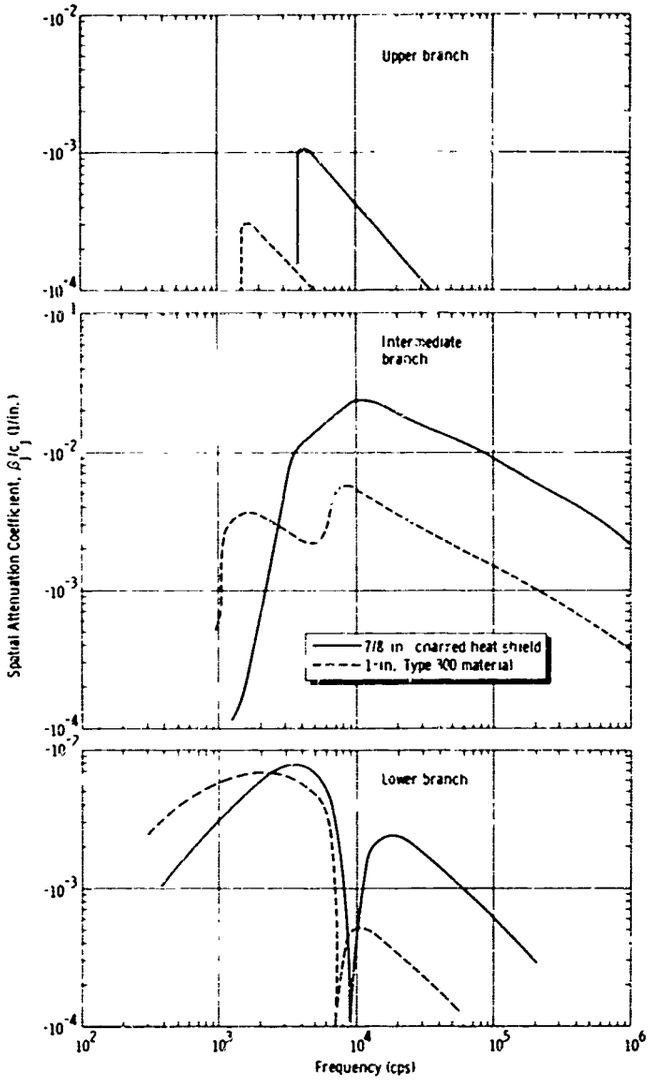


Fig. 3 - Spatial attenuation factor spectrum

and a similar test article (differing only in surface coating) can be contrasted. This procedure, based on an analysis of the wave propagation characteristics of the layered surface, appears to be of wider applicability than the present application. It is especially appropriate where the excitation spectrum is strong in the frequency band corresponding to the higher modes of the structure, where the calculation of response of discrete modes is difficult, if not impossible.

While the extent of mismatch tolerable in wave propagation characteristics will vary with the application, the considerations discussed in this paper should serve as a guide in establishing criteria for acceptability.

## ACKNOWLEDGMENT

The authors wish to thank G. K. Jones for his assistance with the evaluation of the roots of the frequency equation.

## REFERENCES

1. T. J. Mentel and C. C. Fu, "Analytical Formulation of Damped Stress-Strain Relations Based on Experimental Data With Applications to Vibrating Structures," ASD Tech. Rept. 61-623, Nov. 1961

2. N. J. Huffington, Jr., "The Response of Missile Structures to High Velocity Longitudinal Impact," Martin Co. Res. Rept. RR-17, Nov. 1960

3. Nann Ren and Yi-Yuan Yu, "Vibrations of Two-Layered Plates," AFOSR 65-1423, June 1965

## DISCUSSION

Mr. Himelblau (North American Aviation, Inc.): Did you apply a specific shock loading and try to establish the response at some other place in the structure?

Mr. Huffington: This structure was shock tested by firing the actual pyrotechnics. The analysis that I am discussing was used to establish that such tests could be valid. I do not know whether this answers your question or not.

Mr. Himelblau: It almost asks another because I understand that if you use hysteretic damping for shock or random vibration, or anything other than a sinusoid, the solution does not satisfy the basic equations of motion.

Mr. Huffington: I do not think that anyone can argue that hysteretic damping is an exact representation of structural damping, but I think it is better than simply ignoring the dependence on frequency as is done extensively. It is a matter of where to introduce the damping law into the derivation. We chose to introduce it in the stress-strain relation. In any event my solution was for a sine wave so there is no difficulty in treating hysteretic damping.

Mr. Himelblau: I am only concerned really with trying to use this technique to obtain a close form solution to a given shock waveform. This is the context in which my question was asked.

* * *

# PYROTECHNIC SHOCK TESTING OF A FULL-SCALE REENTRY VEHICLE

W. R. Britton and G. K. Jones
The Martin Company
Baltimore, Maryland

A series of pyrotechnic shock tests performed on a lifting reentry vehicle is described. The data presented show the dynamic responses of the vehicle when subjected to shock inputs generated by flexible linear shaped charges, explosive bolts, and pressure cartridges. Due to severe shock transients, various methods of attenuating these shock levels were investigated. The effects of various shock isolation techniques are also shown.

W. R. Britton

## INTRODUCTION

Pyrotechnic devices, due to their light weight and high reliability, are commonly used to initiate flight sequences during a spacecraft mission. One drawback to their use is the high shock transient generated at detonation of these systems. To evaluate the dynamic effects of the pyrotechnic shocks, such tests must be performed on a test model that is structurally identical to the flight article. Pyrotechnic devices used on the Martin SV-5 reentry vehicle (R/V) include flexible linear shaped charge (FLSC), explosive bolts and separation nuts with pressure cartridges.

While it is good design practice to locate shock sensitive components at a distance from the source, the configuration of the reentry vehicle precluded this approach. Therefore, it was necessary to develop and use shock attenuation devices in the regions of the vehicle that experienced shock levels in excess of the equipment qualification levels.

Three isolation techniques were used to reduce the shock levels: (a) isolating the shock source from the vehicle structure, (b) interposing an isolator in the structural path between the shock source and the component mounting location, and (c) isolating the components from the structure.

## TEST DESCRIPTION

### Test Article

Four series of pyrotechnic shock tests were performed on a full-scale Martin SV-5D lifting reentry test vehicle. The test article is an identical structure, including simulated components and a simulated flight-type heat shield. The simulated components represent the mass and center of gravity of the flight components and have identical mounting configurations. The test article heat shield was designed to simulate adequately the wave propagation characteristics of the flight vehicle heat shield [1].

The 7-ft long reentry vehicle weighed 890 lb and consisted of three major subassemblies: (a) the aft body which contained the flight control components and the recovery system; (b) the equipment truss, which was bolted to the aft body section and contained the guidance, control and electrical system components; and (c) the forward structure (glove), which was bolted to the aft body and served as an enclosure for the equipment truss. Figure 1 illustrates these major assemblies.

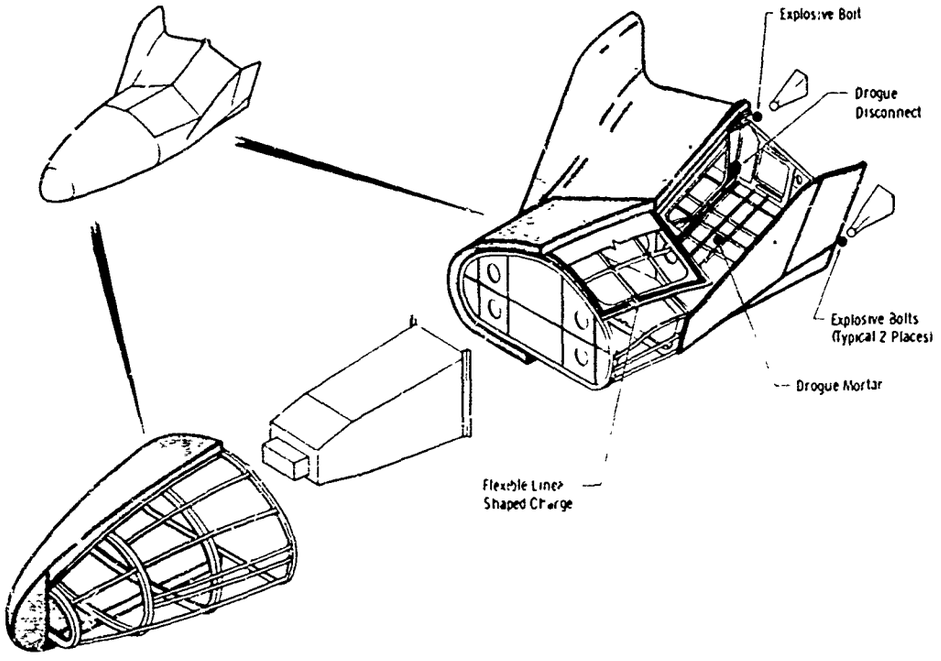


Fig. 1 - Location of pyrotechnic devices

## Pyrotechnic Devices

During the flight of the SV-5 vehicle, four major pyrotechnic devices will be detonated to initiate specific phases of that flight. Vehicle separation will be performed by the detonation of three explosive bolts attaching the aft bulkhead of the vehicle to the booster interstage.

The recovery compartment hatch, centrally located on the vehicle, is severed from the vehicle structure by the detonation of FLSC placed in the coaming around the perimeter of the hatch. The FLSC used in this configuration is 7 ft long with a charge density of 5 grains/ft.

The drogue, used to stabilize the R/V before deployment of the main parachute, is ejected for deployment by a mortar charge. This device is a gas-generating pyrotechnic, rather than the fragmentary type. The mortar charge generates an internal pressure in the drogue container and propels the drogue chute from the vehicle.

The drogue is separated from the vehicle by a pyrotechnic device (drogue disconnect) located on the aft bulkhead. The drogue disconnect consists of a pressure cartridge and separation nut.

## Instrumentation

Eighteen piezoelectric accelerometers were mounted on the test vehicle at selected locations on the structure (Fig. 2). The accelerometers were Endevco Model 2225 shock accelerometers designed for 20.000 g with a flat frequency response to 15 kHz and a mounting resonance of 80 kHz. Accelerometers were mounted on aluminum cubes, bolted and cemented to the structure. Usually two or three accelerometers were mounted on each cube providing multi-axis instrumentation. Response signals were processed through charge amplifiers and recorded on magnetic tape at 60 ips. Tape records of accelerometer signals were processed by playback at 1-7/8 ips to produce high-speed (63-ips) oscillograph records for on-site evaluation. The taped data were then processed using a recursive filter technique to obtain shock response spectra.

## Test Setup

The vehicle was mounted on a low-frequency suspension system, using 3/4-in. diameter shock absorber cord. Approximate flight attitudes were maintained to determine if trajectories cleared vehicle projections. High-speed

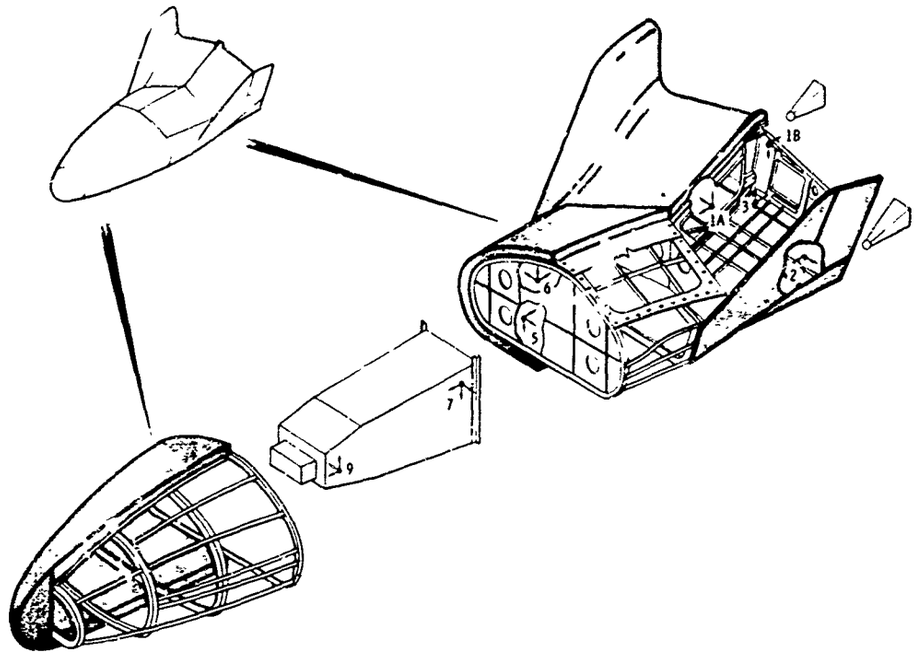


Fig. 2 - Accelerometer locations

Fig. 3 - Typical test arrangement (hatch separation test)

(1200 frames/sec) motion pictures showed total vehicle response and verified adequate clearances. A typical test is shown in Fig. 3.

## PRESENTATION AND DISCUSSION OF DATA

The severity and magnitude of the pyrotechnic shock transient was investigated through the use of shock response spectra. Shock response spectra were obtained from three drogue mortar tests, six drogue disconnect tests, five hatch separation tests and three booster separation tests. A selected number of the measured shock response spectra are presented in this paper.

### Drogue Mortar

The envelopes of the shock spectra measured at various locations on the test article during the drogue mortar tests are presented in Fig. 4. The peak shock spectrum levels ranged from 1790 g at 3.2 kHz measured 2 in. from the source to 35 g at 0.6 kHz measured on the equipment beam, 57 in. from the source. Comparison of the measured shock spectra indicated that the higher frequency portion of the shock (1 to 5 kHz) was considerably more attenuated than the lower frequency portion ($<1$ kHz) by traveling through the vehicle structure. Comparison of the shock spectra


Fig. 4 - Drogue mortar tests shock response spectra envelopes

(Fig. 5) measured on the aft cove shelf (location 3) from the three tests indicates that a factor of approximately 2 exists between the peaks of the shock spectra for the three firings.

## Drogue Disconnect

The envelopes of the shock spectra measured during the initial configuration of drogue disconnect tests are presented in Fig. 6. Due to the high spectrum levels, a maximum of 6000 g at 5 kHz measured near the shock source, two basic isolator configurations were tested. One configuration utilized Pyrotex washers in an attempt to isolate the shock source. Tests with this configuration indicated no drop in shock spectrum levels even though the washers were shattered by the shock loads. The other configuration utilized 90 durometer Adiprene washers (Fig. 7). The envelopes of the shock spectra measured for this configuration are presented in Fig. 8. The peak shock spectra levels measured on the vehicle structure near the source were less than 50 percent of that measured for the initial configuration.

Comparison of the shock spectra measured at the same location (Fig. 9) from three of the drogue disconnect tests indicates that a factor of approximately 1.5 exists between the peaks.

## Hatch Separation

The envelopes of the shock spectra measured on the vehicle structure during the initial hatch separation test are presented in Fig. 10. The shock spectra measured near the base equipment beam, with a peak level of 2800 g at 5 kHz, exceeded equipment qualification requirements. The shock spectra measured in the recovery can, with a peak level of 2200 g at 5 kHz did not provide an adequate margin with respect to the equipment qualification requirement. Since it was not feasible to isolate the shock source from the vehicle structure, the shock levels on the equipment beam and recovery can were reduced by isolating these sections from the adjacent structure.

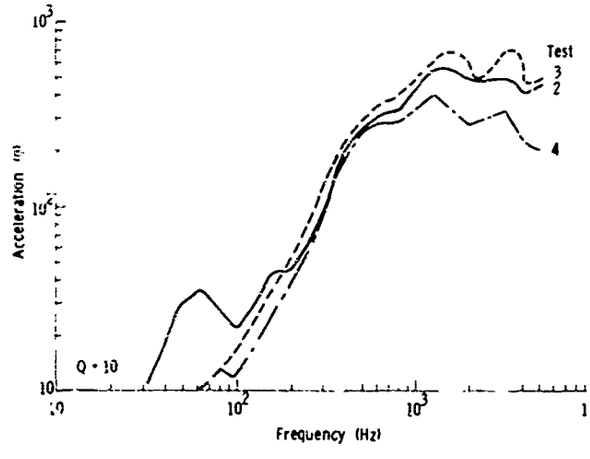


Fig. 5 - Drogue mortar tests comparison of shock response spectra (accelerometer location 3R)

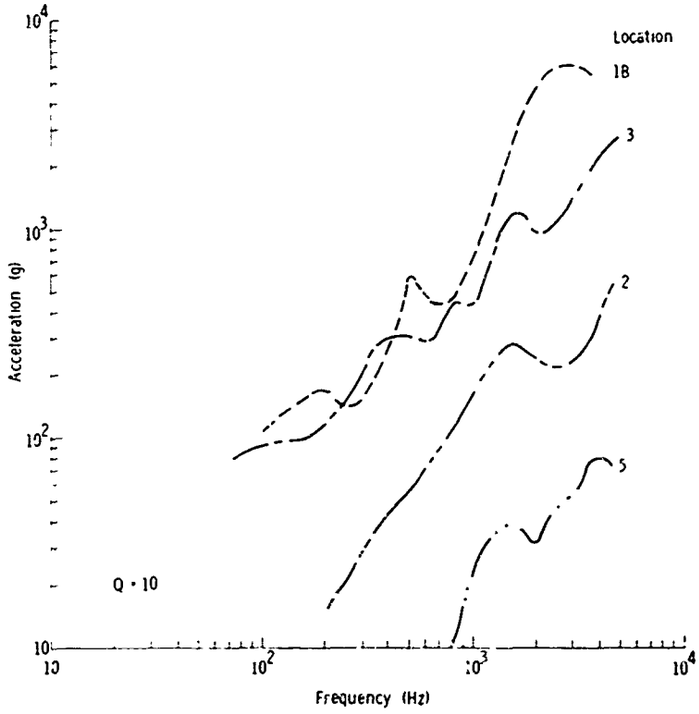


Fig. 6 - Drogue disconnect tests shock response spectra envelopes for original test configuration

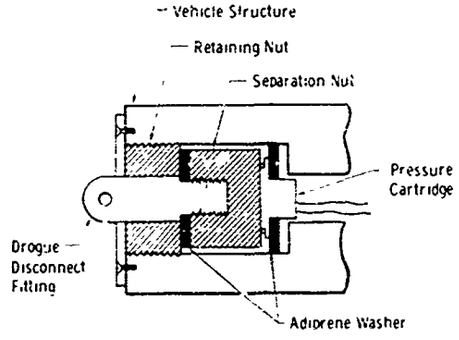


Fig. 7 - Drogue disconnect

The equipment beam was isolated from the station 45 bulkhead by 0.1-in. thick Pyrotex washers and inserts at the primary attachment points and by the omission of the fasteners at the remaining attachment points. The primary constraints satisfied by this design were that the isolator material would not cold flow and the frequency of the fundamental beam mode would not be lowered significantly. Although the measured shock spectra (Fig. 11) at the

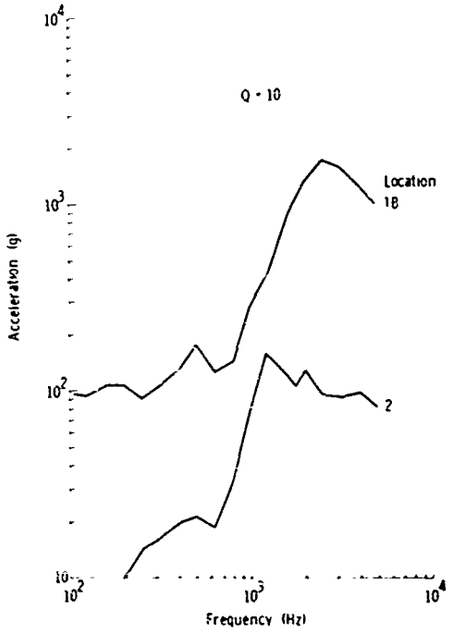


Fig. 8 - Drogue disconnect test 7 response spectra resulting from Adiprene isolators

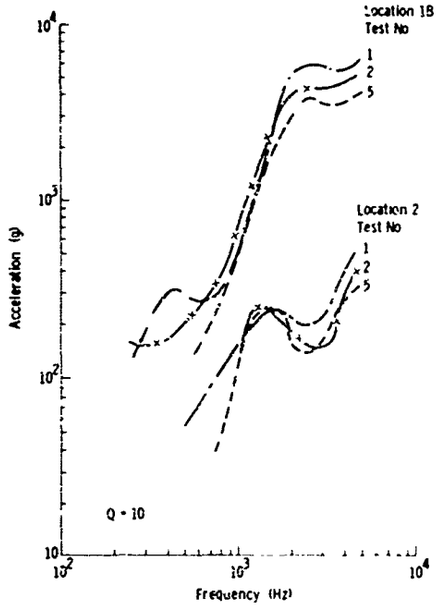


Fig. 9 - Drogue disconnect tests spectra scatter for three identical test configurations

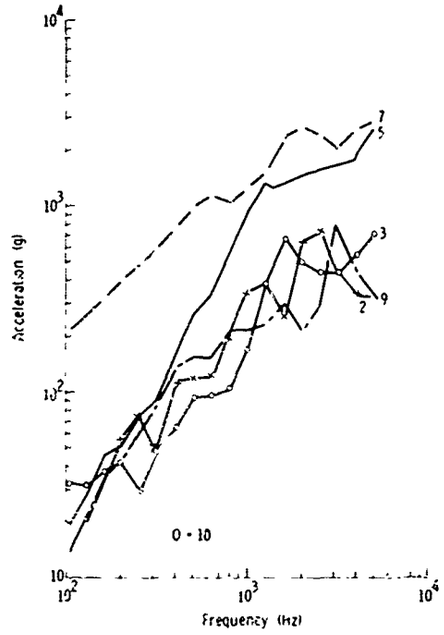


Fig. 10 - Hatch separation test shock response spectra from original configuration

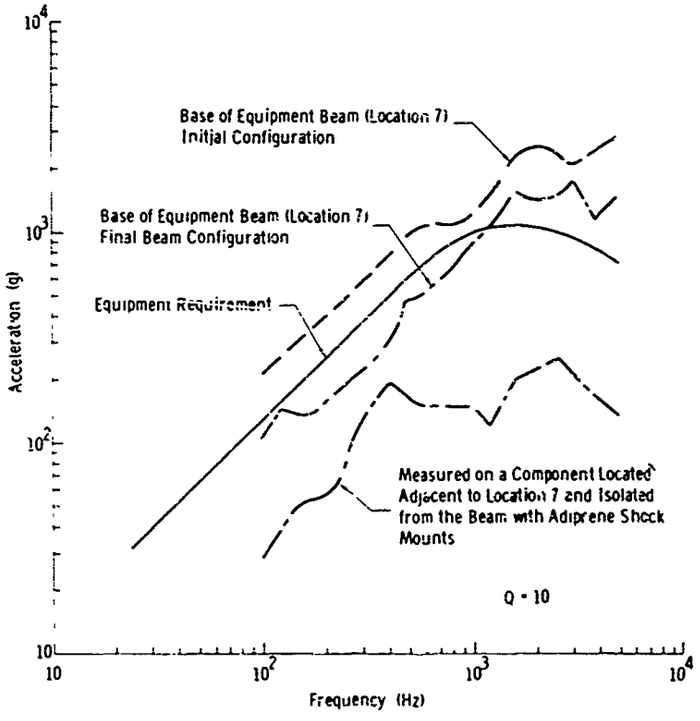


Fig. 11 - Hatch separation test effects of attenuating devices on equipment mounted on equipment truss

base of the beam were reduced by approximately 30 percent with respect to those measured for the initial configuration, they still exceeded the equipment qualification requirement.

To obtain acceptable component shock levels, component shock mounts were developed and tested. The component shock mounts could be separated into two categories, those constructed of relatively hard material (Pyrotex) and those constructed of a softer material (90 durometer Adiprene). In both cases the design of the shock mounts were such that the frequency of the primary resonances of the component-mount system exceeded 1.0 kHz. The Adiprene mounts (Fig. 12) were used with the components mounted near the base of the beam where the shock environment was more severe than elsewhere on the beam; Pyrotex inserts were used with the other beam-mounted equipment. The use of the Adiprene mounts reduced the maximum shock spectrum level by a factor of approximately 7 (Fig. 11). The Pyrotex mounts gave less attenuation (i.e., they reduce the shock by a factor of approximately 2) but were adequate for all equipment locations except near the base of the beam.

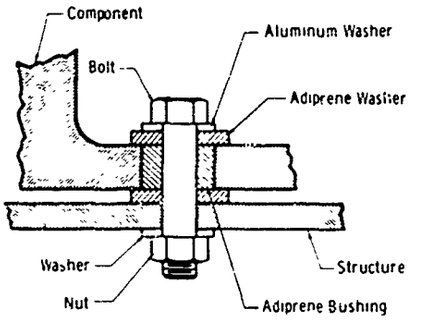


Fig. 12 - Adiprene mount

The recovery can was isolated from the vehicle structure through the use of Lord center-bonded mounts at the mounting points adjacent to the shock source (i.e., the top mounting points). The peak level of the measured shock spectrum (Fig. 13) was reduced to approximately 64 percent of that measured for the original configuration and the shock spectrum levels were sufficiently less than the equipment qualification requirement.

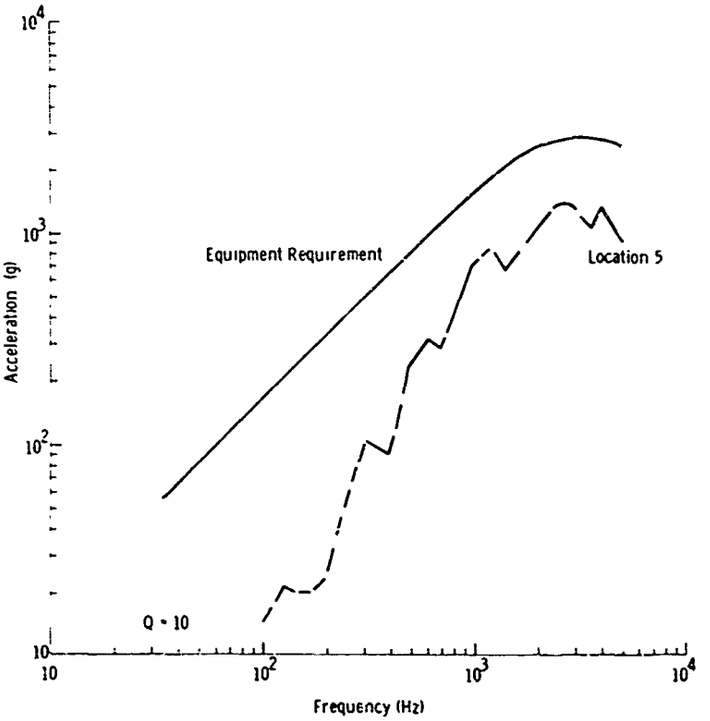


Fig. 13 - Hatch separation test effects of attenuating devices on recovery compartment components

Comparison of the shock spectra measured on the aft cove shelf, location 2, for two tests having the same configuration indicates very little scatter, less than 7 percent difference on peak spectrum levels (Fig. 14).

## Booster Separation

Shock levels were measured during three booster separation tests, and a center bolt firing was performed on the test article.

The first test configuration (Fig. 15) utilized three 285-mg charge, explosive bolts together with crushable aluminum honeycomb absorbers (3.1 pcf). The test results indicated that there was a time difference of approximately 12 msec between the center bolt firing and the outboard bolt firing. Each bolt produced a shock which occurred approximately 1 to 2 msec later. All honeycomb shock absorbers were completely crushed. The measured shock spectra are presented in Fig. 16. Near the source the peak spectrum level was 5000 g at 2 kHz which exceeded the equipment qualification level. The peak shock spectra in the forward section were considerably lower than predicted and indicated that the shock requirements could be reduced.

In an effort to find a way of attenuating the shock, a single 285-mg explosive bolt was fired in the center location using a higher density (5.7-pcf) aluminum honeycomb absorber. The honeycomb isolator was completely crushed by the shock load. The resulting shock spectrum at the measurement location nearest the shock source (location 1A, center rib) indicated an approximately 30 percent reduction with respect to the initial test. However, this reduction was not sufficient and the peak spectrum level still exceeded the equipment qualification requirement.

The configuration used for the next test utilized explosive nuts rather than explosive bolts. Both high- and low-density aluminum honeycomb absorbers were used. The resulting spectra measured at locations on the vehicle were below equipment qualification requirements and represented a reduction in peak level

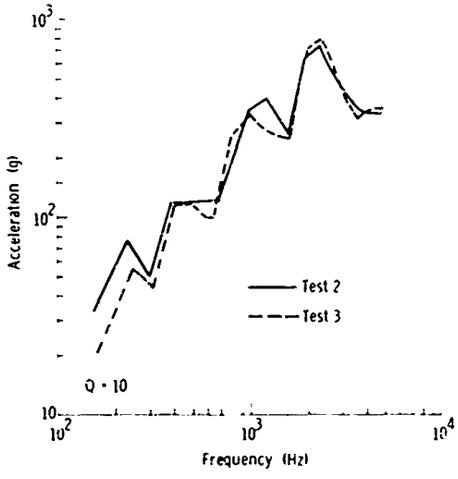


Fig. 14 - Hatch separation test spectra scatter for identical test configuration (accelerometer location 2)

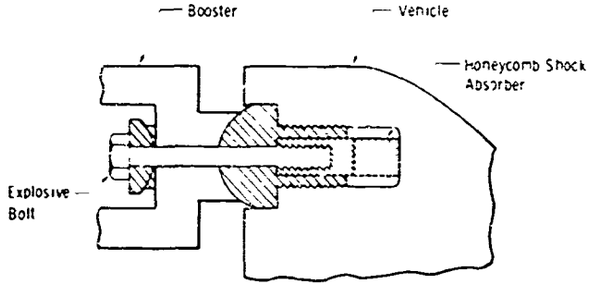


Fig. 15 - Booster separation

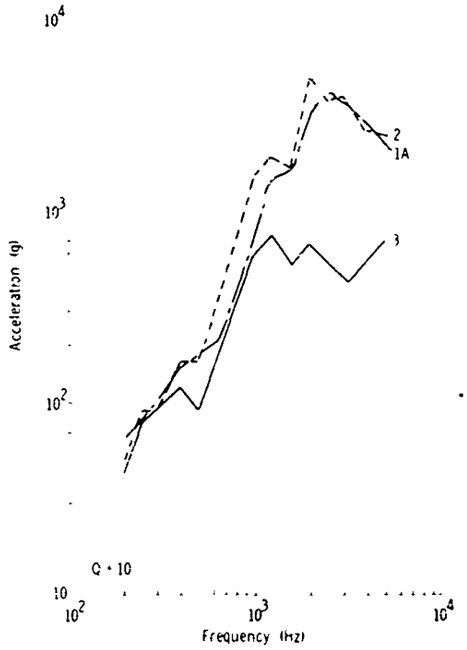


Fig. 16 - Booster separation test shock response spectra generated by 285-mg explosive bolts

of approximately 68 percent with respect to those measured during the previous bolt tests (Fig. 17). It should be noted that the honeycomb attenuators were not crushed by the shock load. Unfortunately, due to the separation design constraints, the explosive nuts could not be used in the flight vehicle-booster configuration.

The configuration utilized for the next test consisted of 235-mg charge explosive bolts in conjunction with 5.7-pcf aluminum honeycomb absorbers at the left and center attachments, while an explosive nut was used at the right attachment together with a low-density (3.1 pcf) aluminum honeycomb absorber. At locations close to the bolts the measured shock spectra (Fig. 18), while slightly exceeding those measured during the previous test using explosive nuts, were less than two-thirds of the equipment qualification level. The aluminum honeycomb isolators used with the explosive bolts were partially crushed by the shock load and the honeycomb isolator used with the explosive nut was not crushed.

## Distance Attenuation

By using data from all tests involving point source type pyrotechnic devices and

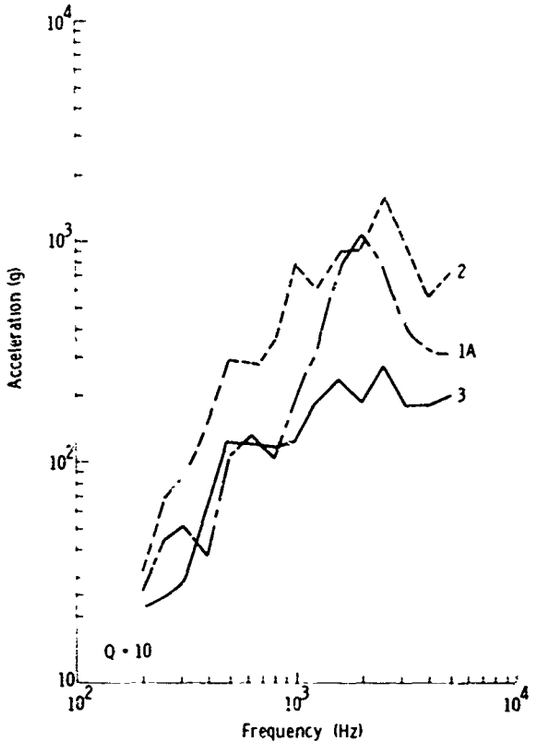


Fig. 17 - Booster separation test shock response spectra generated by separation nuts

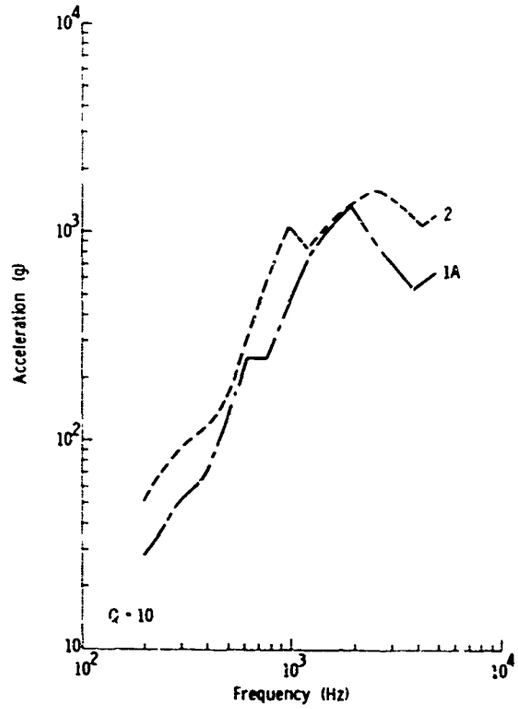


Fig. 18 - Booster separation test shock response spectra generated by 235-mg explosive bolts

renormalizing, a plot was constructed of peak spectrum levels as a function of distance from the source (Fig. 19). It was found that the distance attenuation of peak shock levels was in the range of 9 to 16 db/octave.

## CONCLUSIONS

1. In all cases the shock spectra measured near the source peaked above 2 kHz and had magnitudes in excess of 1000 g.

2. The maximum observed variation in peak spectrum levels between identical pyrotechnic tests did not exceed a factor of 2.

3. The distance attenuation of peak shock spectrum levels from point sources was in the range of 9 to 16 db/octave.

4. With properly designed isolators, substantial reduction in shock spectrum levels could be obtained, even though the resonant frequencies of the isolator-component systems exceeded 1 kHz.

## REFERENCE

1. N. J. Huffington, Jr., and R. J. Goldman, "Simulation of Heat Shield Pyrotechnic Shock Impedance," Shock and Vibration Bull. No. 36, Part II, 1967

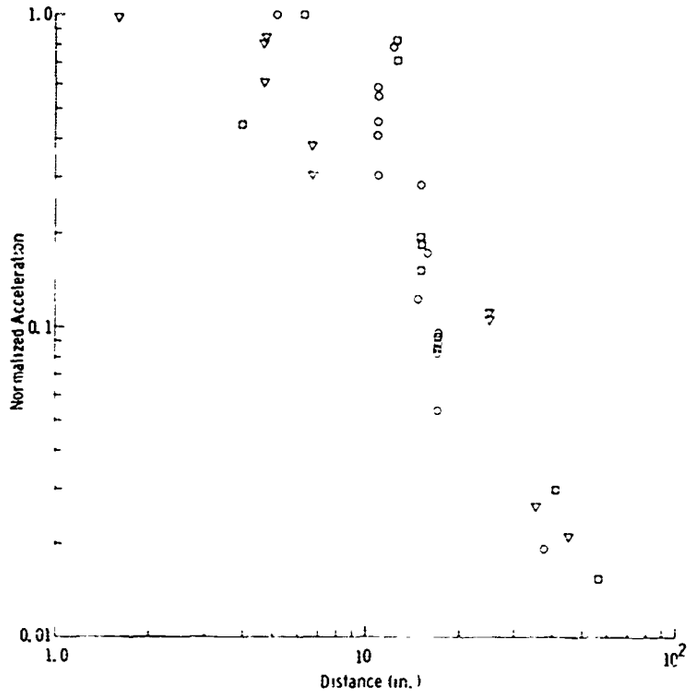


Fig. 19 - Distance attenuation

## DISCUSSION

Mr. Davis (Fairchild-Hiller): You are using a Q of 10 in your shock spectra. Did you find that the shock response spectra were fairly independent of the Q, or would you have gotten higher shock responses had you used, say, a Q of 20?

Mr. Britton: We did not investigate this. We used a nominal Q of 10 in the analysis.

Mr. Davis: I would think that much of the shock time history might have had many sinusoidal components which would tend to increase the shock response if you use higher and higher Q values.

Mr. Bondi (Hughes Aircraft Co.): Since you showed the shock spectrum being reduced with distance, were the accelerometers favorably

oriented radially or longitudinally down the vehicle or were they randomly oriented?

Mr. Britton: We maintained in this attenuation plot primarily a longitudinal orientation of the accelerometers.

Mr. Bondi: When you instrumented the components, did you pick a critical orientation on them and then reduce it?

Mr. Britton: Yes, that is correct.

* * *

# SHOCK TESTING WITH SOLID-PROPELLANT-POWERED GUNS*

Larry O. Seamons
Sandia Corporation
Albuquerque, New Mexico

ABSTRACT

A general description is given of the use to which solid-propellant-powered guns can be put in the field of environmental testing. Emphasis is placed on the inherent flexibility of the shock testing of projectiles in the time interval between ignition of the propellant charge and exit of the projectile from the gun muzzle. A method of computing the shock pulse in this case has been described briefly. Projectile recovery and instrumentation problems have also been cursorily examined.

L. O. Seamons

## INTRODUCTION

Most experimental gun testing and gun design, research and development is conducted to evaluate existing or proposed gun designs or to research new gun systems for possible military applications. In contrast, this paper covers the use of guns as an environmental test facility. The emphasis will not be placed on the development of a gun for a particular test but rather on the use of any gun for a wide variety of environmental tests. A gun can be a versatile testing tool, and that versatility is the point of interest in this paper.

For simplicity and brevity, this discussion will be restricted almost in its entirety to closed-breech, smooth-bore, constant-bore, conventional, solid-propellant-powered guns. This type of gun consists of a powder chamber and a barrel usually of smaller diameter than the chamber. The projectile is seated in the aft end of the barrel, propellant is placed in the chamber, and the propellant is ignited, driving the projectile out of the barrel with an upper velocity limit of 8000 to 9000 fps. For higher velocities, other systems must be used.

## TYPES OF ENVIRONMENTAL GUN TESTS

Guns can be used to support two broad categories of testing. In one case, the gun is used merely as a tool to generate a desired velocity change prior to the actual test. Three examples of this type of testing are described briefly below. The second category is shock testing. Although the other types of tests to be described could also be properly called shock tests, the definition considered in this paper is limited to the case in which a specified shock or acceleration-time pulse is imparted to the projectile or test components mounted inside the projectile while the projectile is still in the gun barrel.

Assume that a gun has been used to produce a desired velocity change for a projectile. If the projectile is the test item, an impact test can be conducted by providing a suitable target. If the projectile is a target material, an impact test can be conducted using a turnaround technique and placing the test item in a desired orientation relative to the projectile. This is often done to facilitate instrumentation of the test item. If the projectile is some type of penetrometer, a penetration test can be conducted

*This work was supported by the U.S. Atomic Energy Commission.

by providing a suitable medium for the penetrometer to pass through. All of these test procedures are common to many different types of environmental test facilities; the only basic differences between facilities are the way in which the velocity change is produced and the type of test item that can be handled. There is no real need to consider using solid propellant guns for these tests unless velocity requirements are high.

Propellant-powered guns become a unique tool when a test item is shock tested (i.e., accelerated in a gun barrel). Guns have a practically unique ability to furnish long-duration (tens of milliseconds) high-amplitude (thousands of g's) shock pulses. Other test facilities are available which can produce one or the other of these characteristics in a shock pulse, but guns can produce both characteristics simultaneously. Also, by introducing a rifling inside the gun barrel, several hundreds of radians per second of angular velocity and hundreds of thousands of radians per second of angular acceleration can be supplied.

Shock tests, to which the remainder of the paper will be devoted, are the more challenging type of test. It is comparatively simpler to produce a desired velocity than to produce a shock pulse exhibiting a particular rise time, duration, and peak amplitude. In gun shock testing, there are a large number of variables affecting the shock pulse shape. The large number of variables involved provide great versatility in the number of pulse shapes that can be generated in a given test gun. In general, all the variables involved can be placed in four categories:

1. Gun geometry – (a) barrel length, (b) powder chamber volume, and (c) bore diameter;

2. Projectile design – (a) projectile weight, and (b) shock mitigation characteristics of onboard test item packaging;

3. Mechanical and thermodynamic properties of the propellant and propellant gas – (a) density, (b) isochoric flame temperature, (c) specific heat ratio, (d) burning rate as a function of pressure, (e) second virial coefficient, and (f) specific gas constant or molecular weight of the propellant gas; and

4. Geometry of the individual propellant grain – surface area of the solid propellant as a function of the fraction of propellant converted to gas.

If all the pertinent variables are known, there still remain the problems of computing the resultant shock pulse for a set of conditions and of mathematically manipulating variables to attain a desired pulse shape. This is imperative since the only other alternative is experimental trial and error which would swallow up a tremendous amount of time and manpower. This then leads to the next subject to be discussed, a macroscopic picture of the computational procedure used by the author to compute gun shock pulses.

## COMPUTATION OF SHOCK PULSES

The computation of shock pulses is done on a digital computer. In general, a finite difference method is used with a fixed time interval as a basis for the calculations. It should be emphasized that this computational method is not unique or original by any means. The computer code used by the author and many much more elaborate codes which deal with all types of gun systems have been developed, and the theory which supports the method is well documented [2, 3].

The mathematical description of the phenomena occurring inside a gun is called interior ballistics. Four fundamental and two supplementary equations are required to define the interior ballistics for the method under discussion.

The first equation, the burning rate equation, is usually experimentally derived. It describes the velocity at which the free surface of a semi-infinite propellant grain regresses or burns away as a function of gas pressure at the free surface. This equation describes the rate at which propellant is being consumed and must be used as long as unburned propellant remains in the gun. A second equation, which must be used as a supplement varies according to the geometry of the propellant under consideration and describes the exposed propellant surface area as a function of the fraction of solid propellant that has been converted to gas. By combining these two equations, it is possible to calculate the amount of propellant converted to gas in a given interval of time.

The second equation, the equation of motion of the projectile, will involve the gas pressure at the base of the projectile as an essential ingredient of the accelerating force. A pressure gradient is incorporated because there are large pressure gradients between the chamber and the projectile base. The equation is

numerically integrated twice to yield velocity and displacement information.

The third equation, an energy balance equation, is used to compute a mean temperature in the gun interior. Here the energy of the burned propellant is equated to the kinetic energy of the projectile, the heat energy transferred to the gun, and the kinetic energy of the propellant gas.

The fourth equation, the equation of state of the propellant gas, includes terms to the second virial coefficient only. It is used to compute a mean pressure in the gun interior.

The computational method can be summarized as follows:

1. Select a finite time interval;

2. Select an artificial starting pressure in the chamber and assume isochoric flame temperature in the chamber;

3. Compute propellant burned during the time interval via the burning rate equation and propellant geometry;

4. Compute acceleration, velocity, and displacement via the equation of motion and the pressure gradient equation;

5. Compute new temperature via an energy balance equation;

6. Compute new pressure via the equation of state;

7. Compute elapsed time; and

8. Return to step 3 and continue cycling until projectile reaches the gun muzzle.

The computer code which forms the core of this method is given by Lubeck [1]. The value of the digital computer in this case is that it simulates actual gun tests and works out the trial-and-error portion of gun testing with huge savings in time and money. One hour of computer time (CDC 3600) will simulate approximately 3000 gun tests using this method. To date, computer predictions are falling within 10 percent on all pertinent parameters for velocity changes less than 4000 fps. For higher velocities, accuracy wanes and more refinements are needed in the method.

## EXAMPLE OF SHOCK PULSE SHAPES ATTAINABLE FROM A SINGLE GUN

The large number of variables involved in determining the final pulse shape makes computation a lengthy process but provides the means to manipulate the pulse shape over a wide range. Some idea of the spectrum of pulse shapes available can be seen in Figs. 1 through 5. These figures are all acceleration-time plots of a projectile being fired from a 75-mm gun. The 75-mm gun was selected arbitrarily and represents a nominal test gun for which experimental data are available.

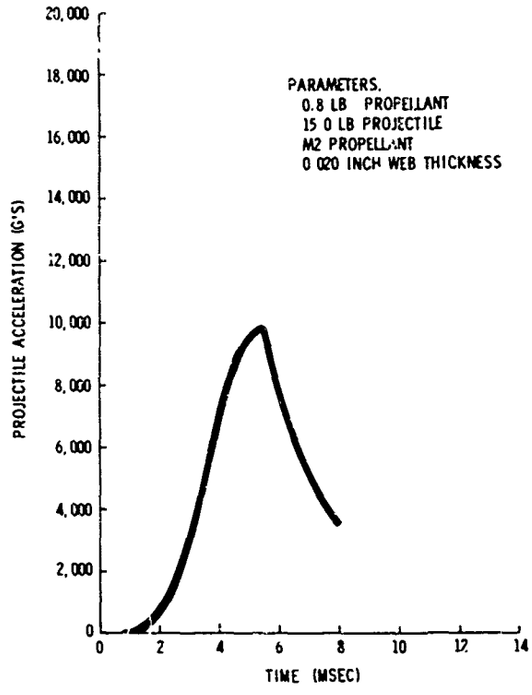


Fig. 1 - Reference shock pulse

Figure 1 shows a reference shock pulse which will be referred to as the standard shock pulse for the gun under discussion. The standard pulse also appears in Figs. 2 through 5 as the thick-lined pulse and thus furnishes a visual comparison among all five figures. All the figures have the same scale on both axes.

The object of this series of figures is to show how the pulse shape changes when one variable is altered and all other conditions remain unchanged. In all, four variables are altered: the propellant weight; the projectile weight; the propellant web thickness, which will be defined later; and the propellant chemical composition. Any of the other variables could be handled similarly, but in lieu of more graphs let the statement that many more possibilities exist suffice.

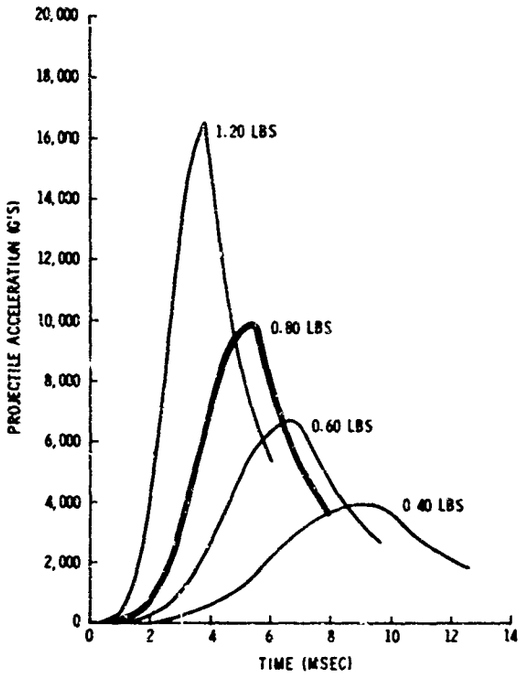


Fig. 2 - Effect on shock pulse shape produced by varying propellant weight

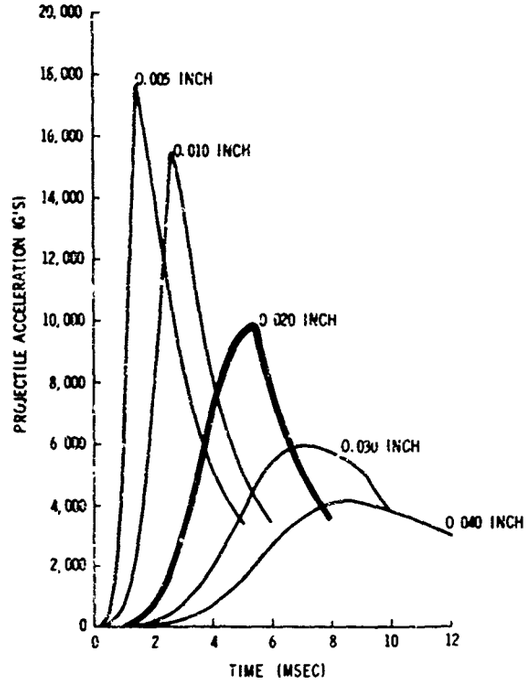


Fig. 4 - Effect on shock pulse shape produced by varying propellant grain web thickness

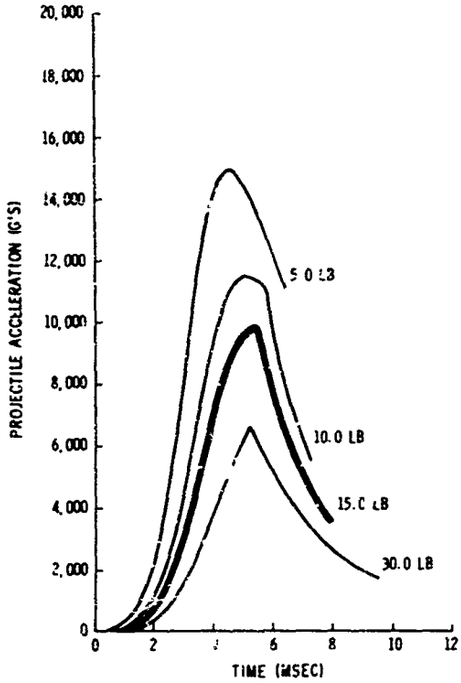


Fig. 3 - Effect on shock pulse shape produced by varying projectile weight

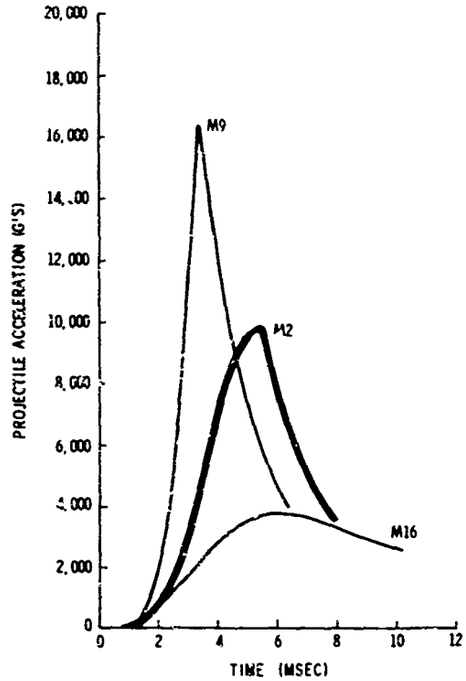


Fig. 5 - Effect on shock pulse shape produced by varying propellant chemical composition

Figure 1 also shows the value of each variable dealt with in the remaining four figures that is required to produce the standard pulse. These are listed in the upper right-hand corner and are preceded by the magnitude of the variable used in the standard pulse. The M2 propellant designation is a military proprietary designation of the chemical composition of the propellant.

Also note in Fig. 1 that the standard pulse has approximately a haversine-shaped rise and an exponential decay. These two shapes are common to many gun shock pulses with the point of transition from one shape to the next occurring about the time that the last of the propellant is converted to gas. The end of the pulse corresponds to the time the projectile clears the gun muzzle. Usually the projectile continues to accelerate outside the muzzle but this portion of the pulse has been omitted.

Figure 2 shows the result of varying the propellant weight. In general, an increase in propellant results in a faster rise time, a shorter duration, and a higher peak acceleration. The velocity change increases approximately as the propellant weight to the 0.7 power. This family of curves and the others shown can be expanded in either direction. In this case, the upper limit is determined by either the physical capacity or the strength limit of the powder chamber. The lower limit is determined for all practical purposes by the smallest propellant weight which will yield repeatable results. Most propellants are characterized by a pressure below which they will not burn predictably; if the propellant weight is depressed far enough, this lower pressure limit will be reached and sporadic pulse shapes will result.

Figure 3 shows the effect of varying projectile weight. Heavier projectiles see a lower peak acceleration and a longer pulse duration. The interesting feature of these curves is that the rise time changes only slightly over a wide range of projectile weights. Also on these curves, it is easier to see the point in time when all the propellant has been converted to gas and the corresponding change in the curve shape takes place. The propellant is "all burnt" at the peak of the bottom curve, and as the projectile becomes lighter the "all burnt" point occurs farther over the curve peak.

Figure 4 shows the effect of varying the web thickness of the propellant grain. The propellant web, if one exists, is defined as the smallest dimension of the propellant grain along a direction normal to the surface at two points of intersection where the direction is in one instance passing into and at the other passing out of the propellant. For example, the web of a long cylindrical propellant grain would correspond to the cylinder diameter, and the web of a thin disc-shaped grain would be the disc thickness. In general, the smaller the web, the faster the propellant is converted to gas. The curves show that small webs lend themselves to shorter pulse durations and higher peak accelerations. Also, a thin web is one of the best ways to achieve a fast rise time. One interesting feature of these curves is that the velocity change does not vary greatly. There is only a 350-fps difference between the top and bottom curves.

Figure 5 gives an indication of the range the pulse shape can cover by changing the chemical composition of the propellant. It is assumed that propellant geometry as well as all other variables are held constant.

Figures 4 and 5 are of great practical interest as a pair since there is a wide variety of military propellant compositions available and usually each composition is available in several different geometries or web sizes. This means that these two items can be optimized for the job at hand in many cases from existing propellant stockpiles.

## OTHER ASPECTS OF GUN SHOCK TESTING

Usually one design problem and one instrumentation problem arise on virtually every shock test. These are, respectively, recovery of the projectile and a direct measurement of the projectile acceleration-time history while the projectile is in the barrel.

The recovery problem is usually accomplished by one of two methods. The projectile can be fired into a large catch box filled with some low-density material, or it can be equipped with a parachute recovery system which is deployed somewhere in the projectile trajectory.

The call out of a maximum allowable recovery acceleration is often part of an environmental test specification. As velocity increases, the severity of the problem of holding down recovery accelerations increases and can become formidable.

Currently, projectile acceleration time is calculated from measurements of chamber pressure time or projectile displacement time. In the first case, it is assumed that the pressure gradient inside the gun is known; in the

second case, the rather inaccurate process of double-differentiation must be performed. Both procedures introduce unwanted inaccuracies, thus pointing out a need for a way to measure projectile accelerations directly.

An attractive aspect of gun testing is that it is a low-cost and rapid way to conduct environmental tests if a gun is a feasible facility.

## SUMMARY

A very general picture of environmental testing with solid-propellant-powered guns has been presented. It is hoped that the flexibility of guns as an environmental test tool has been portrayed and that some of the problem areas which were briefly mentioned may stimulate interest.

## REFERENCES

1. P. T. Lubeck, "A Study of Interior Ballistic Equations on a Digital Computer," Sandia Corp. Livermore Lab., Tech. Memo. TM-66-67, Aug. 1966
2. Hirschfelder, Kershner, and Curtiss, "Interior Ballistics, I," National Defense Res. Comm. Armor and Ordnance Rept. No. A-142 (OSRD-1236), 1943
3. J. Corner, "Theory of the Interior Ballistics of Guns," John Wiley and Sons, New York, 1950

## DISCUSSION

Mr. Hughes (Naval Ordnance Laboratory): How did you calculate acceleration? Was it from the pressure time?

Mr. Seamons: That is correct. It is not a very satisfactory method. We calculate it based on breech pressure measurements and then take into consideration the pressure gradient that exists along the barrel of the gun to arrive at the pressure at the base of the projectile.

Mr. Hughes: When you say breech pressure, do you mean at the base of the powder load? Are you measuring inside the powder or directly behind the projectile?

Mr. Seamons: We are measuring on the periphery of the powder chamber. We do not have anything inside the powder load itself. Most of these are taken from piezoelectric pressure transducer measurements. I might add, it is not a really satisfactory method of getting acceleration.

* * *

# APPLICATION OF POLYURETHANE FOAM TO SHOCK ISOLATION OF LARGE SILO-BASED MISSILES

William A. Volz
Westinghouse Electric Corporation
Sunnyvale, California

In the last few years there has been considerable interest in the application of flexible polyurethane foam to the shock isolation of large silo-based missiles. This is due to the inherent suitability of this material for use in annular configurations and the high space efficiency (ratio of rattle space to the envelope needed for the isolator) that can be achieved. The highlights of a foam isolator feasibility study, recently completed under an Air Force contract, are presented. The program included analysis and design studies followed by tests on a full-diameter isolator. One of the primary goals of this study was to develop and evaluate the analytical tools needed to design a foam shock mount and predict its performance. These analytical methods are the key to transforming foam into an engineering material which is useful and predictable as a shock mount. The paper includes a description of the shock isolator concept considered in the study, a discussion of fundamental foam characteristics, a description of the mathematical model used and the tests run, and a discussion of typical test results.

W. A. Volz

## INTRODUCTION

During the last several years, flexible polyurethane foam has evolved from a packaging material with rather random properties into a contender for the sophisticated application of a shock isolator for large diameter missiles. Polyurethane foam has several inherent properties which make it extremely attractive for use in such applications. The material is particularly suitable for annular configurations and has a high space efficiency (ratio of ratfle space to envelope needed for the isolator). Therefore, there is considerable interest in the development of such a shock absorber system for silo-based missiles.

This paper gives the results of recent work, completed under an Air Force contract [1], to determine the feasibility of a foam shock isolator. The state-of-the-art of foam isolator design is highlighted, particularly the analytical and mathematical modeling procedures used to describe the isolator performance. The results given in this paper are an extension of previous work reported by the author [2].

## ISOLATOR CONCEPT

There are several things to be considered in the design of a shock isolator for a silo-based missile. The missile must be isolated from the silo both vertically and laterally, and must maintain its stability during and after the violent motions of the silo. One of the most common ways of isolating such a missile is by a pendulum vertical suspension with additional mechanisms to apply moments to the bottom of the missile to maintain stability. In this concept, the loads are applied only to the base of the missile, and in most cases, rather large and cumbersome apparatus are required.

In the case of a polyurethane foam shock mount, the vertical suspension consists of a

spring system between the silo floor and the missile (Fig. 1). This isolator could be in the form of coil springs, liquid springs, air springs, or any number of suspension systems that would fit in the volume directly below the missile. The lateral stability and shock isolation would then be provided by the foam isolator located at two or more places along the length of the missile in the annular space between missile and silo. In this concept, there is little or no coupling between the lateral and vertical isolation system. Also, the silo diameter may be a minimum since the radial space needed is the rattle space plus the room required for the fully compressed foam. It is obvious that with this kind of concept, an eject or "cold" launch would be an integral part of the system, as the venting of exhaust gases would not be possible with the foam isolator. Eject launch technology is readily available and has already been proven to be feasible.

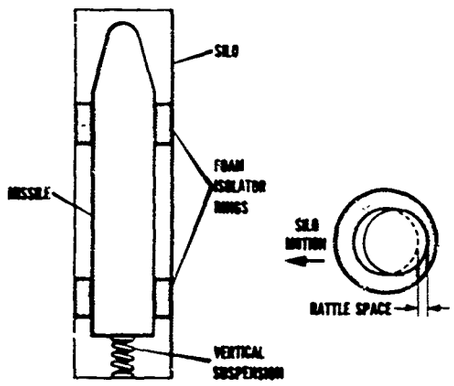


Fig. 1 - Typical foam isolator installation

There are several possible configurations of launch tube, launch adapters, arrangement of the foam isolator, etc. All such concepts have one thing in common, however; the foam isolator is utilized as a ring placed in an annulus between two cylinders having relative motion as shown in Fig. 1. The purpose of this paper is to deal primarily with the prediction of response of the foam ring when it is subjected to the shock environment.

## FOAM CHARACTERISTICS

Polyurethane foam of the type usually considered for shock isolation application is an open-celled foam of low density, between 2 to 10 pcf, and preferably a closely controlled material defined by a weapons specification. The stress-strain characteristics of this material are of primary interest when considering performance under shock. Figure 2 shows a typical stress-strain, or as called in the foam industry, compression load-deflection (C-D) curve. Most foams of this type show a steep slope or modulus for the first 5 to 10 percent compression. A subsequent flattening out occurs as the foam structure buckles, and a "bottoming" characteristic appears in the order of 50 to 70 percent compression. On unloading, the curve drops to a value lower than that of loading, and appreciable hysteresis is obtained. This hysteresis is an important contributor to the damping properties of a foam isolator.

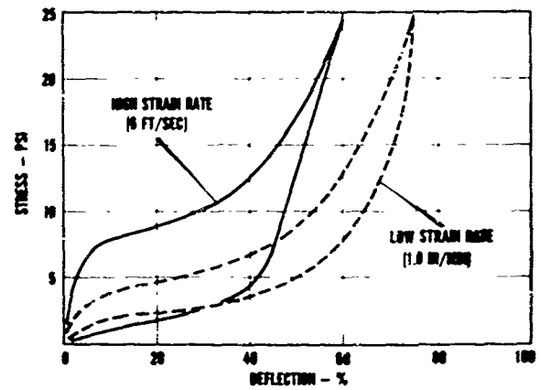


Fig. 2 - Compression load-deflection characteristics of foam

The C-D curves given in Fig. 2 are for two different strain rates. The lower curve is for a strain rate of 1 ipm per inch of thickness, the rate most commonly used for quality control and material description when manufactured. The higher curve is the C-D curve obtained at a rate of 2500 ipm per inch of thickness, which is typical of the strain rate generated during shock environment.

This high rate characteristic is usually obtained by one of two methods. One method is by the use of time-temperature superposition. The time-dependent (viscoelastic) properties of most elastomers are such that high rate effects may be simulated by given decreases in temperature. That is, a material's high strain rate C-D characteristic may be obtained by making a normal (low rate) C-D test at a given low temperature, e.g., -20°F. Therefore, after the necessary time-temperature correlation has been established for the particular polymer

involved, high rate effects may be duplicated with a standard compression testing machine and a temperature control unit. Since the sample tested in this manner is compressed at a low rate, the effects of the air in the cells do not affect the results.

Another method of determining high rate C-D properties is by the use of an impact tester. This is a test where the foam sample is mechanically compressed at the same rate as experienced under shock. The energy for such a test apparatus may be obtained through the dropping of a weight, high-pressure air, or a similar means. The problem with such testing, however, is that the results are often influenced by the compression of air in the sample. As the sample is rapidly compressed, air pressure builds up in the cell structure, and a pressure gradient is obtained from the center of the sample out to the edges. This air compression adds a force to that generated by the elastomer, thereby raising the total force measured on the test.

One way to eliminate this effect is to use a relatively small sample so that the air can flow out easily. This is acceptable for foams that are relatively porous or "breathable." For foams that restrict air flow to a greater degree, however, a vacuum must be applied. In this case, the sample is put into a vacuum chamber and compression at a high rate is applied. Through this procedure, only the forces generated by the elastomer are measured. The results from both time-temperature superposition methods and the high rate test just mentioned have correlated to a reasonable degree for the foam materials tested.

Once the elastomeric C-D properties are known for a foam material, the characteristics of a ring configuration of this material, as used in the isolator, may be calculated. The ring force vs displacement may be obtained readily by a simple numerical integration routine on the computer. Calculating the effects of airflow within the shock isolator and the resultant forces is a more difficult problem, however. The compression of the air in the annular space and the resulting forces are a function of the flow path, the airflow resistance of the foam material, the dimensions of the ring, and the rate at which the ring is compressed. The prediction of the airflow and forces is amenable to treatment by the theory of flow through porous media, the laws of isothermal compression, and conservation of mass. The airflow case to be analyzed is illustrated in Fig. 3.

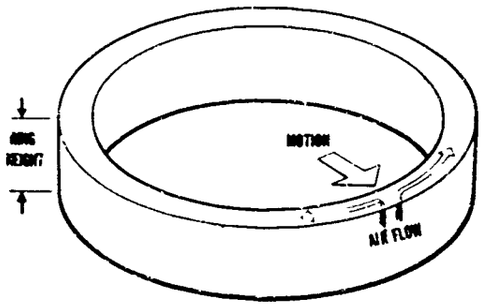


Fig. 3 - Air flow in foam isolator ring

Some of the basic parameters of the foam required for these calculations are the pore size, percent void, and friction factor as obtained by airflow tests on samples. These parameters, along with a definition of the isolator configuration, are put into a computer program, and the pressures and forces generated by the air are calculated. In Fig. 4, some typical results are shown. Several force-deflection curves are given for an annular ring of foam material. These forces are the air compression forces only, and are for various ring heights. (Note that the forces are given per inch of foam height so the airflow properties may be compared directly.) The upper curve is the force-deflection characteristic that would be obtained for an "un-vented" situation where the foam has a very high resistance to airflow and/or the configuration is one where the air has a long path to travel before reaching ambient. It may be seen that the stiffness in this case is quite high, and the damping or hysteresis is very small. The lower curves, however,

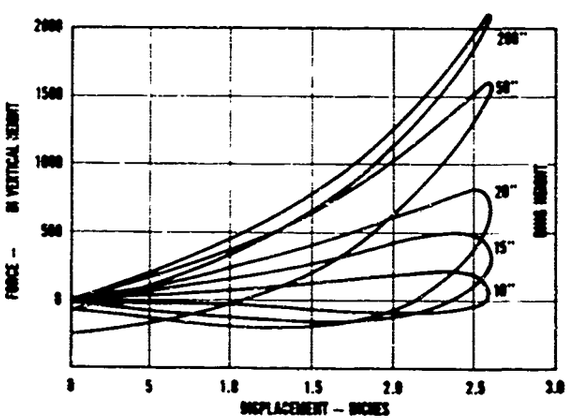


Fig. 4 - Air compression forces for foam ring

represent cases where there is little resistance to flow, and the air compression forces are small. The stiffness obtained is low, and the hysteresis is quite high. From these curves, it may be seen that the stiffness due to air compression and the damping may be readily adjusted by controlling venting properties of the configuration. This is most easily done by varying the height of the foam ring. An optimum trade-off between damping and stiffness of the isolator may be achieved in this manner.

## MATHEMATICAL MODEL

To predict the performance of a foam shock isolator, a mathematical model must be established which adequately describes the forces produced by the isolator under various conditions of displacement and velocity. The mathematical model developed during the foam isolation system feasibility study [1] is given in Fig. 5. This mathematical model is very similar to models used previously [2], with the exception that the airflow element has been added. As shown in the figure, the model is made up of three elements. First, there is a nonlinear spring, $K_s$. This spring describes the nonlinear force-deflection characteristics inherent in the foamed polymer. Secondly, there is a Maxwell element in parallel which is shown as spring $K_1$ and damper C. This Maxwell element serves two functions. It describes the rate sensitivity of the elastomer by providing an increasing force during high rates of compression, which is then added to the basic spring rate force from $K_s$ and provides damping which simulates the hysteresis characteristics.

Therefore, the nonlinear spring $K_s$ and the Maxwell element describe the behavior of the elastomer as determined by sample tests (Fig. 2) and sample-to-ring calculations. The

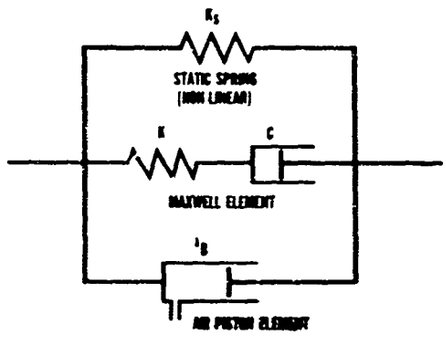


Fig. 5 - Mathematical model of foam shock isolator

third element, the airflow element, simulates the airflow characteristics of the foam ring. In graphical form, this element is essentially a piston and air cylinder with an orifice which varies in area as a function of piston stroke. The piston and cylinder simulate the air pressure buildup in the foam ring, and the orifice accounts for the flow out of the foam and describes the airflow resistance properties, $\lambda_B$, of the foam structure. The airflow resistance of the foam material increases as the compression increases due to change in percent voids. Therefore, a variable orifice is needed.

The effective area of the piston and the parameters of the orifice are obtained from separate airflow calculations for the particular isolator being considered. Once this is done, the model is ready to use for shock analysis calculations. The forces generated by the airflow element in the model are calculated with a set of equations analytically describing the air compression and airflow of such a piston and cylinder arrangement.

## FULL-SCALE TESTS

To establish the feasibility of the foam isolator concept and to verify the adequacy of the mathematical model, a series of tests were run on full-scale foam isolator rings. The tests included a static or low rate compression test and a dynamic test. These tests were run on the Partial Full-Scale Test Machine (PFSTM) at the San Francisco Bay Naval Shipyard – Hunters Point Division. The PFSTM, which is essentially a drop test facility, is shown in Fig. 6. The isolator is placed between the box frame and slug. The box frame and slug are supported by parallelogram linkages which control the drop motion. The box frame and slug are pulled back to the required position, and then, on release, swing down until the box frame impacts the buttress. The box frame is decelerated by lead impact pads in 5 to 10 msec and then is held stationary by anti-recoil latches. The slug compresses the foam isolator after impact and oscillates thereafter as a function of the isolator properties. In this manner, a nearly instantaneous step change in velocity is applied to the system and a high rate of compression is obtained across the foam isolator.

Isolator ring sections up to a total of 50 in. high, representing a portion of the total isolator used in the silo application, are utilized in the test. The parameters obtained from these tests may be simply extrapolated to account for the total amount of foam in the particular silo

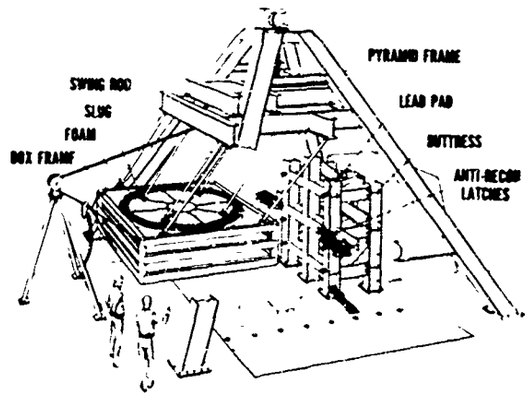


Fig. 6 - Partial Full-Scale Test Machine

application. Through the use of full-scale diameters, unknowns due to diametral effects may be eliminated. In the particular tests run, a series of three foam rings, each 12 in. high, separated by 6.5-in. high venting slots were used. The diameters used were those associated with a large silo-based missile.

During the impact, the acceleration of the slug and relative motion between the slug and box frame are obtained. From these data, time-based response and force-deflection characteristics may be plotted for various drop velocities. These results may then be readily compared to the responses predicted with the mathematical model.

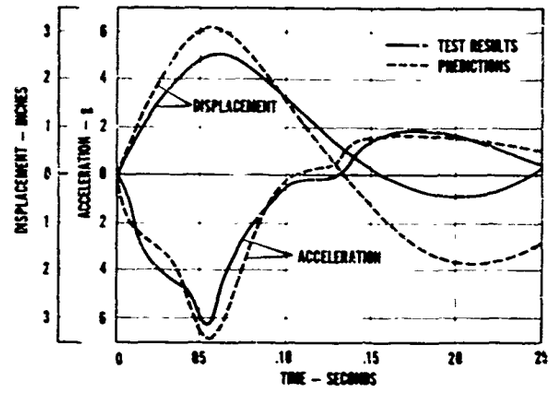


Fig. 7 - Comparison of measured and predicted response

## TEST RESULTS

Typical accelerations and displacements vs time obtained on the test are given in Fig. 7. Plotted along with the test results are the predicted results using the model in Fig. 5. It may be seen that the results and the predictions correlate reasonably well. The accelerations are approximately the same level and follow the same time-history pattern. The most prevalent discrepancies occur in the predicted relative displacements. The predicted displacements are greater than those obtained in the test, especially in the second half cycle. For most silo shock inputs, however, the first half cycle of compression is the most critical, and the degree of correlation is, therefore, felt to be adequate for calculating isolator performance.

Another method of determining the adequacy of the model is through the use of shock spectrum analysis. In Fig. 8, shock spectra of the slug motion are given for the test results and model predictions. The spectrum obtained from the mathematical model response correlates quite well with that obtained from the test results. This implies that when the model is used for predicting the response of a flexible missile, the results should be reliable.

To determine the effectiveness of the shock mount tested, spectrum curves were generated from shock calculations utilizing the model. The results are shown in Fig. 9. The upper curve is a typical shock spectrum of the silo motions. The other curve is a spectrum of the response measured on the isolated missile. The difference between the two shock spectra is the measure of the effectiveness of the foam shock isolator. It may be seen that the environment in the higher frequencies has been reduced considerably.

In summary, a great deal of progress has been made in the use of polyurethane foam as a

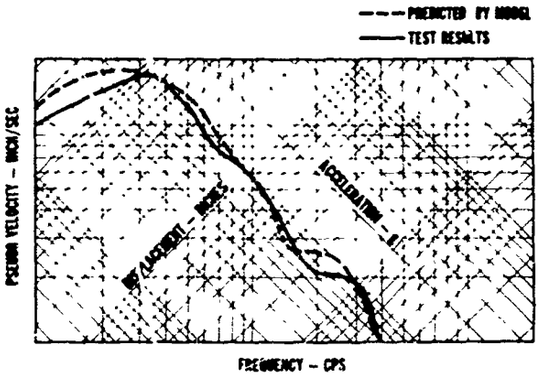


Fig. 8 - Shock spectra of slug response

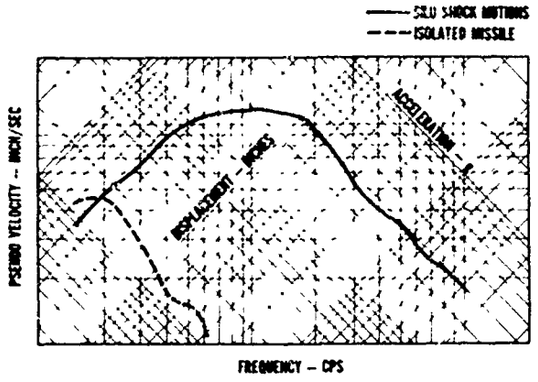


Fig. 9 - Predicted attenuation of silo shock

shock isolator for large diameter missiles. It may now be said that foam can be described as an engineering material with predictable behavior. The feasibility of using a foam shock isolator in a silo-based missile application has been proven. One of the primary contributions to the state-of-the-art has been the mathematical treatment of the airflow properties inherent in such a shock mount. With the mathematical model described, performance of a fully vented foam configuration may now be predicted.

## REFERENCES

1. W. A. Volz, E. J. Barakauskas, and R. H. Strong, "Foam Shock Isolation System Feasibility Study Phase II Summary Report," BSD-TR-66-11, Feb. 1966; Air Force Contract AF04(694)-568

2. W. A. Volz, "Analytical Considerations in the Design of a Polyurethane Foam Shock Mount for Polaris," Shock and Vibration Bull. No. 31, Part 2, pp. 265-271, March 1963

## DISCUSSION

Mr. Scott (Sandia Corp.): You made quite a point of the fact that temperature had a great deal to do with the K of your foam. At what temperature did you test?

Mr. Volz: The tests were run at the local ambient, probably 70°F ± 10°F. Temperature definitely does have an effect on the rate properties but only when it is far removed from the ambient. It has to be close to the glass transition temperature, which is a polymer function and is usually about -30°F or -40°F.

Mr. Crawford (Bell Telephone Laboratories): Was the purpose of the foam rings to decouple vertical response from horizontal response?

Mr. Volz: There are a couple of reasons for this. Usually a smaller silo may be used with a given size of missile with this kind of concept. A relatively simple vertical support system can be used because stability comes from the foam rather than from some apparatus that applies a moment at the bottom. The apparatus can be simplified, and the foam is generally inexpensive.

Mr. Crawford: Was the foam semi-rigid or elastic?

Mr. Volz: It was most definitely an elastic foam, a flexible polyurethane with a density on the order of 2 to 8 pcf. There are several foams defined by weapons specifications as flexible polyurethane foams.

Mr. Galef (National Engineering Science Co.): Most of the foams that I have worked with have been closed celled instead of open celled, so the techniques for separating the air effect from the elastomer effect would not apply. Is it really important to separate these two? You seem to be able to do it, but you must put this error back into the elastomer. Why do you take it out?

Mr. Volz: Because the configuration is very sensitive to the air effect, it is best for the analysis to separate the effects.

* * *

# NEW APPROACH FOR EVALUATING TRANSIENT LOADS FOR ENVIRONMENTAL TESTING OF SPACECRAFT

James T. Howlett and John P. Raney
NASA Langley Research Center
Hampton, Virginia

A new approach is presented for evaluating transient environmental testing of spacecraft. The requirement for using a multi-degree-of-freedom model, rather than the single-degree-of-freedom model of the shock spectra procedure, is established. Since a spacecraft is a complex elastic structure, the response of a specific component is a function not only of its own dynamic characteristics, but of its point of attachment to the spacecraft structure. The effects of component location on maximum response vary several orders of magnitude for representative cases. Furthermore, the added degrees of freedom (i.e., representing the spacecraft by more than one degree of freedom) impose additional constraints in defining a suitable input transient, thus requiring the selection of a more realistic test transient.

A rigorous derivation is presented of a method for determining system response to transient inputs using normal coordinates to represent the multi-degree-of-freedom spacecraft system. Comparison of the envelopes of the amplitudes of the normal coordinates at any time shows the amount of participation of that coordinate and, hence, the contribution of a particular normal mode of vibration to the total system response.

The proposed procedure for evaluating transient environmental testing is illustrated with several examples. The results show the efficacy of multi-degree-of-freedom analytical models of spacecraft for determining system response and the adequacy of proposed input transients for environmental tests, thus providing a more reliable means of selecting appropriate test transient inputs.

J. T. Howlett

## INTRODUCTION

Mission success of spacecraft systems should be assured by adequate, but not overly severe, environmental tests. However, because of the difficulty of simulation of flight environments, the sophistication of experiments which can be carried by a spacecraft may be compromised by ultraconservative environmental testing and qualification procedures. Among the more difficult test environments to evaluate properly are the transient loads.

Ideal test transients should be representative of the transients the spacecraft will experience in flight in the sense, at least, of producing responses which are equivalent to those expected in flight. This objective is not being met at the present time for a number of reasons. The difficulties encountered include the following:

1. Transient inputs are not uniquely definable. The transients measured for a specific spacecraft-launch vehicle combination vary from flight to flight. In addition to this, the spacecraft and launch vehicle interact as dynamic systems so that different types of spacecraft, if flown on the same launch vehicle, would experience different transient inputs.

2. Reproduction of actual flight transients by use of existing vibration test equipment is difficult even if such transients are known.

3. Close estimates of damping are difficult to obtain.

4. Adherence to the widely used shock spectrum technique imposes severe limitations because it does not properly treat the spacecraft as the complex dynamic system which it is.

The limitations imposed by each of these difficulties can be evaluated somewhat independently from the others. This paper is directed to the development of techniques which employ closer representations of the physical systems involved and, hence, are believed to be superior to the shock spectra techniques of item 4.

As a measure of equivalence between proposed ground test transients and typical or expected flight transients, the shock spectrum technique compares envelopes of maximum responses of single-degree-of-freedom systems over the frequency range of interest. Slowly swept sinusoidal inputs are often used as a means of satisfying the requirements dictated by the shock spectrum method. The only equivalence in this type of test is the maximum response of a particular component considered as a single-degree-of-freedom system. Because of the uncertainties associated with simulation of transient responses by sinusoidal testing, large weighting factors are employed which often result in overconservative tests of spacecraft systems. Since the test transient input is not uniquely defined by its shock spectrum, a satisfactory representation of the flight transient cannot be achieved.

The approach presented in this paper for evaluating transient environmental testing of spacecraft idealizes the spacecraft as a complex elastic structure having several degrees of freedom. The method uses conventional procedures of structural analysis. Normal coordinates are used to determine the participation of a particular normal mode of vibration in the total system response. This analytical representation of the spacecraft and its response provides a much improved measure of equivalence between different transient inputs.

## RESPONSE TO TRANSIENT INPUTS

To establish, heuristically at least, the need for a multi-degree-of-freedom representation of the spacecraft (instead of using shock spectra techniques), a few numerical solutions have been worked out. The analytical models and the values of their system parameters are not representative of any specific spacecraft system; however, they are felt to be realistic since the dynamic range of frequencies chosen is representative of spacecraft systems.

### Component Location

The response of a spacecraft component is dependent not only on its own dynamic characteristics, but also on its point of attachment to and the dynamic characteristics of the spacecraft structure. The component response can vary several orders of magnitude for different attachment points. The effect of component location on maximum response to a transient input is shown in Fig. 1. It is assumed that the acceleration input at the base of the models (typically the spacecraft adapter ring) is known. The single-degree-of-freedom system represents a component attached directly to the

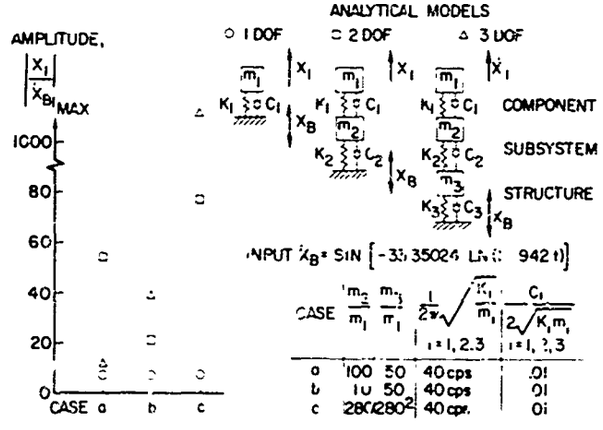


Fig. 1 - Effect of component location on maximum response

spacecraft adapter ring; the two-degree-of-freedom system represents the component attached to a subsystem which is attached to the spacecraft adapter ring. In the three-degree-of freedom system, the subsystem is attached instead to the flexible spacecraft structure which is mounted on the spacecraft adapter ring. Both the assumed subsystem and spacecraft structure are assigned only one degree of freedom for the purpose of the following discussion. The natural frequency of all uncoupled systems is 40 cps. This results, for example, in natural frequencies of approximately 21, 40, and 77 cps for the three-degree-of-freedom system, case a. For case a, the subsystem mass is 100 times the component mass ($m_2/m_1 = 100$) and the mass of the structure is 50 times the component mass ($m_3/m_1 = 50$). The corresponding values for case b are 10 and 50, respectively. In case c, the subsystem mass is 280 times the component mass ($m_2/m_1 = 280$), and the mass of the structure is 280 times the subsystem mass ($m_3/m_2 = 280$). The damping of all systems discussed in this paper is 1 percent of the critical damping of the uncoupled systems.

The acceleration input to the spacecraft adapter ring is represented as the high-speed time-varying sinusoidal sweep,

$$\ddot{X}_B = \sin [-33.35024 \ln (1 - 0.942\, t)] .$$

This is a so-called sin $\ln$ transient and sweeps from 5 to 400 cps in approximately 1.05 sec. The shock spectrum of this transient is essentially constant from 10 to 280 cps.

If the component was mounted directly on the spacecraft adapter ring, its maximum response for the applied transient would be 7 g. If, instead, the spacecraft is considered to be a two-degree-of-freedom system, the results are quite different. The maximum component response is 54, 21, and 77 g for cases a, b, and c, respectively. For the three-degree-of-freedom system, the maximum component response in case a decreases to 12 g; in case b, it increases to 39 g; and in case c, the maximum component response is over 1000 g. In general, the maximum response, $\ddot{X}_1$, is quite different from that of a one-degree-of-freedom system when the spacecraft is treated more realistically as a multi-degree-of-freedom system.

## Response Time History

In addition to the above, there is another very important effect which should not be overlooked in selecting a test transient for an environmental vibration test. In a multi-degree-of-freedom system, two transients which have the same shock spectrum will, in general, produce response time histories and, hence, maximum amplitudes which are quite different from each other. This is shown in Fig. 2a for three different transient inputs. The shock spectra of the transients are shown in Fig. 2b. The coupled system natural frequencies are approximately 11 and 27 cps for the two-degree-of-freedom system and approximately 8.4, 21, and 34 cps for the three-degree-of-freedom system in this figure. The first transient is representative of the acceleration input to the spacecraft adapter ring during sustainer engine cutoff (SECO) of the Ranger 6 flight. The second transient is a 4-oct/min sinusoidal sweep with a shock spectrum which envelopes that of the SECO transient. The third transient is a sin $\ln$ transient which sweeps from 5 to 400 cps in 4.5 sec. The function which generates this transient is

$$\ddot{X}_B = \sin [-157.07963 \ln (1 - 0.2\, t)] .$$

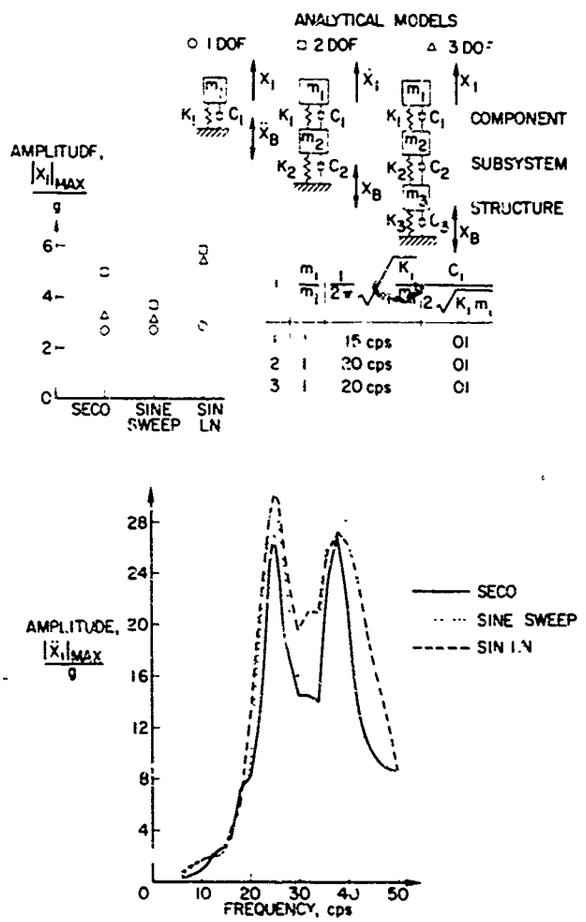


Fig. 2 - (a) Variation of response with type of input, and (b) shock spectra for SECO, sine sweep, and sin $\ln$ transient inputs

The amplitude of this function is modulated to envelope the shock spectrum of the SECO transient for the frequencies of interest.

As Fig. 2 shows, both the 4-oct/min sweep and the sin $\ell$n transient produce slightly greater maximum responses in the one-degree-of-freedom system than the SECO transient. In the two-degree-of-freedom system, using the response to the SECO transient as a reference, the component is undertested by the 4-oct/min sweep and overtested by the sin $\ell$n transient. In the three-degree-of-freedom system, the component is very slightly undertested by the 4-oct/min sweep and considerably overtested by the sin $\ell$n transient. Enveloping of shock spectra is, therefore, not an adequate criterion for transient testing multi-degree-of-freedom systems.

## ANALYSIS

The equations of motion of a multi-degree-of-freedom linear dynamic system can be put in the following form:

$$[M]\{\ddot{X}\} + [C]\{\dot{X}\} + [K]\{X\} = \{f(t)\}. \quad (1)$$

where

$[M]$ = $n \times n$ symmetric positive definite mass matrix,

$[C]$ = $n \times n$ damping matrix,

$[K]$ = $n \times n$ symmetric non-negative definite stiffness matrix,

$\{X\}$ = $n \times 1$ displacement matrix, and

$\{f(t)\}$ = $n \times 1$ matrix of forces.

The solution for the system response in terms of normal coordinates is obtained using established procedures.

Due to the properties of symmetry and definiteness of the matrices $[M]$ and $[K]$, there exists an $n \times n$ matrix $[U]$ with the following two properties [1]:

$$[U]^T[M][U] = [I] \quad (2a)$$

and

$$[U]^T[K][U] = [\omega^2], \quad (2b)$$

where

$[U]^T$ = transpose of $[U]$,

$[I]$ = $n \times n$ identity matrix, and

$[\omega^2]$ = $n \times n$ diagonal matrix of eigenvalues

The matrix $[U]$ is called the modal matrix of the system; the $j$th column of this matrix $\{u_j\}$ is the $j$th mode shape. Let

$$\{X\} = [U]\{q(t)\} = q_1(t)\{u_{11}\} + q_2(t)\{u_{12}\} + \cdots + q_n(t)\{u_{1n}\}. \quad (3)$$

where $q_j(t)$ is the $j$th normal coordinate. Substituting Eq. (3) into Eq. (1) gives

$$[M][U]\{\ddot{q}\} + [C][U]\{\dot{q}\} + [K][U]\{q\} = \{f(t)\}$$

and

$$[U]^T[M][U]\{\ddot{q}\} + [U]^T[C][U]\{\dot{q}\} + [U]^T[K][U]\{q\} = [U]^T\{f(t)\}.$$

From Eq. (2)

$$\{\ddot{q}\} + [U]^T[C][U]\{\dot{q}\} + [\omega^2]\{q\} = \{Q(t)\},$$

where

$$\{Q(t)\} = [U]^T\{f(t)\}$$

is the $n \times 1$ matrix of generalized forces. For proportional damping, the matrix $[U]^T[C][U]$ is a diagonal matrix and the equations are uncoupled [2]. In this case, the $j$th equation can be written

$$\ddot{q}_j + 2\zeta_j\omega_j\dot{q}_j + \omega_j^2 q_j = Q_j(t). \quad (4)$$

The general solution to Eq. (4) for arbitrary $Q_j(t)$ can be obtained by the method of variation of parameters [3]. From the theory of ordinary differential equations, the homogeneous equation $Q_j(t) = 0$, corresponding to Eq. (4), has a solution of the following form:

$$q_{h_j}(t) = Aq_{1_j}(t) + Bq_{2_j}(t).$$

where $q_{1_j}(t)$ and $q_{2_j}(t)$, hereinafter identified as $q_{1_j}$ and $q_{2_j}$, are linearly independent and A and B are the constants of integration. To obtain a particular solution, the arbitrary constants A and B are replaced by $r_1(t)$ and $r_2(t)$. Then $r_1(t)$ and $r_2(t)$, subsequently referred to as $r_1$ and $r_2$, are determined so that Eq. (4) is satisfied. Thus,

$$q_{p_j} = r_1 q_{1_j} + r_2 q_{2_j}$$

and (5)

$$\dot{q}_{p_j} = r_1\dot{q}_{1_j} + r_2\dot{q}_{2_j} + \dot{r}_1 q_{1_j} + \dot{r}_2 q_{2_j}.$$

Imposing the condition

$$\dot{r}_1 q_{1j} + \dot{r}_2 q_{2j} = 0 \qquad (6)$$

leads to

$$\dot{q}_{pj} = r_1 \dot{q}_{1j} + r_2 \dot{q}_{2j} \qquad (7)$$

and

$$\ddot{q}_{pj} = r_1 \ddot{q}_{1j} + r_2 \ddot{q}_{2j} + \dot{r}_1 \dot{q}_{1j} + \dot{r}_2 \dot{q}_{2j} . \qquad (8)$$

Substituting Eqs. (5), (7), and (8) into Eq. (4) and collecting terms yields

$$r_1(\ddot{q}_{1j} + 2\zeta_j \omega_j \dot{q}_{1j} + \omega_j^2 q_{1j})$$

$$+ r_2(\ddot{q}_{2j} + 2\zeta_j \omega_j \dot{q}_{2j} + \omega_j^2 q_{2j}) + \dot{r}_1 \dot{q}_{1j} + \dot{r}_2 \dot{q}_{2j} = Q_j .$$

Since $q_{1j}$ and $q_{2j}$ satisfy the homogeneous equation,

$$\dot{r}_1 \dot{q}_{1j} + \dot{r}_2 \dot{q}_{2j} = Q_j . \qquad (9)$$

Equations (6) and (9) can be solved by Cramer's rule for $\dot{r}_1$ and $\dot{r}_2$:

$$\dot{r}_1 = -\frac{q_{2j} Q_j}{W} \qquad (10a)$$

and

$$\dot{r}_2 = \frac{q_{1j} Q_j}{W} , \qquad (10b)$$

where

$$W = q_{1j} \dot{q}_{2j} - \dot{q}_{1j} q_{2j}$$

is the Wronskian. Note that $W \neq 0$ since $q_{1j}$ and $q_{2j}$ are linearly independent. By integrating Eqs. (10),

$$r_1 = -\int \frac{q_{2j} Q_j}{W} \, dt \qquad (11a)$$

and

$$r_2 = \int \frac{q_{1j} Q_j}{W} \, dt . \qquad (11b)$$

The general solution to Eq. (4) is

$$q_j = q_{hj} + q_{pj} = A q_{1j} + B q_{2j} + r_1 q_{1j} + r_2 q_{2j}$$

$$= q_{1j}[A + r_1] + q_{2j}[B + r_2] . \qquad (12)$$

where A and B are the constants of integration and $r_1$ and $r_2$ are given by Eqs. (11). It should be noted that the time-varying functions $q_{1j}$ and $q_{2j}$ appearing in Eq. (12) depend only on the parameters of the system and oscillate at the $j$th natural frequency of the system; they are independent of the generalized force $Q_j$. On the other hand, $r_1$ and $r_2$ are relatively complicated functions of both the system parameters and the forcing function.

Equation (12) indicates the influence of the forcing function on the general solution to the problem. The bracketed quantities in Eq. (12) can be thought of as time-varying amplitudes which modulate $q_{1j}$ and $q_{2j}$. The effect of changing the forcing function is to change the time variation of the bracketed terms. Therefore, the time-varying amplitude of the normal coordinate $q_j$ provides an indication of the effect of different forcing functions on the participation of the $j$th mode in the response of the system. The information contained in the response time histories of the $\ddot{q}_j$'s provides an excellent basis for the evaluation and selection of test transients.

## EQUIVALENCE OF TRANSIENTS

The following scheme is used to determine a satisfactory test transient for an environmental vibration test of a particular spacecraft:

1. The spacecraft is analyzed and an acceptable structural idealization, Eq. (1), is established.

2. Equation (1) is solved numerically for $\{\ddot{X}\}$.

3. Equation (3) is used to compute $\{\ddot{q}\}$:

$$\{\ddot{q}\} = [U]^{-1}\{\ddot{X}\} .$$

A typical time history for $\ddot{q}_j(t)$ is shown in Fig. 3a.

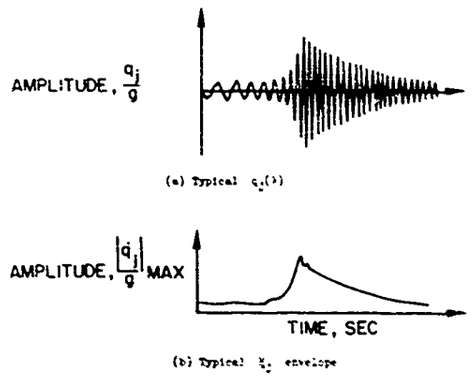


Fig. 3 - Typical normal coordinate response $\ddot{q}_j(t)$ and envelope

4. The envelopes of absolute values are computed for $\ddot{q}_j$, $j = 1, \ldots, n$. Figure 3b shows the envelope for the $\ddot{q}_j$ in Fig. 3a.

5. The $\ddot{q}$ envelopes for the representative measured flight transient and for the test transients under consideration are compared on the basis of maximum amplitude versus time and, if fatigue is a consideration, then the other characteristics of the individual time histories may be studied.

6. The test transient is selected which best approximates the $\ddot{q}$ envelopes produced by the flight transient. In this regard, however, the selected test transient may be modified to conform to whatever degree of conservatism is desired. This modification might take the form of increasing the amplitude of the test transient to produce slightly higher levels of response than the measured transient. In addition, the test transient may be modified to contain a minimum energy level over a frequency band thought to include all unknown resonances of the actual spacecraft.

## EXAMPLES OF APPLICATION

### Evaluation of Slow Sinusoidal Sweep Test

The $\ddot{q}$ envelopes for the SECO transient input to the two-degree-of-freedom system of Fig. 2a are shown in Fig. 4a. The envelope of $\ddot{q}_1$ has a maximum value of 1.75 g; the envelope of $\ddot{q}_2$ has a maximum value of 9 g. Both modes respond simultaneously and the duration of the response is less than 1 sec.

Figure 4b shows plots of the $\ddot{q}$ envelopes for the 4-oct/min sinusoidal sweep of Fig. 2.

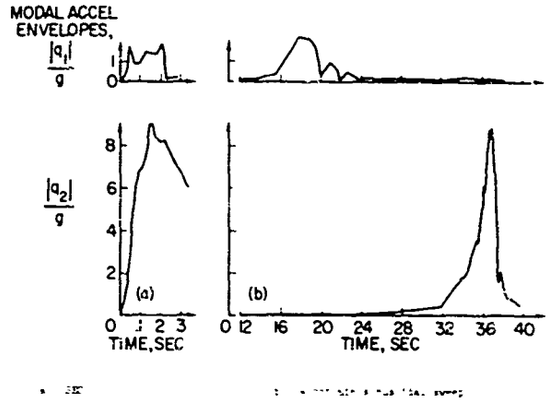


Fig. 4 - Modal responses of two-degree-of-freedom system to (a) SECO input, and (b) 4 oct/min sinusoidal sweep input

Their maximum amplitudes are approximately the same as those of the SECO transient. However, there are very important differences between the $\ddot{q}$ envelopes for the sinusoidal sweep and those for the SECO transient. For the sinusoidal sweep, the modes do not respond simultaneously, resulting in the variation of maximum component responses shown in Fig. 2a. For the SECO transient, the first and second modes combine to produce a maximum response which is greater than either of these two individual modes excited by the sinusoidal sweep. For the sinusoidal sweep, the maximum component response occurs in mode 2. The contribution from the first mode at this time is negligible and, hence, the spacecraft is undertested as far as maximum response is concerned, even though this sinusoidal sweep conservatively envelopes the shock spectrum of the SECO transient.

On the other hand, the duration of the response for the sinusoidal sweep is much longer than it is for the SECO transient. The sinusoidal sweep would be more likely to produce a fatigue failure than would the flight transient.

These comparisons show that the sinusoidal sweep is a poor environmental test of this spacecraft's response to the SECO transient. The system is undertested on the basis of maximum response and is overtested on the basis of fatigue life.

Figure 5a shows the $\ddot{q}$ envelopes for the SECO input to the three-degree-of-freedom system of Fig. 2a. The maximums for the 1st, 2nd, and 3rd modes are 1, 5.5, and 3.5 g, respectively. All modes respond simultaneously. The $\ddot{q}$ envelopes for the sinusoidal sweep input to this system are shown in Fig. 5b. As with the two-degree-of-freedom system, the amplitudes are approximately the same as those of the SECO transient, but the modes respond at different times. This raises a question. The comparison of maximum component response shown in Fig. 2a indicates that for the three-degree-of-freedom system, the sinusoidal sweep produces only slightly less maximum component response than the SECO transient. On the basis of the information conveyed by the $\ddot{q}$ envelopes, however, the sinusoidal sweep may appear to be a severe undertest of maximum response. This apparent discrepancy is explained by examining the modal participation for the three-degree-of-freedom system at the time of maximum component response. In this case, Eq. (3) becomes

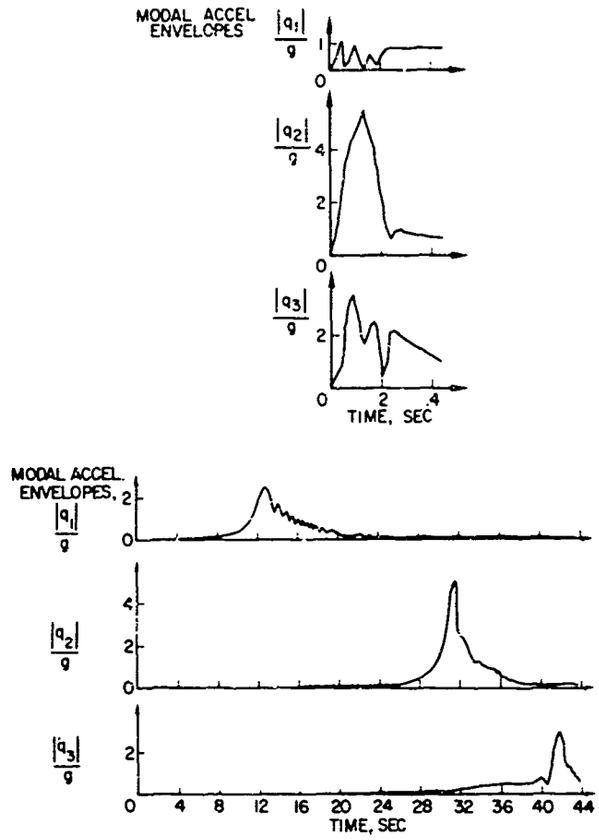


Fig. 5 - Modal responses of three-degree-of-freedom system to (a) SECO input, and (b) 4 oct/min sinusoidal sweep input

$$\begin{Bmatrix} \ddot{X}_1 \\ \ddot{X}_2 \\ \ddot{X}_3 \end{Bmatrix} = \ddot{q}_1 \begin{Bmatrix} 0.791 \\ 0.53 \\ 0.29 \end{Bmatrix} + \ddot{q}_2 \begin{Bmatrix} 0.591 \\ -0.54 \\ -0.59 \end{Bmatrix} + \ddot{q}_3 \begin{Bmatrix} -0.157 \\ 0.64 \\ -0.74 \end{Bmatrix}.$$

The values of the normal coordinates at the time of maximum response of $\ddot{X}_1$ to the SECO input are

$$\ddot{q}_1 = 0.31,$$

$$\ddot{q}_2 = 4.6,$$

and

$$\ddot{q}_3 = -1.97.$$

Therefore,

$$\ddot{X}_{1_{MAX}} = 0.24521 + 2.7186 + 0.30929 = 3.2731.$$

The contribution from the second mode, 2.7186, is over 83 percent of the total maximum response. Hence, the component's maximum response is only slightly undertested by the sinusoidal sweep.

For the substructure, however, this is not the case. The values of the normal coordinates at the time of maximum response of the substructure $\ddot{X}_2$ are

$$\ddot{q}_1 = 0.3,$$

$$\ddot{q}_2 = -4.0,$$

and

$$\ddot{q}_3 = 3.5.$$

Therefore,

$$\ddot{X}_{2_{MAX}} = 0.159 + 2.1[illegible].4 = 4.559.$$

The second mode contribute[illegible]1.4 percent; the third mode contributes 49.1 percent; however, with the slow sinusoidal sweep, $\ddot{X}_2$ reaches its maximum when the second mode only is responding. The approximate values of the normal coordinates at this time are

$$\ddot{q}_1 = 0.1,$$

$$\ddot{q}_2 = -5.0.$$

and

$$\ddot{q}_3 = 0.15 .$$

Hence, in this case,

$$\ddot{X}_{2_{MAX}} = 0.053 + 2.7 + 0.096 = 2.849 .$$

The slow sinusoidal sweep undertests the substructure by 37.5 percent. For the three-degree-of-freedom system, also, the slow sinusoidal sweep is a poor environmental test of the response of the system to the SECO input.

### Evaluation of sin $\ell n$ Test Transient

The $\ddot{q}$ envelopes for the sin $\ell n$ input to the three-degree-of-freedom system of Fig. 2a are shown in Fig. 6. The maximum values of the $\ddot{q}$ envelopes for the sin $\ell n$ input (which conservatively envelopes the shock spectrum of the SECO transient) are approximately 50 to 150 percent greater than those for the SECO input. The modes respond very nearly simultaneously and the duration of their response is on the order of 1 sec. A 25 percent reduction in the input amplitude of the sin $\ell n$ function would give $\ddot{q}$ envelopes with maximum amplitudes which are still conservative by 70 percent for the first mode and 10 percent for the second and third modes. It should be noted, however, that this reduction produces a shock spectrum which is considerably underconservative for the sin $\ell n$ input. Nevertheless, all three masses of the three-degree-of-freedom system still have maximum responses which are greater than those for the SECO input. The values are given in Table 1.

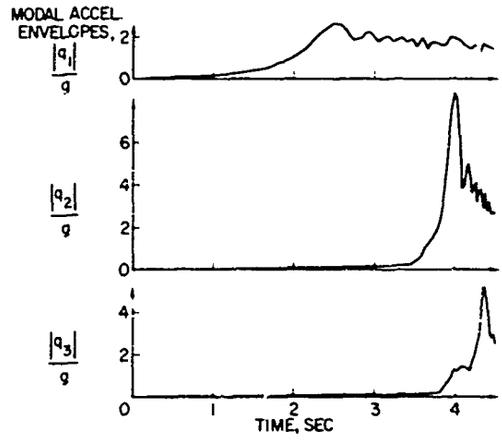


Fig. 6 - Modal response of three-degree-of-freedom system to 4.5-sec sin $\ell n$ input

TABLE 1
Maximum Responses of Three-Degree-of-Freedom System to SECO and 0.75 sin $\ell n$ Inputs

| Mass | Response (g) | |
|---|---|---|
| | SECO | 0.75 sin $\ell n$ |
| $m_1$ | 3.28 | 4.07 |
| $m_2$ | 4.6 | 4.7 |
| $m_3$ | 4.56 | 4.6 |

The 4.5-sec 0.75 sin $\ell n$ transient, therefore, appears to be nearly acceptable in lieu of the actual SECO transient for testing the three-degree-of-freedom system of Fig. 2a. With a little effort, it could be modified to provide a test identical to the SECO input.

## CONCLUDING REMARKS

This paper has demonstrated that the shock spectrum technique is not, in general, capable of accurately predicting maximum responses of complex elastic spacecraft structures to transient inputs and that a more sophisticated approach is needed.

A method has been developed for evaluating transient environmental testing of complex spacecraft. The technique presented, which is within the current capability for structural analysis, represents the spacecraft as a multi-degree-of-freedom system and uses normal coordinates to determine the participation of each mode in the total system response. This method is required to predict accurately the maximum responses of systems which have significant interactions between the various modes. The method provides a suitable measure of equivalence between various proposed test transients as well as between transient and sinusoidal testing.

In the application of this scheme to an actual spacecraft, it is desirable to include as many degrees of freedom in the analytical model as can be identified as significant since each additional degree of freedom (each additional normal coordinate) acts as an additional constraint in selecting a suitable test transient. Thus, a more suitable input can be achieved.

The results presented herein prompt the authors to recommend the extension of this approach for possible application to construction of suitable test transients for the environmental testing of spacecraft.

## REFERENCES


1. F. B. Hildebrand, Methods of Applied Mathematics. Prentice-Hall, 1952

2. T. K. Caughey and M. E. J. O'Kelly, "Classical Normal Modes in Damped Linear Dynamic Systems," J. Appl. Mech., Vol. 32, Ser. E, pp. 583-588, Sept. 1965

3. Erwin Kreyszig, Advanced Engineering Mathematics. John Wiley, New York, 1962


## DISCUSSION

Mr. Roberts (Martin Co.): I suggest there is a very strong limitation to the proposed method: the delta t of the input slopes is of the same order as the periods of the low modes of the structure being analyzed. If the shock wave impingement on this structure is an abrupt impingement from a wave propagation through the structure, the number of modes that would be required to illustrate the maximum responses of the complex structure would be of the order of 50 or 100 or 1000.

Mr. Howlett: The method is based, in the first place, on a finite element approach. We are representing the spacecraft by a finite number of degrees of freedom; it is always possible that this is not a good representation. There are surely some cases in which a continuous representation and, actually, wave theory must be used to predict what is happening.

Dr. Sevin (IIT Research Inst.): I do not argue the limitations of single-degree-of-freedom shock spectra, but I was puzzled about several things. The comparison of the one, two, and three degrees of freedom seemed to me perhaps a bit unfair. I was not sure whether you ment to say that the one-degree-of-freedom system was the best model of what was more properly, a three-degree-of-freedom system. I am sure you could have picked a better single-degree-of-freedom system approximation which would have shown far greater agreement. In principle, you are keeping the same parameter values for each of the elements of the model; you can stack them, you know, ad infinitum and get any kind of comparison that you like, but I think that is perhaps a bit unfair. Secondly, I was surprised that you had not mentioned that in a linear multi-degree-of-freedom system, assuming that the modal components are in phase and their absolute values are added, the single-degree-of-freedom system spectrum certainly provides an upper bound to the response. Therefore, you would expect that if the SECO loadings truely envelope the others on the spectra, they would also envelope the responses on the multi-degree-of-freedom system. It seemed to me, also, that you were showing a slight trend upward in maximum acceleration of your single-degree-of-freedom model for the three inputs. This couldn't occur if the SECO envelope really enveloped the other two. So, I guess I am basically saying that there seems to be a question of your ability to model the system adequately. If you really knew how to model the system, you certainly would be in a much better position to say in what sense one input is equivalent to another.

Mr. Howlett: Yes, that is true. We are assuming that you must have a correct analytical model of the system. This is done quite frequently throughout the aerospace industry; spacecraft structures are being modeled by finite element approaches with very good agreement. You were right that when all the modes respond at the same time, the shock spectrum technique gives an upper bound on the maximum response. When this does not happen, when maybe only the first and third modes respond and the second does not, this approach would give a lower upper bound and a more realistic interpretation.

Dr. Sevin: If you propose to treat the modes in their actual phasing, you have to be extremely concerned about whether your model is adequate or not. It would have been interesting with these examples to investigate how conservative the upper bound was for the various loadings. It is conservative but I am not sure there has been sufficient experience to know how conservative it is.

Mr. Howlett: There is more work needed to determine the number of degrees of freedom required and how accurate the model is. In the paper there are some numbers which might give you an idea of how close the upper bound was. Where the input amplitude was reduced by 25 percent, there is very close agreement between the sin $\delta n$ input and the SECO transient for two of the three maximum responses.

Dr. Morrow (Aerospace Corp.): I do not think there should be any question that a spacecraft is a multi-degree-of-freedom system. The shock spectrum should never have been used as an indication of the responses of such a

system. I am not quite sure what we mean by specifying responses. What we should be specifying, if anything, is inputs. But, in any event, there are other problems that go somewhat beyond what has been presented here. In the first place, if we have a shock transmitted, say, through the airframe to the payload of one of these spacecraft -- I assume we are talking about a payload for a booster -- we have a very clear-cut case of a low impedance structure driving something of very high impedance. Under these circumstances we really should be looking at force rather than at the motions provided. If we are merely trying to reproduce the actual shock that took place on a particular flight and use a shaker, equalization and so forth, it does not matter. But if we are trying to simulate one shock by another, a force comparison would be very much more worthwhile. There are other considerations. I am not entirely clear why we should be subjecting the whole spacecraft to a shock. Probably the tradition got started with a specification I helped to write, but I remember shock got specified in that way as an unsteady compromise arrived at after quite a bit of arguing. The specification should be subject to review. In short, when things are very large and very difficult to test there is something to be said for the design approaches we use on the rest of the airframe. After all, the spacecraft may be expected to be more rugged than the structure that transmits it. What we are probably more concerned with here is the equipment on board which may be damaged by shocks. If this equipment is considered, creating a model which includes not only the spacecraft shell but the equipment is a really formidable problem. Adapting the shock so meticulously to the thing you are testing becomes a little more of a problem. In fact, the data shown here give some idea of whether the structure is overtested but no indication of whether the equipment on board is overtested or undertested.

Mr. Howlett: What I called the $m_1$ on the figures was considered to be an actual component, for instance, a tube. It is set into the supporting frame which is mounted on the structure.

Dr. Morrow: But to do this, we have to simplify so drastically that the results may not be reliable. You do not necessarily get repeatable stresses from one situation to another from the shock spectrum. One reason is that we have rather prolonged pulses or transients; the other is that no phase relationships are measured in connection with the shock spectrum. We have the same kind of uncertainty we would have if we measure a number of sinusoids at the same time and did not keep their phase relationships recorded. However, if instead of the shock spectrum you use a Fourier transform which can readily be applied to either force or motion and which includes phase information as well as amplitude, you can calculate the response of any linear system quite accurately. Maybe we really need more work on plotting Fourier transforms using the magnitude in much the same way as we have been using the shock spectrum. Magnitude conveys essentially the same information. We should have the phase information for anybody who wants to investigate a few detailed cases a little more thoroughly.

Mr. Howlett: Some work is being done right now along that line. The trouble with the Fourier transform is that you do not have a unique input to any of these spacecraft, even though it may appear so from two supposedly identical slides. With the Fourier transform the phase relationship is extremely important, and work has been done on this. We know how to envelope the amplitude, but exactly how to envelope the phases of several different inputs is a big problem. Widely varying results have been found, depending on what is done with this phase.

Dr. Morrow: I do not think you can do anything with enveloping the phase; however, if you wanted to calculate the response in any particular instance it does enable you to do it. You may have a serious problem trying to make two different pulses give exactly the same effect on a complicated system; maybe there is no way out of that. Maybe we simply have to make compromises for most of our testing and then take a closer look when needed.

Mr. Matteson (Naval Ordnance Laboratory): In your analysis you appeared to compare vibrational inputs. Did you analyze any shock inputs with vibrational overtones?

Mr. Howlett: No, we just used an acceleration input to the base and not what you would really call a shock. But the same thing could be done using this method. I do not see any problems that would arise.

Mr. Matteson: Do you feel that the conclusions that you have drawn from this analysis would be applicable to the shock with a vibrational overtone?

Mr. Howlett: I do not see why it wouldn't. As far as I know, it would work quite well. But we have not actually done it.

* * *

# SPECIFICATION OF SHOCK TESTS

## Panel Session

Moderator: Max McWhirter, Sandia Corp., Albuquerque, N.M.

Panelists: R. W. Hager, Boeing Co., Seattle, Wash.
M. Gertel, Allied Research Assoc., Inc., Concord, Mass.
E. H. Schell, Air Force Flight Dynamics Lab., Wright-Patterson AFB, Ohio
G. W. Painter, Lockheed-California Co., Burbank, Calif.
R. T. Othmer, Sandia Corp., Albuquerque, N.M.
J. R. Sullivan, Naval Ship Systems Command Headquarters, Washington, D.C.

The material on the following pages was presented during the panel session on specification of shock tests. All remarks have been edited for clarity, and some have been omitted, usually because they repeated points brought out earlier in the discussion.

### OPENING STATEMENTS

Mr. Sullivan: There is no single best way to specify a shock test. However, for a given set of circumstances there is always a preferred way of working. This simple truth is seldom recognized in the heat of arguments among people who think they are trying to do the same thing, but are really doing something different.

The uncertainties and variations of most real problems are such that simulation, per se, is not possible. Specification requirements, rather than attempting to achieve simulation, should be aimed at providing the minimum acceptable level of confidence that the item will perform satisfactorily under actual service conditions. The problem in most cases is statistical and will always leave a finite element of risk concerning in-service reliability. The real problem of the specifier is to identify the extent of this risk and to develop criteria which will provide an acceptable level of performance for the need and the cost of obtaining it in the most effective way.

During formal acceptance tests, sophisticated instrumentation and precision testing seldom serve to reduce the element of in-service risk. Controls employed during such testing usually need only be precise in a contractual sense and should be based on parameters that can be simply measured and interpreted. Developmental tests, as opposed to the formal specification testing, are often carried out by a contractor or vendor to minimize rejection risk during the formal testing period. Because the formal or contract test requirements are, at least hopefully, clearly identified, they are subject to further rigorous interpretation. Hence, informal developmental tests can lead to very complex and sophisticated test setups simply because they are aimed at a recognizable goal. While these requirements themselves may be precisely defined, they are often based on satisfying in-service needs which are seldom amenable to such rigorous treatment. Mature engineering judgment must be exercised during the developmental testing phase to prevent data collection and testing which are without worth or meaning.

Mr. Painter: Two technical requirements can be considered in evaluating a shock test method: (a) the test should produce an acceptable simulation of the service environment, and (b) test results should be reproducible in the sense that if two laboratories are testing a piece of equipment made to a certain design, approximately the same damage potential will be applied in both cases. The relative importance of these two requirements is not constant. In many cases we know little or nothing about the service environment, and a general specification is used. For this situation certainly the second

requirement becomes the predominant concern. On the other hand, there are situations where we know a great deal about the service environment which might have some very peculiar and important characteristics. These should then be considered in choosing the test method.

Consider a very common shock situation, a shipping container shock in which the item to be protected has shock mountings between it and the container. The service environment test in this case consists of dropping the container and producing a half-sine transient on the packaged item. Almost certainly this environment would be simulated in the laboratory by a drop test in which the item is attached to a reasonably rigid structure, allowed to fall, strike a spring, and rebound. If we look into the situation further, we find that there are other types of pulse phenomena occurring in the service environment. All of these have a large velocity change associated with them. If we know that a pulse-type phenomenon exists in the service environment, then this is probably the best type of test to use in the laboratory because it should be fairly easy to reproduce. However, as pulse shapes become shorter and shorter, it becomes much more difficult to satisfy the requirement of reproducibility. Then we have to start worrying about the excitation of the natural modes in the equipment and the fixturing.

A second type of shock is the oscillatory or complex shock transient which occurs quite often in aerospace vehicles. It usually results from a very sudden energy input to the system with the resultant ringing of the structure. In this case a pulse-type shock test is not suitable because it does not satisfy either the first or the second requirement.

At this point, it might be useful to see why pulse-type shock testing originated because there is a widespread practice of using simple pulses to simulate oscillatory transients. After World War II there was considerable interest in shipping-container shock and in the half-sine phenomenon. In the later 1940's Blake and Walsh at NRL were working with reed gages to analyze the shock spectra of the Navy Hi Impact Shock Machines. By the early 1950's the shock spectrum was considered probably the best measure of damage potential available, although it was not perfect. Before long the philosophy was expressed that it did not matter a great deal in a shock test whether or not the time function was reproduced in great detail; the important thing was to produce something that would provide an envelope of the service environment shock. However, to apply this approach to oscillatory shock transients, a pulse has to be produced which will truly approximate the shock spectrum of these transients. These spectra are normally peaked at a fairly high frequency with little energy in the low frequencies, and with a fairly low velocity change. They simply cannot be approximated. A pulse can be produced with a spectrum that will, at all frequencies, envelope the spectra of the oscillatory transients, but this results in a great deal of overtesting at certain frequencies. But suppose we allow overtesting; what about reproducibility with a pulse type test? If an attempt is made to produce the spectrum of an oscillatory transient with a pulse, at least to optimize the spectrum a very short duration pulse must be used. Immediately system ringing becomes a problem. It is analogous to two different laboratories conducting a sinusoidal vibration test using the same sweep and amplitude out of the oscillators, but with no equalizing equipment. Unless considerable effort is exerted to have exactly the same type of fixturing and so forth, it is unlikely that they would end up with the same type of test. A pulse test is essentially an open loop test. There is no way of minimizing the difference between desired and actual results.

About three or four years ago we developed a test at the Lockheed-California Co. for the transients occurring in the Polaris vehicle during stage separation. This method fulfills both requirements admirably. Complex transients can be reproduced on an electromagnetic shaker, as long as difficulties with the force and motion capability of the shaker system are not encountered. With this method, a very short duration voltage pulse goes into an array of bandpass filters with separate gain controls; the outputs of these filters are summed and fed into the shaker system. All the equalizing capabilities of a random vibration test are available so it is essentially a closed loop test.

In a test such as the half-sine, which is specified quite often, the first requirement is no problem; there is only the question of whether or not the test is reproducible. If the specification calls for a pulse of sufficiently long duration and not too short a rise time so that there is no concentration of spectral energy at fairly high frequencies, it is easy to reproduce the test. But when tests call for very short duration pulses, control again becomes difficult. It is exceedingly unlikely that two laboratories conducting these short duration tests will have the same damage potential in their tests. Finally, when laboratory A is testing to a half-sine pulse and laboratory B wants to use an oscillatory transient to produce the damage potential of the half-sine pulse, the situation must be

watched closely because there can be considerable difference in damage potentials with a complex transient. But, if laboratory B were willing to accept the possibility that its test was more conservative and if a fairly low value of Q were used in shaping the transient, there could be reasonable assurance that the equipment was subjected to about the same damage potential as that tested by laboratory A.

Dr. Othmer: Ideally the best method for specifying a shock test is that which is the simplest for the technician, who invariably has to perform the test, to understand. To arrive at the simplest presentation requires a team effort. Invariably the person most concerned about the item being investigated is the design engineer who often does not really know quite how to go about specifying a good test for his particular item. He needs to be involved in any group determination of the test to be used. The result of the investigation should be the output from a design engineer, a dynamicist, an environmentalist and a test engineer. The test engineer knows his equipment best, and will be the one who eventually sees that the technicians perform the test.

To define the environment prior to the development of any hardware requires some knowledge of previous applications and some analysis to know what the system may be doing in the particular environment involved. Of course, in many cases the information can be obtained from previously performed tests. Since the actual shock environment for a system or component is generally far from a simple pulse, analyses must be performed to find the best simple shock pulse. For a pulse with a large velocity change, of course, a test pulse containing a large velocity change is needed For the oscillatory pulse with a short transient, the large velocity change is not necessary and many different procedures may be used to arrive at a reasonable solution. Care must be taken to assure that inputs, not responses, are used. A fairly good correlation can be made with a complex shock input in the environment by obtaining shock spectra which cover several inputs and by comparing these with that of the test pulse. This does not mean that for multidegree-of-freedom systems the input can be taken at the base of the system and a good test be made of the component on the uppermost item. For the investigation of that component, the input should come from close to the component mounting. If it is not possible, of course, to make these measurements, analyses will have to be used to find the best input. In situations where large velocity changes occur, the standard half-sine, square wave, sawtooth, parabolic cusp, and so on, are excellent initial selections for the test pulse. But when considering the actual test machine, the pulse it produces should be the one investigated. The shock spectrum of the pulse finally selected should encompass that of the environmental input. Certainly in many cases, there can be overtests, but these can be evaluated and, if necessary, eliminated.

Generally, then, I believe that the best shock test is the simplest available, that a team of engineers should evaluate the test, that mathematical analyses should play an important part in the test selection, and that shock spectra can be used in selecting the shock specification.

Mr. Schell: Although most of my position on specifications is anti spectrum, I do not mean to imply that the shock spectrum is not a useful tool in arriving at a test motion. Shock spectra should be specified, but I would rather specify the motion. In general, there are three test methods in common use today. There is the machine specification in which the test machine is described by drawings and specifications so that all machines used are the same. The test is given by stating, for example, a simple drop height for the table and carriage of the sandpit machine, or the drop height of a hammer in the Navy Hi Impact Machines. These tests do suffer somewhat from nonrepeatability, and the input is very difficult for a designer to specify. In other words, the motion-time history cannot be known with certainty. However, the test condition may be produced very simply and easily by an inexperienced operator. In the sandpit machine, there is some variability resulting from unevenness of the sand.

More recently the pulse-type specification has been set in which the actual input shock motion is defined along with its tolerances. Any machine meeting the specification can be used, and the test is not limited to a single input wave form as in the sandpit and Hi Impact shock machines. The modern shock machines can produce a variety of waveforms. Pulse tolerances are not easy to specify, but it can be done. The pulse itself, or the acceleration-time history, can be used in exact analytical design procedures, thereby aiding the preliminary designer in estimating what is going to happen to a piece of equipment when it is tested to this type of input.

The third method is specification of the shock spectrum, which defines how a collection of linear oscillators must respond to a test motion. An analysis has to be made to verify that they are going to respond in this way. This type of specification has become very popular in

recent years, but, I am opposed to the practice. Reduction of shock motions to a shock spectrum is a difficult process requiring complex and expensive data analysis equipment. The data analysis also requires some time to find out whether the shock test has actually been performed as specified. The results are never available at the end of the test. The most serious indictment, however, of the shock spectrum specification is that it is an incomplete description of the shock motion. The consequences of this fact are reflected in the inability to reproduce test results, in undue restrictions on the use of analytical design techniques, and in overconservatism of designs. A paper I gave at the IES meeting in April 1966 showed that waveforms as different as a sawtooth and a rapid sweep sinusoid could produce the same spectrum. However, the sawtooth has a much larger velocity change than does the swept sine wave, so with only a spectrum specification given, two vastly different inputs will meet the same requirement. The paper also showed that even a damped single-degree-of-freedom system will pass one of these tests and will fail the other because one of them is oscillatory, and damping greatly reduces the oscillatory response. The same is true for nonlinear and multiple-degree-of-freedom systems. It can be reasoned further that if two waveforms differ, the responses of a given system to each waveform will differ. If these responses differ, a system can always be found which will fail one test and pass the other. For very small differences, this may not be important. It does become important if the waveforms are greatly different. Thus, any test specification which allows two different waveforms, for example the sawtooth and sine, can result in a great difference in the test conditions or in the test responses. This is the case with the shock spectrum specifications as used today. Specification of the test motion characteristics, the acceleration-time history of the shock motion, allows a simpler, quicker, less expensive test requiring a minimum of equipment. Furthermore, because it is a complete description of the test motion it provides reproducibility of results not obtainable with the shock spectrum method. Additionally, the motion specification can be used in any analytical design technique and the results need not be overconservative. While a shock spectrum is possibly the best method available today for indicating damage potential in the frequency domain, nobody can tell just how good an indicator of damage potential it is. It may actually be a very poor indicator. Furthermore, there are some very powerful indicators in the time history record, the most important being the peak amplitude, the duration and the velocity change. To a lesser extent the waveform is also an indicator of damage potential. All of these indicators can be determined very simply from the time history without the use of a computer, which is required for the difficult processes of frequency domain analysis.

Adequate measurements of the environment are seldom available. Data analysis methods do not predict how a real equipment will respond. The impedance of the driving source or of the equipment being tested is rarely known. Finally, the simple single-degree-of-freedom system is only one of a small army of possible failure models, each of which can fail in a different way. With our tremendous ignorance of the physical phenomena of environmental shock failure, it makes little sense to use such sophisticated techniques as are now being proposed to specify shock tests. Our efforts should be devoted to getting a simple test which is repeatable and provides the gross simulation of the environment. No matter how you get there you will always test with a shock motion. Thus, the specification of a simple shock motion makes more sense to me than does any other specification of a shock test.

Mr. Hager: Many of the comments that I am going to make have already been stated, sometimes a little differently from the way I am going to state them. I am going to discuss a little broader scope. I will also attempt to explain later why I am pro shock spectra. There are a number of methods in current use for specifying the shock test requirements. These methods range all the way from simply duplicating the actual service environment, such as with a drop test, to those which require mathematical analysis of the input to show that the specification has been met. Shock spectra fit in the latter category. All these methods have, or at least should have, a common purpose which must be determined before one starts to establish shock spectra. This purpose is to produce responses in the equipment which are some factor greater than those which will be produced under the service environment. Definition of response, of course, is a little more complicated than this simple statement implies. Response, as used here, would be defined as deflections, structural loads, stresses, relative motions, or any other behavior of the equipment which would produce failure or malfunction in that equipment. The type of shock test requirement to be used in each particular case should be based on a number of considerations. The intent, of course, is to insure satisfactory performance under the service environment with the simplest and least expensive test technique. One of the factors which should be considered before the test requirements are set is the

possibility of the actual service condition being imposed on the equipment. This may be the most feasible and complete technique to use in testing. Another consideration is the limitations of the available test equipment or test machines used for the test. The service environment must be known, but many times it can only be estimated. The dynamics of the equipment being tested must be known. Where this equipment is a part of a much larger system, the dynamics of the total system and the relationship of the equipment to the system must be known. Lastly, the relative importance of this piece of equipment to the overall performance of the weapons system should be known. In some cases, the item to be shock tested is very large and complex; in this case it may be much easier actually to duplicate the service environment than to try to do it by simulated laboratory testing. An example of this type of testing is a large missile road transporter which must pass a rough road or chuckhole condition. To simulate this kind of operation in the laboratory would be very complex. The best technique, of course, would be to construct a chuckhole and drive the vehicle over it at service speeds. In most cases, however, the service environment cannot be duplicated. The piece of equipment is a part of a much larger system and must be qualified prior to the operation of the system. In these cases the service environment must be simulated in the laboratory and some technique of specifying the shock test is required. To produce responses in the equipment which are some factor greater than those which would be produced under the service environment, we must have knowledge of the equipment responses and, where the equipment is a part of a much larger system, the dynamic responses of the larger system. Some of this knowledge can be obtained from measurements of the actual operating system under a service condition. Many times only measurements from a similar operation are available. When the system is totally new and no data are available, analytical approaches must be used. To obtain all the necessary data requires fairly complex analyses, but this is possible with today's computer capability. Once the responses of the equipment and the system are established and understood, a test requirement can be established which will produce the desired responses. The particular test requirement established must consider the dynamics of the test machine to be used, since this arrangement will probably be much different dynamically from the actual operating system of which the equipment is a part. The time history of the shock pulse, or whatever is being used is not as important as the responses produced in the equipment. The test could be conducted by controlling the response, and oftentimes this is done in vibration testing. It is not a very practical technique for shock testing because of the short durations. Here the control will generally be at the input to the equipment. Whether the test input is defined as an acceleration-time history or the dynamic response of an acceleration-time history, such as a shock spectrum, is purely a matter of choice. They are really the same thing, methods of describing what the actual input is. In either case, the best requirement has been selected to produce the critical responses in the equipment.

Most of my discussion so far is from an analytical or theoretical standpoint. There are some practical considerations which must be kept in mind. If an acceleration-time history is established as the input, it may very well limit the number of machines which can be used for testing. On the other hand, if the shock spectrum technique is established, as Mr. Schell has pointed out, it may limit the number of organizations which can conduct the test. These must be realistic considerations when establishing test requirements. In many cases the shock environment is a very complex pulse which produces significantly different results depending on the damping of the modes of the equipment. If a slow sinusoidal sweep test is used to induce the corresponding responses, an unrealistically long duration for the test will result. On the other hand, if the standard impulse or impact shock test is used, the input is unrealistically high to simulate these complex waves. A technique used at Boeing is transient vibration testing; it employs a very rapid sinusoidal sweep and has been developed for more realistic testing. The input is specified by two shock spectra corresponding to two different values of critical damping. These spectra control the magnitude, the sweep rate, and the duration of the input. We are using a number of different techniques for developing shock test requirements, and we will probably continue to do this. Many of our shock test requirements come from specifications which are imposed on us contractually. For simulation testing in the laboratory however, we have found that the shock spectrum technique is workable and very adaptable to a wide range of service environments, such as the complex wave. Of course, tolerances and such items as the damping in the shock spectra must be controlled. We must not limit ourselves to purely undamped systems. The role of the dynamicist is to select the best technique of the many available, based on the factors involved.

Mr. Gertel: I agree with almost everything the panelists have stated, but I take some

specialized views of some of the things they have said. I am, if I were to summarize my position, anti motion specification and pro shock spectrum. Motion specification is fine if we are dealing with a simple half-sine pulse or ramp pulse or something that can be adequately described in words of that nature. But actual shocks are not simple pulses; they are usually quite complex and cannot be meaningfully described by motion specification.

Specifying a shock test has two aspects. The first is to specify a shock design requirement. When a shock test is specified, designers no longer have to be concerned with the real environment, since the item now only has to pass the laboratory shock test. Also, in establishing a laboratory shock test, it can be determined whether or not the designers have adequately achieved their objectives. Our previous panelists have touched on these two aspects of specifying shock tests. I think most of the audience will agree that the problems arise when we try to interpret how to go about this. The controversy usually centers on three leading questions: (a) what parameters should be used for defining shock, and should a peak motion, time history, or some spectral characteristic be used; (b) should we select a representative sample from the universe of shock environments for a particular application, or should we attempt to synthesize an arbitrary severe composite environment by some sort of enveloping or superposition process; and (c) should we attempt to account for or control the differences between the mechanical impedances of service and test machine installations? On the first question, presently five parameters have been touched on: peak acceleration, peak shock velocity, shock time history, Fourier spectrum, and shock spectrum. Also, the shock machine or the shock testing apparatus to be used can be specified. I would like to qualify my position of being pro shock spectrum, by pointing out that the shock spectrum is not unique. There are many different inputs that can produce a given spectrum, for example, the vibration test arrangements and the various types of machines. If uniformity of test is desired, the machine has to be specified. This avoids the problems of equivalence between one test method and another. It is nonsense to say that if a shock spectrum is specified as the means of controlling a test, it has to be identified for each run from the measurement output of the machine. It is done once under controlled conditions for a particular testing device. Thereafter, when the same device is used, whether it is a sweep shaker or some shock machine, we need only follow the procedure outlined by the people who define the test.

On the question of design shock conditions, it is important to distinguish between a measured shock environment and a design shock condition. We very seldom utilize a single measured sample of a shock environment as a design condition. It is a popular concept that the design condition should reflect the worst possible envelope of environments that the equipment might experience. Consequently, the enveloping process, usually in connection with shock spectra, has become a popular approach to defining a design condition. This approach is quite satisfactory if we are concerned with the effects of a transient environment on rather small components whose resonances will not affect the motion at their support. I think it is widely known that equipments at their resonant frequencies will tend to behave like tuned dampers and null the motion at their support. Consequently, in a shock spectrum of this kind, there will be notches, sometimes referred to as shock spectrum dips. The process of enveloping shock spectra from varied measured conditions, by its very nature, obliterates these dips or notches, and the resulting envelope is based on the maximum responses that have been encountered. This tends to imply inadvertently that the support in every case was of infinite impedance with respect to the item mounted on it. So, the enveloping process has certain disadvantages if we are trying to use a shock spectrum to establish design conditions. It has been suggested, and this is a subject for some further consideration, that envelopes of the valleys of the shock spectra, as well as envelopes of the maxima, should be examined with regard to setting up design conditions. Fourier spectrum techniques perhaps can provide a better definition of shock testing or shock design conditions. Much background work has been done, but no specification has as yet been derived. We may see this in the next decade.

Mechanical impedance considerations was the third controversial item. The same problem exists with the test machine as with the installed equipment in service. The simplest practical way of avoiding the problem of mechanical impedance mismatch is to specify the particular machine to be used. Within reasonable tolerances, there is then a fixed mechanical impedance in the laboratory on which the test item is applied.

Considerable additional research is needed to define shock design requirements from measured environmental data. A major problem here is to obtain a composite severe environment without obscuring the modifying effects due to finite mechanical impedances of actual equipment supporting structures. For design purposes,

the shock spectrum method of presenting the effects of a shock in terms of equivalent static load accelerations as a function of component natural frequencies transforms a dynamics problem into an equivalent statics problem. It is a designer-oriented approach which is useful and highly recommended. For shock testing purposes the greatest uniformity results from specifying the test machine, fixtures and method of test. The shock spectral characteristics of the shock machine should be presented as reference data. The shock spectrum, of course is a single-degree-of-freedom concept. It can be applied successfully to multidegree-of-freedom systems by the concept of modal participation factors applied to the shock spectrum results. The modal participation factor is a method of identifying the sensitivity to the shock-excited input of a particular mode of a complex multidegree-of-freedom system.

GENERAL DISCUSSION

Dr. Sevin (IIT Research Inst.): There seemed to be a disparity in emphasis among all the panelists. The concern was the simulation or the effect of reproducing the input environment by test, with very little attention to the damage mechanisms of the failure models or the essential characteristics of the inputs in terms of their ultimate effect on the component, equipment or structure, or their combination. I understand that the shock spectrum in its original introduction by Biot was intended principally as a characterization of response behavior and not as a description of the input. It has been extended in the sense that it is used today, in terms of input characterization, of which it is not unique. In a plot of acceleration vs frequency, even for one degree of freedom, most certainly it is tacitly assumed that peak acceleration is to be reproduced. This may or may not be. How well are the mechanisms of damage understood? Is work going on to explore that in greater depth? The ability to reproduce the actual environment, as ideal as that approach might be, seems to be somewhat impractical both in terms of its characterization and its uniqueness. Even in the chuckhole example, there probably isn't a unique distribution of chuckholes. Yet, if the characteristics of the response to be simulated could be described in adequate quantitative fashion, one or more waveforms could be chosen and easily or practically reproduced, although not uniquely, by analytical techniques. These waveforms would in some sense come closest to reproducing the particular kinds of response characteristics desired.

Mr. Schell: When Biot originally introduced the concept, I think he did have response in mind. However, in the past few years the shock spectrum has been used more to characterize input waveforms in environment than to indicate the particular response of anything but the simplest equipments. The shock spectrum is actually used as input data for multidegree-of-freedom mode analysis techniques in which modal superposition is used. So it actually has developed from a response to an input characterization. I think it is in this that it gets its best use.

Mr. Othmer: I don't believe that the shock spectrum is representative of the input; it is representative of the effect of the input on a group of individual single-degree-of-freedom systems.

Mr. Kuoppamaki (Consultant): I am in full agreement with Mr. Schell that there are many unknowns in shock testing. However, I would like to refer to an earlier phase of this development. Shock testing was started on dynamic shakers because it was substantially less expensive and reproduction was easier than on other test machines. There were great difficulties in producing specified motion with shock machines. Therefore, what is the difference whether we specify motion or response? It is always possible to use the conventional drop test machines, but if motion is specified, shakers are excluded as possible test facilities. Shouldn't that be a condition to consider as the next step in coming closer to the actual space age in shock testing?

Mr. Schell: I have no intention of excluding shakers as shock machines. If the data analysis indicates that the shock transient has essentially a very small velocity change, the test probably should be performed on a shaker. However, it is not impossible to specify the motion on the shaker. The spectrum need not be specified.

Mr. Bort (Naval Research Lab.): I think that one of Mr. Gertel's points is very important and is sometimes apt to be overlooked—that the shock spectrum depends a great deal on the weight of the equipment or the component to be subjected to the shock. The component will interact on the input and produce notches and peaks in the shock spectrum from what are really minor changes in the input time histories. In many cases when a shock spectrum is calculated from a particular input motion, it is calculated mathematically with essentially an imaginary oscillator having zero mass scanned

through a frequency range. This does not necessarily give a shock spectrum that can then be applied to a massive piece of equipment. An experiment was run quite a while ago at the Naval Research Laboratory in which a 300-lb piece of equipment was mounted to the 4000-lb anvil on the medium-weight shock machine. The equipment's frequency could be varied without changing its weight by changing some spacer blocks and beams. As a shock spectrum was mapped out for the 300-lb piece of equipment by changing its frequency and measuring its response, one was found at 200 lb which was on the order of 1/5th to 1/10th of the shock spectrum found for a mathematical zero weight system by doing calculations on the input. Sometimes when shock spectra calculated by envelope methods are combined, requirements are obtained that are too large. Perhaps looking for the peaks and notches in the spectrum is much more significant than combining them by envelopes.

Mr. McWhirter: I would like to ask Mr. Painter a question. Do you equalize the shaker with the component on it, thereby forcing a large amount of energy in at the resonant frequency, or do you equalize the shaker just for the sake of equalizing it and allow the component to do something to the environment?

Mr. Painter: The method is limited primarily by what is known about what is to be accomplished. Either method can be used. To allow the equipment to introduce notches in the shock spectrum, broadband equalization can be used. Real narrowband equalization can also be obtained.

Mr. McWhirter: I think it is rather important whether force control or acceleration control is used. Which do you think we should be using?

Mr. Painter: Both. I will be giving a paper* in which I recommended that both acceleration and force be monitored in the service environment and force control be used when a piece of equipment tries to stop the thing it is attached to, either in a shock or vibration test.

Mr. Rommel (Lockheed-California Co.): The comments just made on source impedance are more or less a function of the inability to acquire all of the information needed about either shock or vibration environments in service. Whether a waveform time history or a shock spectrum is used, this problem is not avoided. So, assuming that there is a service measurement, how is this transformed into a simple pulse?

Mr. Schell: You can look for the maximum velocity change in the environmental data. You may have a number of environmental measurements and you might want to find some sort of an average velocity change. Perhaps, to be more conservative, all these environmental measurements might give the total velocity change. You would certainly want to look at the peak accelerations in the environment and get some sort of a measure to give a conservative test for peak acceleration. You would also want to look at durations and would, hopefully, try to extend them to their actual length in the environment. Then you might also analyze the data to the shock spectrum. From these results a waveform could be drawn which had at least as much acceleration, velocity change and duration as the environment had, and had a shock spectrum which was the minimum of the environmental envelope of the shock spectra. I do not know of anybody who has used this technique; certainly, we haven't used it. We have been saddled with some preliminary documents that get carried over from year to year. We have to coordinate them with other services who are reluctant to give up sinusoidal testing. The technique seems to me a logical way of arriving at a test waveform. It could be a pulse or it could be oscillatory, depending primarily on the data analysis indications.

Mr. Rommel: You commented on using a test machine. I am not sure what your position is on that as a specification, but a few years ago an RCA electronic packaging designer told about the first piece of equipment that he had to design. He found out after it was built that there were certification tests that had to be performed, and he took it to an environmental laboratory to have these tests run. He gave the equipment, a radio, to the test engineer, who held it 2 ft above a concrete work bench, dropped it, and passed him back the broken parts. This sort of testing is simple and can be done by an untrained person very easily, but the designer did spend a couple of years trying to build a good piece of equipment. I feel that to simplify a test to make it easy to do, or so that an untrained person can run it, is not really what we want to do.

Mr. McWhirter: If the man designed the equipment and built it without knowing the test was to be run, his problem was communication, not testing.

*G. W. Painter, "Use of Force and Acceleration Measurements in Specifying and Monitoring Laboratory Vibration Tests," Shock and Vibration Bull. No. 36, Part 3, Jan. 1967.

Mr. Schell: I would like to clarify my position on machine testing. At present I prefer motion specification. I would not be averse to a specification in which the motion was specified, and then machines were qualified to this motion. Then such a simple thing as a drop test could be specified. If, for example, a machine were built that would generate a pulse of known characteristics, such as a 30-msec half sine, under certain conditions, the result would be a combination of machine specification and pulse specification. I would prefer this over a machine specification alone, because the pulse specification gives the designer information that he does not have otherwise.

Mr. Gertel: Thirty g's means nothing to the designer. If he attempted to design a low natural frequency piece of equipment just using the 30 g and multiplying that by some static stress, he would have a horrible design. The shock spectrum gives much more information. It indicates what happens to a low-frequency component, to the middle-frequency range, and to the high frequency. These frequencies needn't be looked on as single-degree-of-freedom responses, but can be considered modal responses for complex pieces of equipment. Then, usual modal participation factors, such as correction inputs, give the designer something to work with.

Mr. Schell: If the pulse is specified, the shock is completely specified. This need only be analyzed to obtain the shock spectrum. Secondly, with the pulse, analytical techniques can be used that are exact, rather than approximate as are the analytical techniques with normal mode superposition methods using the shock spectrum. Very unconservative results can be obtained by summing modes simply because phasing is not considered.

Mr. Painter: I don't think Mr. Schell has answered the question of what to do when the pulse won't produce a spectrum or when an oscillatory pulse has to be used to get the desired effect Mr. Hager commented on the advantages of shock spectrum analysis If more than one value of Q assumed, the shock spectrum gives a great deal of insight into what occurs in a shock transient. It will show immediately, for instance, from a shock spectrum which is very high with low damping assumed in the analyzer and quite low with high damping assumed, that there is a transient with a lot of ringing at concentrated, fairly narrow frequency bands. On the other hand, if the damped and undamped spectra are about the same, the phenomenon approaches a pulse.

Mr. Forkois (Naval Research Lab.): About 3 or 4 months ago, an electronics man called me and said he was making a proposal on a piece of equipment. He said a shock spectrum test defined by six frequencies and six g levels was specified. I asked what were the lowest and the highest values. The lowest was, for instance, 30 cps and 30 g's, and the highest was 2000 cps and 3000 g's. He asked if I could do this test. I said I didn't know now. This is the way the specification was stated to a small company. I would like to know what your answer would have been to this question.

Mr. Hager: I think some clarifications are required. First, he should have indicated if this was a response spectrum. Did he indicate the Q factor that had been used to define the response spectrum?

Mr. Forkois: I imagine it was undamped. The man was not knowledgeable on the subject. I don't suppose the specification gave this information either.

Mr. Hager: This is a very important consideration. When specifications are written, the requirements must be described completely. I would be able to say that we could conduct that test, but it would require a definition of the characteristics of the particular piece of equipment to be tested and a knowledge of the available test machine. In this particular case, a fast sine sweep test could be used, but I think the specification was incorrectly posed to the designer and should have contained more information.

Mr. Forkois: My answer was that it would be nice to know what phenomenon they were trying to duplicate. I suspected that it was pyrotechnic shock, but neither I nor the man who asked me the question knew anything about it. More needs to be given than just 6 values in g's and 6 values in frequency to perform a shock test.

Mr. Rommel: Have we been talking just about the primary spectrum, or also about the residual spectrum? Should the residual spectrum be used as a supplement to the test specification?

Mr. Hager: In this case, the residual spectrum will always exist, since the particular pulse shapes used in these tests will have both the positive and the residual or the initial and the residual spectra. In all cases we are testing with a pulse shape. No testing is done with a spectrum as an input. The spectrum is just a

means of describing the particular pulse shape and of monitoring the test results. A residual spectrum can be used, and often both are specified. Many times, however, only the initial portion is specified and the test must be conducted in both directions so that maximum conditions are obtained.

Mr. Rommel: What I had in mind was the cumulative damage difference that results from using different pulse shapes, of which the residual spectrum might be some indication.

Mr. Hager: That's correct. In many of the tests the particular pulse shape used will be significantly different in the residual spectrum. It can be controlled. We are not doing this generally in our application.

Mr. Smith (Bell Aerosystems Co.): My experience until recently has been confined to the flutter and vibration field. It has been very interesting to see that there are roughly as many opinions as there are people present. But it seems to me that Mr. Othmer's team approach can be used to illustrate the general situation. I would include on the team not only the design engineer, the dynamicist, the environmental engineer and the test engineer, as he indicated, but the customer as well.

I don't see how the shock spectrum can be expected to apply to anything but the input since we are generally concerned with multidegree-of-freedom systems. We have heard arguments about many points which seem to me to be cleared up only by putting the whole picture together. First of all, let's take the shock spectrum specification. I would suppose that the simpler the specification of the shock is, the lower is the level of confidence that it really represents the environment. A pure impulse is the simplest specification; it never occurs in practice. If the time-dependent input is very carefully specified, it surely has been derived from some very confident measurements in practice and represents a nearly true environment, except for the variability that will always exist. This then should be combined with the two other basic factors, equipment dynamics and equipment capability. Supposedly the dynamic characteristics of the equipment have been calculated for other purposes. Also in any good shock testing setup, the equipment's capabilities, including shaping devices, should be readily available. Surely when all of these things are combined, we can begin to answer some of the basic questions listed as the reasons for holding this panel. For example, what are the advantages and disadvantages of specifying shock spectra? If I was right in assuming that the spectrum specifies the shock as an input, not as an output, it does depend on the confidence with which the shock represents the environment. If the spectrum is simple, the confidence is low; if it is detailed, the confidence is high. Should the specification include an acceptable motion? This would again surely depend on putting together the confidence level of the spectrum, the dynamics of the test machine and the piece of equipment to be tested. The results will determine the necessity of a motion specification. Should the specification be based on enveloping shock spectra? If the environment is detailed, the test can be designed so that it lies close to the specification. If the specification has very low confidence, presumably an envelope must be used which lies farther away from the specification. The equivalence between a shock spectrum produced by a pulse and that produced by a relatively sustained vibration has already been established by the paper in which some of the characteristics of single- and multidegree-of-freedom systems were compared to various kinds of input.

Mr. Schell: The fact that the motion or the specification is complex does not necessarily imply a great deal of confidence in that specification. I think that a shock spectrum specification is much more complex than a simple pulse. Nevertheless, I have no more confidence in the shock spectrum specification than I do in the simple pulse specification.

Mr. Gertel: The shock spectrum is by origin a designer-oriented tool. It presents the response to a particular arbitrary input as a plot of many single-degree-of-freedom systems making up the model. It is used to define the input in an indirect sense in that if there is a second motion, its shock spectrum can be compared to that of a first motion. In a general way if the plotted equivalent static accelerations or the plotted shock spectrum is higher in value for certain frequency ranges than the second motion, we can conclude on the basis of quasi-stress analysis applied to some simple systems that those systems will be stressed more highly than for the other motion. Consequently the types of systems or the frequency ranges which might be more critical in one motion than in another can be identified.

Mr. Stallard (AVCO Corp.): I have heard comments about shock spectra vs shock pulses, but eventually we are going to have to make hardware. I've also heard some comments about being able to give the designer information for his dynamic analysis. I have yet to meet the designer who has ever run a dynamic analysis

of a little box, 6×6×6 in., that weighs 5 lb. He probably does not know how to perform such a dynamic analysis, and I don't think any dynamic analyst does either. I must agree with the gentleman from Wright Field that we must give this designer of little black boxes a number to which to test, such as a versine pulse of 100 g for 6 msec. We cannot give him a shock spectrum because he wouldn't know what to do with it. He will get a versine pulse when he runs a half-sine pulse because there cannot be an abrupt discontinuity in the pulse. It does not happen physically. For shock spectrum purists, the spectrum for the versine is close to that of the half sine anyway.

Mr. Hager: We do indeed run dynamic analyses of 6-×6-×6-in. black boxes. It is not beyond the capability of dynamic analysts at this time. The analyst has as much difficulty, of course, approaching it with a pulse as he does by using a shock spectrum with proper identification of what it is.

Dr. Morrow (Aerospace Corp.): Since there has been some question as to whether it is legitimate to use a shock spectrum to describe an input, I would like to remind us that the residual shock spectrum measured for infinite Q differs from the magnitude of the Fourier spectrum only by a factor of $2\pi$ times the frequency. The use of the shock spectrum as a description of a shock input predates that discovery, but the Fourier spectrum is an exact measure of the input if phase is included. There is a very simple quantitative relationship between the two magnitudes. Furthermore, the shock spectrum does provide some insight into potential damage. This, I think, provides some justification for using either as a description of the input. After all, with a complex system it is very confusing to try to describe all the responses at once. There is a need for test methods that are simple to apply and to specify, and do not require too many dollars in decision making. We should remember that a pulse does not uniquely specify a shock unless tolerances are placed on it. One of the advantages of the shock spectrum is that introducing tolerances is very simple. A minimum shock spectrum can be specified which can be made more elaborate if desired. I would like to suggest a compromise among the various points of view. Suppose we had a fundamental specification which referred in particular to a minimum shock spectrum or minimum values of the Fourier transform. In addition, suppose we indicated generally what kind of pulse or transient would be acceptable for producing this. In other words, if one wants to use something wildly different from what one had in mind, it has to be discussed. But this, at least, keeps down the variation somewhat. It doesn't follow that a shock spectrum should have to be measured from the first time the machine is set up to the routine testing in production. Further compromises can be made such as observing the pulse shape once the test has been proven, is in use, or even in the production test. If the test produces the desired shock spectrum and the main consideration is to insure that it is reproducible, the machine could be used as the test, providing it is checked at intervals with a dummy load by a shock spectrum to make certain that the characteristics have not changed. We have seen that the shock spectrum is not a unique description in that some variability of the effect can persist with the same shock spectrum, but it can be shown by a shock spectrum that two shocks are widely different in their effects. Regardless of what compromise we make in the matters under discussion, it might be illuminating to go back to the late 1940's and examine the type of equivalence between field tests and laboratory tests that were arrived at without using spectra. Often there is no similarity whatsoever to be discerned in the effect, and the shock spectra should be compared.

Mr. Beal (Monterey Research Lab.): Mr. Painter has said the one flaw of the pulse test is that it is an open loop test. Is his test method a closed loop test in the sense that corrections can be made to the input during the course of an individual input?

Mr. Painter: Yes. The method has the same capability as a random vibration test. When ringing of the equipment being tested is found, it can be corrected very readily using peak notch filters.

Mr. Hager: Maybe I should answer that question from our standpoint also. We do have feedback in the system which controls the table input. At these resonances, there is feedback much as with a shaker.

Mr. Beal: As I understand it, an individual pulse input might last about a second or two. Can you correct the pulse during one of these inputs, making this a closed-loop test?

Mr. Painter: There may be some confusion when we talk about pulses. We actually start the transient with a very short pulse, perhaps of 300 $\mu$sec. This is not the actual test transient; it is the pulse being fed into the filters. As a transient with a very flat Fourier spectrum over the frequency range of interest, it would probably be flat up to about 4000 cps or even above, depending on how high it was taken.

But this very short duration pulse is fed to a bank of filters which ring. Therefore, to take care of the feedback problem, a sinusoidal sweep is first fed into the shaker system, and the table is equalized using peak notch filters to get a flat response of the system, over the entire frequency range of interest, wherever accelerometers are located. Then the transient can be shaped to get the desired result. A shock spectrum analyzer at the output of this system indicates if the transient is the one desired. It is not necessary to know the details of the transient.

Mr. McWhirter: Are you saying that you are only concerned with peak response, that time history is not important?

Mr. Painter: No, indeed. I am saying that we are interested in producing a desired shock spectrum envelope.

Mr. McWhirter: Are you concerned only with the peak response as shown by the spectrum at various frequencies? Don't you care whether the complex wave produces peak response 10 times or only once.

Mr. Painter: Well, how long it goes really is well defined by the spectrum. If there are a lot of low-frequency components in the spectrum, naturally there will be several wiggles at a fairly low frequency that will take some time to die out. On the other hand, if the spectrum is concentrated in the very high-frequency regions, there will be a number of very rapid oscillations which will soon be over. The desired damping in the shock spectrum analyzer can be selected. For example, a Q of 10 or of 50 may be selected and the transient shaped to it. Actually, it might be well in this synthesis to assume a couple of levels of damping and try to stay within a certain region for each of those levels. This apparently is the technique that Mr. Hager is using with his swept sine method.

Mr. Wishart (Naval Construction Research Establishment): It seems there has been a tendency to assume that a shock pulse, whether defined in terms of maximum acceleration, maximum velocity in time, or in terms of a shock spectrum, is in some way unique. I don't see that this can be the case at all. I'm concerned with providing design information to designers of naval equipment. If we take a real piece of equipment, this equipment may find itself on the bottom or on the deck of a destroyer, near a bulkhead or near a turbine. It might be in a submarine; it might be subjected to the explosion of a 50- or 1500-lb TNT charge. The shock spectrum of that equipment will vary considerably, depending on its location. The designer of that equipment must make it capable of withstanding the shock environment of all those positions in all those ships. How can you describe a shock spectrum that will enable him to design and test that equipment? How can you make a machine that will give that spectrum and if it didn't, how can you vary it? I would like to introduce one other point here. If your aim is really good simulation of the in-ship environment, you should really try also to include the vertical and the athwartship components. To my knowledge, no attempt is made to do this in a shock test. You test vertical and horizontal components independently. Even when you tilt the equipment, you are still far from the real environment. I have some sympathy, therefore, for Mr. Schell's point of view that whatever you like to do you are still going to be a long way from the truth. You might, therefore, admit it and assume that your test is only a test of ruggedness, nothing more, nothing less.

Mr. Gertel: I grant that what you have stated comes very close to the truth, but do you suggest that we give up and do nothing about it? We have to do the best we can with the tools we have at our disposal, and a shock spectrum is a starting point. I am not saying that it is the final solution. With regard to the problem of the variety of situations or locations in which a particular equipment can be installed, one gets stuck in a sense with the envelope of shock spectra. This implies an infinite impedance which will not permit approximate modification for the interaction effects of heavy equipment. The entire problem of shock requires continuing investigation, but we are really trying to take our first step up the ladder so that we don't have to wait until the system is installed on a ship to subject it to service shock conditions to find out what we want to know.

Mr. Wishart: I am not suggesting you do nothing. I'm merely suggesting that you accept the fact that you have a very inaccurate method at present and not try to make it sound so very much better than it really is.

Mr. Schell: I would like to add to that. I say also that we should not give up, that we should keep on doing research. At present these results belong in the research laboratory, and until valuable practical applications can be derived from them, that is where they should stay.

Mr. Kuoppamaki: Regarding the practical applications, the response spectrum is no longer a research item. The basis of it is well known. I would suggest that, once we specify the response

spectrum, each drop test machine manufacturer will produce equipment which will cover this spectrum. Then we could apply the actual measurements which we obtain from our environment. This will make it possible to relate the response spectrum to the second requirement, repeatability.

Mr. Pendleton (Lockheed Missiles & Space Co.): As a result of the contradiction stated this morning, the capabilities of the small company vs the large company in trying to design equipment, we are trying to specify two criteria for the equipment. We specify a shock spectrum criterion which we can use in our laboratories and a half-sine or simpler pulse which can be used by vendors without sophisticated equipment and capability. Generally, we feel that the half-sine pulse is a more conservative test, and the vendor can, if he wishes, risk running a more conservative test to qualify his package and to save expense. We then can use a more realistic test, as Mr. Painter said, in qualifying the package after we have received it in our shop.

* * *

THIS DOCUMENT CONTAINED
BLANK PAGES THAT HAVE
BEEN DELETED